

**ALTERNATIVE LEAST-SQUARES FINITE ELEMENT MODELS OF
NAVIER-STOKES EQUATIONS FOR POWER-LAW FLUIDS**

A Thesis

by

VENKAT PRADEEP VALLALA

Submitted to the Office of Graduate Studies of
Texas A&M University
in partial fulfillment of the requirements for the degree of

MASTER OF SCIENCE

May 2009

Major Subject: Mechanical Engineering

**ALTERNATIVE LEAST-SQUARES FINITE ELEMENT MODELS OF
NAVIER-STOKES EQUATIONS FOR POWER-LAW FLUIDS**

A Thesis

by

VENKAT PRADEEP VALLALA

Submitted to the Office of Graduate Studies of
Texas A&M University
in partial fulfillment of the requirements for the degree of

MASTER OF SCIENCE

Approved by:

Chair of Committee,	J. N. Reddy
Committee Members,	H. C. Chen
	Chii-Der Suh
Head of Department,	Dennis L. O'Neal

May 2009

Major Subject: Mechanical Engineering

ABSTRACT

Alternative Least-Squares Finite Element Models of Navier-Stokes Equations for
Power-Law Fluids. (May 2009)

Venkat Pradeep Vallala, B.E., Osmania University College of Engineering, Hyderabad

Chair of Advisory Committee: Dr. J. N. Reddy

The Navier-Stokes equations can be expressed in terms of the primary variables (e.g., velocities and pressure), secondary variables (velocity gradients, vorticity, stream function, stresses, etc.), or a combination of the two. The Least-Squares formulations of the original partial differential equations (PDE's) in terms of primary variables require C^1 continuity of the finite element spaces across inter-element boundaries. This higher-order continuity requirement for PDE's in primary variables is a setback to Least-Squares formulation when compared to the weak form Galerkin formulation. To overcome this requirement, the PDE or PDE's are first transformed into an equivalent lower order system by introducing additional independent variables, sometimes termed auxiliary variables, and then formulating the Least-Squares model based on the equivalent lower order system. These additional variables can be selected to represent physically meaningful variables, e.g., fluxes, stresses or rotations, and can be directly approximated in the model. Using these auxiliary variables, different alternative Least-Squares finite element models are developed and investigated.

In this research, the vorticity and stress based alternative Least-Squares finite element formulations of Navier-Stokes equations are developed and are verified with the

benchmark problems. The Least-Squares formulations are developed for both the Newtonian and non-Newtonian fluids (based on the Power-Law model) and the effects of linearization before and after minimization are investigated using the benchmark problems. For the non-Newtonian fluids both the shear thinning and shear thickening fluids have been studied by varying the Power-Law index from 0.25 to 1.5. Also, the traditional weak form based penalty method is formulated for the non-Newtonian case and the results are compared with the Least-Squares formulation.

The results matched with the benchmark problems for Newtonian and non-Newtonian fluids, irrespective of the formulation. There was no effect of linearization in the case of Newtonian fluids. However for non-Newtonian fluids, there was some tangible effect of linearization on the accuracy of the solution. The effect was more pronounced for lower power-law indices compared to higher power-law indices. And there seemed to have some kind of locking that caused the matrices to be ill-conditioned especially for lower values of power-law indices.

To my parents and to my school

ACKNOWLEDGMENTS

I would like to express my gratitude to my advisor Dr. J. N. Reddy for his support and guidance throughout this research. I would like to thank him for the way in which he introduced us to the field of computational mechanics during his courses on linear and nonlinear finite element analysis. I have learned many fundamental things regarding the art of various finite element formulations and their implementation using Fortran. In spite of his busy schedule he always had time to clarify all my doubts during the course of my research. He has been a very good mentor and a guide whose support was always there for me to bank on. These aspects helped me a lot in completing my Master of Science program at Texas A&M University. I would also like to thank my committee members for their support and the time they spent serving on my committee.

Special thanks to Dr. K. S. Surana, University of Kansas, for his time in explaining about his work on Least-Squares finite element formulations for Power-Law fluids. I appreciate Dr. Vivek Prabhakar (former doctoral student of Professor Reddy) for all the clarifications he provided on his doctoral thesis work. Finally, I would also like to thank my friends at Advanced Computational Mechanics Laboratory (ACML) for all their support and help during the course of my research.

TABLE OF CONTENTS

CHAPTER	Page
I INTRODUCTION.....	1
Background	1
Present Status	5
Research Objectives	14
Procedure.....	15
Newtonian Fluids	15
Non-Newtonian Fluids (Power-Law).....	16
II LEAST-SQUARES FORMULATION FOR POISSON'S EQUATION	17
Introduction	17
Least-Squares Formulation	18
Finite Element Model.....	19
Numerical Procedures	21
Numerical Example.....	23
Results	25
Conclusions	28
III LEAST-SQUARES FORMULATION OF VORTICITY BASED FIRST-ORDER SYSTEM FOR NEWTONIAN FLUIDS	29
Introduction	29
The Vorticity Based First-Order System.....	31
Least-Squares Formulation	32
Finite Element Model.....	33
Numerical Example.....	36
Results	37
Conclusions	43
IV LEAST-SQUARES FORMULATION OF STRESS BASED FIRST-ORDER SYSTEM FOR NEWTONIAN FLUIDS	44
Introduction	44
Least-Squares Formulation	45
Method I.....	47
Finite Element Model.....	49
Numerical Example.....	50

CHAPTER	Page
Results	52
Case-I (Linearization before Minimization).....	52
Case-II (Linearization after Minimization)	53
Method II.....	55
Finite Element Model.....	57
Numerical Example.....	58
Results	59
Conclusions	63
 V LEAST-SQUARES FORMULATION OF STRESS BASED FIRST-ORDER SYSTEM FOR POWER-LAW FLUIDS	 65
Introduction	65
Power-Law Fluids	66
Least-Squares Formulation	67
Finite Element Model.....	72
Numerical Example.....	74
Results	75
Case-I (Linearization before Minimization).....	75
Case-II (Linearization after Minimization)	77
Conclusions	78
 VI LEAST-SQUARES FORMULATION OF VORTICITY BASED SYSTEM FOR POWER-LAW FLUIDS	 79
Introduction	79
Least-Squares Formulation	81
Finite Element Model.....	82
Numerical Example.....	83
Results	85
Case-I (Linearization before Minimization).....	85
Case-II (Linearization after Minimization)	87
Conclusions	88
 VII REDUCED INTEGRATION PENALTY FINITE ELEMENT MODEL FOR POWER-LAW FLUIDS	 90
Introduction	90
Penalty Finite Element Formulation	92
Reduced Integration Penalty Finite Element Formulation	95
Power-Law Fluids	98
Numerical Example.....	99

CHAPTER	Page
Results	100
Conclusions	102
VIII SUMMARY AND CONCLUSIONS.....	103
REFERENCES.....	110
VITA.....	117

LIST OF FIGURES

FIGURE	Page
1 A uniform mesh of four elements on which the poisson problem is defined.....	24
2 Velocity vector profile for polynomial order of P=5	25
3 Velocity contour plot for polynomial order of P=5.....	26
4 Comparison of primary variable ϕ for P=3 and 5 with analytical solution at Y=-1.0	26
5 Comparison of primary variable u for P=3 and 5 with analytical solution at Y=-1.0	27
6 Comparison of primary variable v for P=3 and 5 with analytical solution at Y=-0.8	28
7 Computational domain using eight rectangular elements	37
8 Isobars over the domain for P=3	38
9 Velocity contour plot for polynomial order of P=3.....	39
10 Comparison of pressure p for P=3 for linearization before (BL) and after (AL) minimization cases with analytical solution at Y=-0.5.....	39
11 Comparison of pressure p for P=5 for linearization before (BL) and after (AL) minimization cases with analytical solution at Y=-0.5.....	40
12 Comparison of horizontal velocity u for P=3 for linearization before (BL) and after (AL) minimization cases with analytical solution at Y=-0.5.....	41
13 Comparison of horizontal velocity u for P=5 for linearization before (BL) and after (AL) minimization cases with analytical solution at Y=-0.5.....	41

FIGURE	Page
14 Comparison of vertical velocity v for $P=3$ for linearization before (BL) and after (AL) minimization cases with analytical solution at $Y=-0.5$	42
15 Comparison of vertical velocity v for $P=5$ for linearization before (BL) and after (AL) minimization cases with analytical solution at $Y=-0.5$	42
16 Computational domain using graded 25 rectangular elements	51
17 Plots of horizontal velocity u at $X=0.5$ with $P=5$ for linearization before minimization case	52
18 Plots of vertical velocity v at $Y=0.5$ with $P=5$ for linearization before minimization case	53
19 Plots of horizontal velocity u at $X=0.5$ with $P=5$ for linearization after minimization case	54
20 Plots of vertical velocity v at $Y=0.5$ with $P=5$ for linearization after minimization case	54
21 Computational domain using 2x4 rectangular elements	59
22 Comparison of pressure p for $P=3$ for linearization before (BL) and after (AL) minimization cases with analytical solution at $Y=-0.5$	60
23 Comparison of pressure p for $P=5$ for linearization before (BL) and after (AL) minimization cases with analytical solution at $Y=-0.5$	60
24 Comparison of horizontal velocity u for $P=3$ for linearization before (BL) and after (AL) minimization cases with analytical solution at $Y=-0.5$	61
25 Comparison of horizontal velocity u for $P=5$ for linearization before (BL) and after (AL) minimization cases with analytical solution at $Y=-0.5$	62

FIGURE	Page
26 Comparison of vertical velocity v for $P=3$ for linearization before (BL) and after (AL) minimization cases with analytical solution at $Y=-0.5$	62
27 Comparison of vertical velocity v for $P=5$ for linearization before (BL) and after (AL) minimization cases with analytical solution at $Y=-0.5$	63
28 Computational domain using graded 5x5 rectangular elements	74
29 Plots of horizontal velocity u at $X=0.5$ with $P=7$ for various values of Power-Law index for linearization before minimization.....	76
30 Plots of vertical velocity v at $Y=0.5$ with $P=7$ for various values of Power-Law index for linearization before minimization.....	76
31 Plots of horizontal velocity u at $X=0.5$ with $P=7$ for various values of Power-Law index	77
32 Plots of vertical velocity v at $Y=0.5$ with $P=7$ for various values of Power-Law index	78
33 Computational domain using non-uniform 5x5 rectangular elements	84
34 Plots of horizontal velocity u at $X=0.5$ with $P=5$ for various values of Power-Law index for linearization before minimization.....	86
35 Plots of vertical velocity v at $Y=0.5$ with $P=5$ for various values of Power-Law index for linearization before minimization.....	86
36 Plots of horizontal velocity u at $X=0.5$ with $P=5$ for various values of Power-Law index	87
37 Plots of vertical velocity v at $Y=0.5$ with $P=5$ for various values of Power-Law index	88
38 Computational domain using uniform 16 rectangular elements	99
39 Plots of horizontal velocity u at $X=0.5$ with $P=5$ for various values of Power-Law index using RIP	101

FIGURE	Page
40 Plots of vertical velocity v at $Y=0.5$ with $P=5$ for various values of Power-Law index using RIP	101

CHAPTER I

INTRODUCTION

Background

The Navier-Stokes equations are one of the most widely used equations in the area of computational fluid dynamics. Many methods have been proposed for the numerical solution of the Navier-Stokes equations governing flows of viscous incompressible fluids. In the past many researchers have used finite difference or finite volume techniques to study Navier-Stokes equations. However, during the last few decades researchers have started using the finite element method to study the Navier-Stokes equations governing a variety of viscous incompressible fluids. The finite element method (FEM) has enjoyed a great success in solid mechanics and heat conduction applications but has not yet achieved the same level of success in computational fluid dynamics. However, the FEM can be used for a wide variety of problems that involve multiphysics and are complex in nature, such as non-Newtonian fluids and fluid-solid interaction problems.

Most of the finite element formulations are based on weighted-residual (integral) methods. Among these, the weak form Galerkin formulation is most commonly used.

This thesis follows the style of Computer Methods in Applied Mechanics and Engineering.

Although the Least-Squares formulation can be considered as a special case of the weighted-residual method, it has its own standing as the true variational method as it involves the minimization of a functional, whereas the other weighted-residual methods may not have a corresponding functional whose first variation is equivalent to the governing equations. Variational methods (i.e., methods based on the existence of a functional whose extremum is equivalent to the governing equations) are considered to produce the ‘best’ approximation to the exact solution of the equations being modeled. Most solid mechanics problems allow the construction of a functional (based on energy considerations) whose extremum would provide the basis for the construction of associated finite element models. Unfortunately, such a functional based on the energy concept cannot be constructed for the Navier-Stokes equations. Consequently, most finite element models of the Navier-Stokes equations are based on the weak form Galerkin formulation. The only exception is that there exists few works that use the Least-Squares formulation to construct the finite element models.

The Navier-Stokes equations can be expressed in terms of the primary variables (e.g., velocities and pressure), secondary variables (velocity gradients, vorticity, stream function, stresses, etc.), or a combination of the two. Consequently, a large number of finite element models, irrespective of the formulation, can be developed. The successful application of the finite element method to fluids requires a judicial choice of the method (i.e., weak form Galerkin, Least-Squares, etc.) and also the variables. The weak form Galerkin formulations of the Navier-Stokes equations in terms of the primitive variables (p, u, v) have several disadvantages. These are:

- (i) the coefficient matrices are non-symmetric and ill-conditioned due to the absence of pressure variable in the continuity equation;
- (ii) the choice of approximation spaces must satisfy ‘in-sup’ or the Ladyzhenskaya-Babuska-Brezzi (LBB) condition [1,2]. This precludes the use of compatible approximation spaces for velocity and pressure;
- (iii) for nonlinear equations, coefficient matrix is nonsymmetric and the computational cost is high; and
- (iv) the converged solution exhibits non-physical oscillations similar to those observed in finite difference schemes.

Several methods of circumventing these problems have been reported in the literature ([3]-[7]). These methods are problem-dependent and require an arbitrary choice of parameters. The Least-Squares method gives a more general, flexible and robust formulation procedure than the weak form Galerkin-based methods. The first known mathematical analysis of Least-Squares finite element formulations can be traced back to the work of Bramble and Schatz [8] and Bramble and Nitsche [9]. Bramble and Schatz [8] analyzed Least-Squares models for the original elliptic boundary value problems, where the Least-Squares functional were defined in terms of the L_2 norm. This implies a minimum of C^1 continuity of the finite element spaces across inter-element boundaries. As a result, Least-Squares formulations lost appeal and failed to gain popularity due to the higher order continuity requirements when compared to the weak form Galerkin formulation. To overcome this requirement, the partial differential equations (PDE or PDE's) are first transformed into an equivalent lower order system by introducing

additional independent variables, sometimes termed auxiliary variables, and then formulating the Least-Squares model based on the equivalent lower order system. These additional variables imply an increase in cost, but they can be selected to represent physically meaningful variables, e.g., fluxes, stresses or rotations, and can be directly approximated in the model. This approach is believed to be first explored by Jespersen [10] and is the preferred approach in modern implementations of Least-Squares finite element models. For second-order PDE's, if an equivalent first order system is introduced, and the Least-Squares functional is defined in terms of the L_2 norms only (which in turn is defined in terms of the first-order PDE's only), the finite element model allows the use of approximation spaces with merely C^0 continuity. In this formulation the required boundary conditions can be imposed either strongly or, alternatively, in a weak sense through the Least-Squares functional.

The Least-Squares method satisfies the criteria desirable in the variational method. This has drawn considerable attention to the solution of the Stokes and Navier-Stokes equations ([11]-[17]). The Least-Squares formulation has several theoretical and computational advantages. Notably, it circumvents the 'in-sup' condition of LBB. As a result equal order interpolation can be used for all the variables. It also results in symmetric, positive-definite coefficient matrix; hence robust iterative solvers can be employed to solve the system of algebraic equations. Now it has been applied to elliptic [18], hyperbolic [19], and mixed [20] partial differential equations. Practical applications include boundary layer flow [21], gas dynamics [22], Stokes flow [23], inviscid compressible flow [24], convection-diffusion [25], and phase change problems [26].

Present Status

The vorticity based first-order system is the most popular and widely accepted first-order system for the incompressible Navier–Stokes equations. This type of transformation is used by Jiang ([27]-[28]) and Jiang et al. ([29]-[30]). In two dimensions the total number of variables is only increased by one but vorticity, which is of physical significance, can be known directly from the program. Jiang and Sonnad [31] implemented a p -version Least-Squares formulation for the numerical solution of the stationary incompressible Navier–Stokes equations based on the velocity–pressure–vorticity first-order system. However, no detail numerical results were reported. Yet another approach is to introduce the stresses as independent variables. This leads to a stress based first-order system. In two dimensions the total number of variables is increased by three; Surana and co-workers ([32]-[33]), presented numerical results for the stationary incompressible Navier–Stokes system using a p -version Least-Squares formulation. They used Newton’s method with Line-Search in their iterative process. A third option is to introduce all components of the gradient of the velocity vector field as independent variables. This is generally referred to as the velocity gradient based first-order system. Such an approach was first suggested and studied by Cai et al. [34] and Bochev et al. ([35]-[36]). In two dimensions the total number of variables is increased by four and this formulation has the added benefit to easily compute (in the post processing stage) physical quantities of interest that are linear combinations of the partial derivatives of the velocity vector field, e.g., vorticity and stresses. Each of the three formulations has practical and mathematical advantages and disadvantages. In general the vorticity based

formulation achieves the same order of accuracy at a lower degree-of-freedom count, and is thus the preferred formulation in this work.

In previous works, Jiang and et al [28], concerning the Least-Squares finite element formulations for the Navier–Stokes equations, predominantly low-order nodal expansions have been used to develop the discrete finite element model. The low-order nodal expansions tend to lock and reduced integration techniques must be used to obtain acceptable numerical results. Even with reduced integration techniques the quality of solution is not always guaranteed. When enough redundant degrees of freedom are constrained the Least-Squares finite element solution using reduced integration may yield Least-Squares collocation finite element solution. Thus these are not bona-fide Least-Squares based models, but rather collocation Least-Squares based models. The related work on this is done by Pontaza and Reddy [28] on Least-Squares finite element formulations for viscous incompressible and compressible fluid flows. In such a formulation, the Least-Squares functional are defined as the sum of the weighted Squares of the equations residuals evaluated at a finite number of (collocation) points. The concept of the effectivity (or reliability) index was introduced as a guideline to determine a priori whether or not a collocation Least-Squares solution is reliable. It is important to note that reduced integration techniques will only result in a collocation solution if a strict balance between the number of collocation points and total number of degrees of freedom is satisfied.

In [37], the equivalent first-order systems for the incompressible and compressible Navier–Stokes equations obtained by introducing vorticity, stresses, or

velocity gradients as additional independent variables, with focus on the incompressible Navier–Stokes vorticity based first-order system and present a L^2 Least-Squares formulation. The norm-equivalence is explained and how high p -levels can offset the ills of non-equivalence is discussed through a numerical example. The effectivity index notion is presented and its role in obtaining reliable Least-Squares collocation solutions at low p -levels is explained. Numerical results are verified for flow over a backward-facing step, steady flow past a circular cylinder, three-dimensional lid-driven cavity flow, and low-speed compressible buoyant flow inside a square enclosure with corresponding benchmark solutions. The effects of h -refinement, p -refinement and distorted meshes were studied using Kovasznay flow [38]. A discontinuous Least-Squares formulation where the finite element spaces are allowed to retain higher regularity across inter-element boundaries is also presented. The first example of a discontinuous Least-Squares formulation is due to Aziz et al. [39] for a two-domain transmission problem, for which mathematical analysis and numerical results were given by Cao and Gunzburger [40]. Application of the discontinuous Least-Squares finite element formulation has been also demonstrated by Gerritsma and Proot [41] in the context of a first-order one-dimensional model problem, and by Heinrichs [42] in the context of a one-dimensional singular perturbation model problem. Such formulations do not require that auxiliary variables be introduced and may result in better Least-Squares finite element formulations, in the sense that a better compromise between optimality and practicality may be achieved. But this requires the use of higher conditioning number than the corresponding first-order forms.

Recently, interest has shifted towards high-order accurate numerical solutions of the Navier–Stokes equations and it is here that spectral/*hp* finite element formulations have proven to be more efficient [15]. Encouraged by the success of spectral/*hp* methods in computational fluid dynamics, Pontaza and Reddy [15], combined these ideas with Least-Squares variational principles, which offer many theoretical and computational advantages in the implementation of the corresponding finite element model that are not present in the weak form Galerkin finite element model. The Navier–Stokes equations are expressed as an equivalent set of first-order equations by introducing vorticity or velocity gradients as additional independent variables and the Least-Squares method is used to develop the finite element model. Outflow boundary conditions were imposed in a weak sense through the Least-Squares functional. High-order element expansions were used to construct the discrete model and linearized by Newton’s method, resulting in a linear system of equations with a symmetric positive definite coefficient matrix that is solved in a fully coupled manner by a preconditioned conjugate gradient method. Spectral convergence of the L_2 Least-Squares functional and L_2 error norms is verified using smooth solutions to the two-dimensional stationary Poisson and incompressible Navier–Stokes equations. Numerical results for incompressible flow over a backward-facing step, steady flow past a circular cylinder, three-dimensional lid-driven cavity flow, and low-speed compressible buoyant flow inside a square enclosure were presented and found to be in excellent agreement with benchmark solutions. Low-order nodal expansions were used to verify the locking phenomenon in Navier–Stokes equations by Least-Squares finite element formulations. Low-order nodal expansions have been found to lock for

non-equivalent formulations and reduced integration was needed to yield acceptable numerical results. With the reduced integration, it is found that the resulting assembled matrix is nearly singular. Furthermore, the numerical solution may not be smooth at the nodes and post-processing is needed to recover nodal values from the reduced integration points. The vorticity based first-order systems were found to give equally accurate results when compared to the velocity gradient based first-order systems, at significantly lower CPU solve times due to having introduced fewer additional degrees of freedom. Hence it can be conclude that, for the incompressible and low-speed compressible Navier–Stokes equations, the vorticity based formulations are the most efficient. Pontaza and Reddy have extended the formulation to the non-stationary Navier–Stokes equations [43] and viscous compressible flows for subsonic/transonic flow conditions.

When the standard weak form Galerkin method is for velocity–pressure finite element formulation, the biggest problem faced is that of ‘in-sup’ (or LBB) condition ([1]-[2]). The penalty finite element formulation [44] circumvents this problem. It also reduces one independent variable (pressure). However, in the penalty formulation a very high penalty parameter of $(10^8 - 10^{12})$ is required to obtain accurate solutions. For high penalty parameters, the contribution from the viscous terms would be negligibly small compared to the penalty terms in the computer, and a trivial solution is obtained. This is termed as ‘locking’. To circumvent locking and to obtain acceptable solution, under integration (reduced integration) of penalty terms has been proposed [45]. The other problem with this formulation is inaccurate prediction of the pressure from the penalty equation.

When C^0 -continuous shape functions are used to interpolate velocities, pressure is discontinuous along element boundaries, and an averaging is needed to obtain acceptable pressure field [3]. However, pressure field computed in this manner is not very accurate; a very high penalty parameter is needed to obtain accurate pressure. For large values of penalty parameters, the condition number of the finite element coefficient matrix is very high and hence the convergence of iterative solvers is very poor. Due to ill-conditioning of coefficient matrix penalty based weak form Galerkin finite element formulation did not gain much popularity.

Bochov and Gunzburger [46] proposed Least-Squares based penalty formulation for Stokes equations but their study was mathematical and no numerical results were reported. Hasthaven and co-workers ([47]-[48]) have proposed spectral/ hp penalty methods where they implemented boundary conditions using this approach. Prabhakar and Reddy [16] studied Spectral/ hp penalty Least-Squares finite element formulation for the steady incompressible Navier–Stokes equations. The continuity equation is treated as a constraint on velocity field and the constraint is enforced using the penalty method. Instead of traditional penalty method, iterative penalty method proposed by Gunzberger [49] is used. The modified Navier–Stokes equations are expressed as an equivalent set of first-order equations by introducing vorticity–dilatation or stresses as additional independent variables and the Least-Squares method is used to develop the finite element model. High-order basis functions are used to construct the discrete model. Unlike other penalty finite element formulations, equal order integration is used for all terms of the coefficient matrix. The best feature of this formulation is that it requires very small

penalty parameter, 10–40 to yield very accurate solution. For such small penalty parameters, the coefficient matrix is better conditioned and convergence is not slow as in the traditional penalty finite element model. Due to the use of high-order expansions, a very accurate velocity as well as pressure fields is obtained. Thus, the disadvantages of the weak form penalty finite element model are overcome by the penalty Least-Squares finite element model.

The formulation is an alternative to the spectral/*hp* Least-Squares finite element formulation presented by Pontaza and Reddy ([15], [43]) for steady and unsteady problems. In their formulation the divergence-free constraint on the velocity field is enforced directly through the Least-Squares functional, and pressure is retained as an independent variable. For unsteady problems, this approach seems to have disadvantages as the time-evolution of the pressure field is not well-behaved. It is believed that it lacks a strong pressure–velocity coupling. The present formulation avoids this problem altogether by eliminating pressure via iterative penalty method proposed by Gunzberger [49]. First, the spectral convergence is verified using the exact solution of the Kovasznay flow problem. Then, the results for 2D lid-driven cavity problem are compared with Jiang et al.[50]. Next, the 2D flow over a backward-facing step is compared with the benchmark solutions of Gartling [51] and Pontaza and Reddy [15] and flow past a circular cylinder at low Reynolds number is compared with experimental measurements of Grove et al. [52]. The mass conservation is tested by solving 2D flow past a large circular cylinder in a channel. Lastly, this formulation is developed for velocity–

temperature coupled problems and results for buoyant flow inside a square enclosure are compared with the benchmark solution of Davis et al. [53].

In case of non-Newtonian fluids the viscosity is not constant. For Power-Law fluids the viscosity varies with the second invariant of the strain rate tensor and introduces further nonlinearity in case of Navier-Stokes equations. Fluids for which, the viscosity decreases with increase in shear rate, are called shear-thinning fluids and they have Power-Law index less than unity. Fluids with Power-Law index greater than unity are called shear-thickening. Padhye and Reddy [54] worked on penalty finite element model for axisymmetric flows of non-Newtonian fluids. Padhye and Reddy also solved unsteady, plane and axisymmetric flows of Power-Law and viscoelastic fluids using penalty finite element models. For Power-Law fluids they used both velocity formulation and mixed formulation. Iga and Reddy [55] applied it to the free surface flows of Power-Law fluids. Finite element models based on the velocity-pressure (and stress) formulation for flows of incompressible, viscous, Power-Law fluids in axisymmetric or plane flows were developed by many authors ([56]-[65]). But most of them evaluated the viscosity based on latest known values of the velocities (lagging velocities). This is generally called linearization before minimization of Least-square functional. Even though this gave correct numerical results, it is not in accordance with the principles of mathematics.

For Least-Squares especially, the velocity-stress formulation is very attractive for the use in conjunction with Non-Newtonian fluids because the stresses are available as unknowns. Publications from Bell and Surana [66], Edgar and Surana [67], Surana and others ([68]-[71]), analyze this application of the Least-Squares formulation. They do not

use any linearization techniques before minimization of the Least-square functional. However the second variation terms of the viscosity are dropped after minimization. This makes the coefficient matrix symmetric and hence robust iterative solvers can be employed to solve the algebraic equations. Newton's Method with Line-Search is employed to improve the convergence rate. Dropping the second variation of the viscous terms, reduces the complexity of the problem and is believed drastically improve the rate of convergence. Some say it only alters the direction of search, but no mathematical reasoning given in any of the papers. Others consider it more or less a heuristic approach, which seems to work through the general robustness of the LSFEM. From the mathematical point of view it is not clear, if that approach works or converges under all circumstances.

In [67] the equations of the axisymmetric case are examined, while [66] uses the two-dimensional form in Cartesian coordinates. The constitutive equation for the fluid is a Power-Law that leads to a nonlinear variation of governing equations. In [66] this model is enriched by the energy equation, which models the heat transfer inside the fluid. Two interdependencies between the fluid and the temperature field are modeled. The viscosity depends on the temperature and the heat is generated by viscous dissipation. Both papers present a shear flow, a driven cavity and a sudden expansion as numerical examples for the non-Newtonian fluid. A driven cavity flow is used as the test case for isothermal case. A shear flow and a sudden contraction are the test cases for the non-isothermal coupled model. For higher polynomial degrees the results are in good agreement with analytical solutions or benchmark problems. The results are only

compared with the bench mark solutions for Newtonian cases as they are the only ones available in literature. For non-Newtonian case there are no available results for the bench mark problems.

Research Objectives

For Newtonian fluids the viscosity is constant and generally the convective terms are linearized by lagging velocities (u , v). This method is called linearization before minimization. Though this method gave good results in many (Least-square) cases, this is not in accordance with the principles of mathematics. In Least-Squares formulation, there are no studies on the effects of linearization (before and after minimization) on the convergence of Newtonian fluids. For Newtonian fluids, as only convective terms are nonlinear, it is quite simple to linearize them, but it is not easy and some times not possible to linearize (without dropping some terms) for Power-Law fluids due to the non linearity of the viscous terms. One simple way is to linearize both convective and viscous terms before minimization (which is not mathematically correct). The other way is to linearize after minimization of the Least-square functional. For non-Newtonian fluids, too, there are no studies on the effects of linearizations (before and after minimization) on the accuracy and convergence of the solution. Most work on Power-Law fluids is done on the stress based Navier-Stokes equations; Least-Squares formulation for vorticity based Power-Law fluids has not been explored yet. Also there has been no work on the weak form Galerkin formulation using the Reduced Integration Penalty method (RIP) for Power-Law fluids. The objectives can be summarized as below:

- (i) To study the effects of linearization before and after minimization for Newtonian fluids.
- (ii) To formulate the Least-Squares finite element model for Power-Law fluids and study the effects of linearization before and after minimization.
- (iii) To formulate the weak form Galerkin formulation using Reduced Integration Penalty method (RIP) for Power-Law fluids and compare it with Least-Squares formulations.

Procedure

Newtonian Fluids

- (i) Formulate Least-Squares finite element model (LSFEM) for Poisson's equation and verify the LSFEM procedure using a manufactured flow problem. Study the effects of p -refinement on the accuracy and convergence of solution.
- (ii) Formulate the vorticity based LSFEM for steady state, incompressible, Navier-Stokes equations in two-dimensions. Study the effects of linearization before and after minimization on the accuracy and convergence by using the Kovasznay flow. Also perform a p -refinement study on the same.
- (iii) Formulate the stress based LSFEM for steady state, incompressible, Navier-Stokes equations in two-dimensions. Study the effects of linearization before and after minimization on the accuracy and convergence of solution. Also perform a p -refinement study on the same.

Non-Newtonian Fluids (Power-Law)

(iv) Formulate the stress based LSFEM for steady state, incompressible, Navier-Stokes equations in two-dimensions with variable viscosity as per Power-Law model. Study the effects of linearization before and after minimization on the accuracy and convergence by using 2D lid-driven cavity flow. Also study any possible occurrences of 'locking' phenomenon.

(v) Formulate the vorticity based LSFEM for steady state, incompressible, Navier-Stokes equations in two-dimensions with variable viscosity as per Power-Law model. Study the effects of linearization before and after minimization on the accuracy and convergence by using 2D lid-driven cavity flow. Also study any possible occurrences of 'locking' phenomenon.

(vi) Formulate the weak form Galerkin finite element model using Reduced Integration Penalty (RIP) method for steady state, incompressible, Navier-Stokes equations in two-dimensions with variable viscosity as per Power-Law model using 2D lid-driven cavity flow. Also study any possible occurrences of 'locking' phenomenon.

CHAPTER II

LEAST-SQUARES FORMULATION FOR POISSON'S EQUATION

Introduction

In this chapter the Poisson's equation is considered to explain the Least-Squares finite element method (LSFEM), the iterative solving procedures, and applications to numerical problems. The Poisson equation can be written as:

$$-\nabla^2 \phi = f \text{ in } \Omega, \quad (2.1)$$

$$\phi = \phi^s \text{ on } \Gamma_\phi, \quad (2.2)$$

$$\hat{n} \cdot \nabla \phi = q_n^s \text{ on } \Gamma_q \quad (2.3)$$

where $\Gamma = \Gamma_\phi \cup \Gamma_q$ and $\phi = \Gamma_\phi \cap \Gamma_q$, f is the source term, \hat{n} is the outward unit normal on the boundary of Ω , ϕ^s is the prescribed value of ϕ on the boundary Γ_ϕ , and q_n^s is the prescribed normal flux on the boundary Γ_q .

The Least-Squares variational principle could be directly applied to the above equation, but this requires continuous higher order differentiable spaces and hence the LSFEM does not provide any computational advantage over traditional weak form Galerkin method. To fully harness the power of LSFEM, the above equations are cast in first-order equivalent system as below:

$$-\nabla \cdot \mathbf{V} = f \text{ in } \Omega, \quad (2.4)$$

$$\nabla \phi - V = 0 \text{ in } \Omega, \quad (2.5)$$

$$\phi = \phi^s \text{ on } \Gamma_\phi, \quad (2.6)$$

$$\hat{n} \cdot \nabla \phi = q_n^s \text{ on } \Gamma_q \quad (2.7)$$

Least-Squares Formulation

The Least-Squares functional associated with the above set over a typical element Ω^e is:

$$I(\phi, V, f) = \frac{1}{2} \int_{\Omega^e} \left[(-\nabla \cdot V - f)^2 + (\nabla \phi - V)^2 \right] d\Omega \quad (2.8)$$

and the necessary condition for the minimum of I is:

$$\delta I(\phi, V, f) = \int_{\Omega^e} \left[(-\nabla \cdot V - f)(-\nabla \cdot \delta V) + (\nabla \phi - V) \cdot (\nabla \delta \phi - \delta V) \right] d\Omega = 0 \quad (2.9)$$

The variational problem associated with the above functional is obtained from the minimization condition $\delta I = 0$. It can be stated as: find (ϕ, V) in a suitable vector space for all $(\delta \phi, \delta V)$ in the same vector space such that the following equation holds:

$$B((\phi, V), (\delta \phi, \delta V)) = l(\delta \phi, \delta V) \quad (2.10)$$

where $B((\phi, V), (\delta \phi, \delta V)) = \int_{\Omega^e} \left[(-\nabla \cdot V)(-\nabla \cdot \delta V) + (\nabla \phi - V) \cdot (\nabla \delta \phi - \delta V) \right] d\Omega$ is the bilinear form and $l(\delta \phi, \delta V) = \int_{\Omega^e} \left[(f)(-\nabla \cdot \delta V) \right] d\Omega$ is the linear form. The first variation

in two-dimensions can be expressed as:

$$\delta I(\phi, V, f) = \int_{\Omega} \left[\left(-\frac{\partial u}{\partial x} - \frac{\partial v}{\partial y} - f \right) \left(-\frac{\partial \delta u}{\partial x} - \frac{\partial \delta v}{\partial y} \right) + \left(\frac{\partial \phi}{\partial x} - u \right) \left(\frac{\partial \delta \phi}{\partial x} - \delta u \right) + \left(\frac{\partial \phi}{\partial y} - v \right) \left(\frac{\partial \delta \phi}{\partial y} - \delta v \right) \right] d\Omega = 0 \quad (2.11)$$

where (u, v) are the horizontal and vertical components of V .

Collecting the similar variational terms and applying the fundamental lemma of calculus of variation the above is equivalent to the following integral statements:

$$\int_{\Omega} \left[\left(\frac{\partial \phi}{\partial x} - u \right) \left(\frac{\partial \delta \phi}{\partial x} \right) + \left(\frac{\partial \phi}{\partial y} - v \right) \left(\frac{\partial \delta \phi}{\partial y} \right) \right] d\Omega = 0 \quad (2.12)$$

$$\int_{\Omega} \left[\left(-\frac{\partial u}{\partial x} - \frac{\partial v}{\partial y} - f \right) \left(-\frac{\partial \delta u}{\partial x} \right) + \left(\frac{\partial \phi}{\partial x} - u \right) (-\delta u) \right] d\Omega = 0 \quad (2.13)$$

$$\int_{\Omega} \left[\left(-\frac{\partial u}{\partial x} - \frac{\partial v}{\partial y} - f \right) \left(-\frac{\partial \delta v}{\partial y} \right) + \left(\frac{\partial \phi}{\partial y} - v \right) (-\delta v) \right] d\Omega = 0 \quad (2.14)$$

This can be expressed as bilinear and linear forms as:

$$B((\phi, u, v), (\delta \phi, \delta u, \delta v)) = l(\delta \phi, \delta u, \delta v) \quad (2.15)$$

Finite Element Model

Assuming the approximations of ϕ, u, v as:

$$\phi(\Omega) = \sum_{j=1}^n \phi_j \Psi_j(\Omega), u(\Omega) = \sum_{j=1}^n u_j \Psi_j(\Omega), v(\Omega) = \sum_{j=1}^n v_j \Psi_j(\Omega) \quad (2.16)$$

and substituting in the above integral statements, we obtain the finite element model:

$$\begin{bmatrix} [K^{11}] & [K^{12}] & [K^{13}] \\ [K^{21}] & [K^{22}] & [K^{23}] \\ [K^{31}] & [K^{32}] & [K^{33}] \end{bmatrix} \begin{Bmatrix} \{\phi\} \\ \{u\} \\ \{v\} \end{Bmatrix} = \begin{Bmatrix} \{f^1\} \\ \{f^2\} \\ \{f^3\} \end{Bmatrix} \quad (2.17)$$

In addition, if the $\nabla \times V$ is used as a constraint (to insure the coersivity of the Least-Squares functional) the above integral statements are modified as:

$$\int_{\Omega^e} \left[\left(\frac{\partial \phi}{\partial x} - u \right) \left(\frac{\partial \delta \phi}{\partial x} \right) + \left(\frac{\partial \phi}{\partial y} - v \right) \left(\frac{\partial \delta \phi}{\partial y} \right) \right] d\Omega = 0 \quad (2.18)$$

$$\int_{\Omega^e} \left[\left(-\frac{\partial u}{\partial x} - \frac{\partial v}{\partial y} - f \right) \left(-\frac{\partial \delta u}{\partial x} \right) + \left(\frac{\partial \phi}{\partial x} - u \right) (-\delta u) + \left(\frac{\partial \delta u}{\partial y} \right) \left(\frac{\partial u}{\partial y} - \frac{\partial v}{\partial x} \right) \right] d\Omega = 0 \quad (2.19)$$

$$\int_{\Omega^e} \left[\left(-\frac{\partial u}{\partial x} - \frac{\partial v}{\partial y} - f \right) \left(-\frac{\partial \delta v}{\partial y} \right) + \left(\frac{\partial \phi}{\partial y} - v \right) (-\delta v) + \left(\frac{\partial \delta v}{\partial x} \right) \left(\frac{\partial u}{\partial y} - \frac{\partial v}{\partial x} \right) \right] d\Omega = 0 \quad (2.20)$$

Then the coefficients $[K^{\alpha\beta}]$ can be evaluated and finite element model can be obtained.

The above can be represented as $[K^e \{u^e\}] \{u^e\} = \{f^e\}$. It is to be noted that the coefficient matrix $[K^e]$ in this case is not a function of nodal values, however in other cases it can depend on the unknown nodal primary variables. The present problem is called a linear problem and in cases when coefficient matrix $[K^e]$ depends on unknown nodal primary variables, it is called a nonlinear problem. In this chapter, the iterative procedure for a general nonlinear case is explained and the same can be used for a linear case too. After assembling the above elemental equations the assembled system of equations are obtained. It can be represented as:

$$[K(\{U\})] \{U\} = \{F\} \quad (2.21)$$

where $[K]$ and $\{F\}$ denote the global coefficient matrix and the right-hand side vector respectively. The above algebraic equations can be solved by applying the boundary conditions using iterative procedures explained below.

Numerical Procedures

The numerical procedures used to solve the nonlinear algebraic equations are iterative in nature. In this we begin by assuming that the solution $\{U\}^{(r-1)}$ at the $(r-1)$ st iteration is known, and we wish to seek the solution $\{U\}^{(r)}$ at the r th iteration. At the beginning of the iteration, i.e. when $r=1$, the solution $\{U\}^{(0)}$ is assumed or “guessed” consistent to the problem data. Using the solution $\{U\}^{(r-1)}$ the coefficient matrix $\left[K\left(\{U\}^{(r-1)}\right) \right]$ is computed. Since $[K]$ is evaluated using the estimated vector $\{U\}$, in general $\left[K\left(\{U\}^{(r-1)}\right) \right] \{U\} \neq \{F\}$. Hence we are left with a residual:

$$\{R\} = \left[K\left(\{U\}^{(r-1)}\right) \right] \{U\} - \{F\} \quad (2.22)$$

The objective of the iterative process is to reduce a very small value, negligible value. This can be done by calculating the Euclidean norm between the solutions of two consecutive iterations. There are two popular iterative techniques one is direct-iteration, also known as *Picard iteration* method and other known as *Newton-Raphson* or *Tangent Matrix* method.

The direct iteration method is the simpler of the two methods. In this the solution at r th iteration is determined from the equation:

$$\left[K\left(\{U\}^{(r-1)}\right) \right] \{U\} = \{F\} \quad (2.23)$$

where the coefficient matrix $[K]$ is evaluated using the known solution from the $(r-1)$ st iteration. It is assumed that the coefficient matrix $[K]$ is invertible after the imposition of the boundary conditions. Thus the initial guess vector $\{U\}^{(0)}$ should be such that it satisfies the specified essential boundary conditions and $[K]$ is invertible. The direct iteration converges if the nonlinearity is mild and it diverges if the nonlinearity is severe. Divergence is more likely for hardening type nonlinearity. Acceleration of the convergence may be achieved by using the weighted-average of solutions from last two iterations.

In Newton-Raphson method the residual vector $\{R\} = [K]\{U\} - \{F\} = 0$ is expanded in Taylor's series and the terms of order 2 and higher are omitted to obtain:

$$\left(\frac{\partial \{R\}}{\partial \{U\}} \right)^{(r-1)} \cdot \{\delta U\} = - \left\{ R \left(\{U\}^{(r-1)} \right) \right\} \quad (2.24)$$

$$\left[T \left(\{U\}^{(r-1)} \right) \right] \cdot \{\delta U\} = - \left\{ R \left(\{U\}^{(r-1)} \right) \right\} \quad (2.25)$$

where $[T]$ is the *tangent matrix* given by:

$$\left[T \left(\{U\}^{(r-1)} \right) \right] \equiv \left(\frac{\partial \{R\}}{\partial \{U\}} \right)^{(r-1)} \quad (2.26)$$

The component definition of the tangent matrix at the element level is:

$$T_{ij}^e \equiv \frac{\partial R_i^e}{\partial u_i^e} = \sum_{m=1}^n \frac{\partial K_{im}^e}{\partial u_i^e} u_m^e + K_{ij}^e \quad (2.27)$$

and the residual vector after the $(r-1)$ st iteration is given by:

$$-\left\{\mathbf{R}\left(\left\{\mathbf{U}\right\}^{(r-1)}\right)\right\}=\left\{\mathbf{F}\right\}-\left[\mathbf{K}\left(\left\{\mathbf{U}\right\}^{(r-1)}\right)\right]\left\{\mathbf{U}\right\}^{(r-1)} \quad (2.28)$$

The finite element model for an element can be represented as:

$$\begin{bmatrix} [T^{11}] & [T^{12}] & [T^{13}] \\ [T^{21}] & [T^{22}] & [T^{23}] \\ [T^{31}] & [T^{32}] & [T^{33}] \end{bmatrix} \begin{Bmatrix} \{\Delta\phi\} \\ \{\Delta u\} \\ \{\Delta v\} \end{Bmatrix} = \begin{Bmatrix} \{R^1\} \\ \{R^2\} \\ \{R^3\} \end{Bmatrix} \quad (2.29)$$

The solution at the r th iteration is then given by:

$$\left\{\mathbf{U}\right\}^{(r)}=\left\{\mathbf{U}\right\}^{(r-1)}+\left\{\delta \mathbf{U}\right\} \quad (2.30)$$

The Newton-Raphson method converges for hardening as well as softening type nonlinearities. For hardening type the convergence may be accelerated by using the weighted-averages of the solutions of last two iterations. More details about these two methods can be found in the book on nonlinear finite element analysis by Dr. Reddy [72]. In this chapter direct iteration method is used to solve the Poisson's equation. And since it is a linear problem the coefficient matrix $[\mathbf{K}]$ is independent of the solution of $(r-1)$ st iteration. Hence the direct iteration procedure converges in first iteration itself. Also both the coefficient matrices for direct iteration and for Newton-Raphson method will be one and the same. The Newton-Raphson method is used in the coming chapters on non-Newtonian fluid flows.

Numerical Example

To verify the LSFEM formulation, a manufactured solution [15] of the Poisson equation in (2.1) is considered:

$$\phi(x, y) = (7x + x^7) \cos \pi y, -1 < x, y < +1 \quad (2.31)$$

over a square domain of as shown in Figure 1. Substitution of the above equation into original Poisson equation (2.1) yields:

$$f(x, y) = -\nabla^2 \phi = (7\pi^2 x - 42x^5 + \pi^2 x^7) \cos \pi y \quad (2.32)$$

We also have

$$u(x, y) \equiv \frac{\partial \phi}{\partial x} = 7(1 + x^6) \cos \pi y, v(x, y) \equiv \frac{\partial \phi}{\partial y} = -\pi(7x + x^7) \sin \pi y \quad (2.33)$$

Thus, the following boundary conditions can be imposed on the square domain:

$$u(-1, y) = 14 \cos \pi y, v(x, \pm 1) = 0, \phi(1, y) = 8 \cos \pi y \quad (2.34)$$

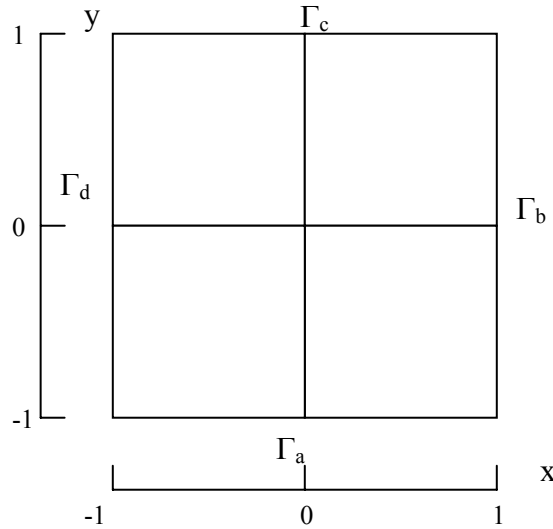


Figure 1. A uniform mesh of four elements on which the poisson problem is defined

The above problem is solved by direct-iteration method with order of polynomials ranging from P=2 to P=7. The coefficient matrix is evaluated using a

Gaussian quadrature of $(P+1)$ in both the co-ordinate directions. The Reynolds number Re is fixed as 1000 for all the cases. Convergence is declared when the Euclidean norm is less than 10^{-3} , which typically took 5-7 iterations.

Results

For $P=2$, the program did not give correct results when compared to the exact solution. For $P=3$, the results were better compared to the previous case. For $P=5$, the results matched the exact solution for all the variables. And, for $P=7$, there was hardly any improvement in the solution compared to the previous case. The accuracy of the solution can be noted from the figures. Figure 2 and Figure 3 show the velocity vector profile and velocity contour profile over the domain for polynomial order of $P=5$.

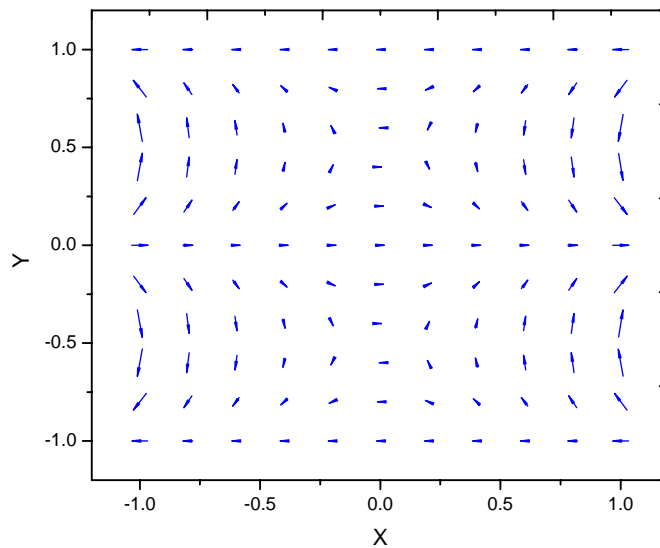


Figure 2. Velocity vector profile for polynomial order of $P=5$

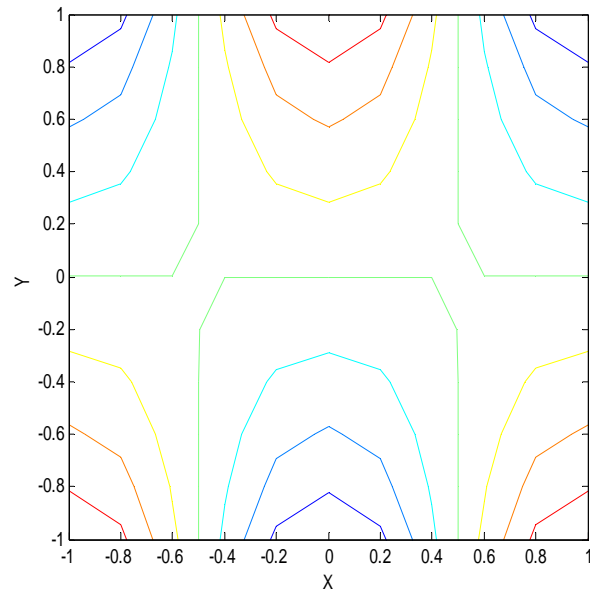


Figure 3.Velocity contour plot for polynomial order of P=5

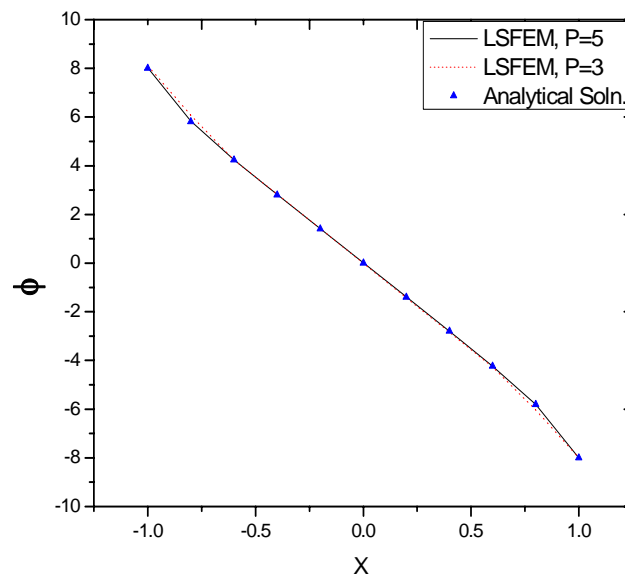


Figure 4.Comparison of primary variable ϕ for P=3 and 5 with analytical solution at Y=-1.0

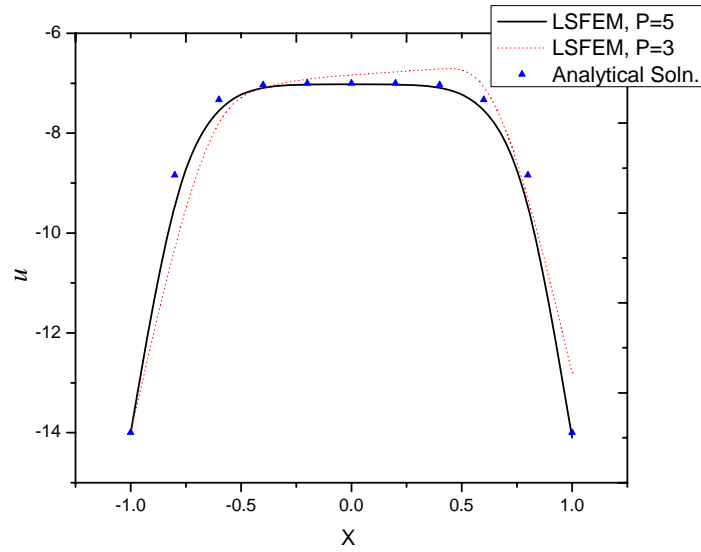


Figure 5. Comparison of primary variable u for $P=3$ and 5 with analytical solution at $Y=-1.0$

Figure 4 and Figure 5 show the comparison of primary variables ϕ and u for $P=3$ and $P=5$ with analytical solution at $Y=-1.0$. Figure 6 shows the comparison of primary variable v for $P=3$ and $P=5$ with analytical solution at $Y=-0.8$.

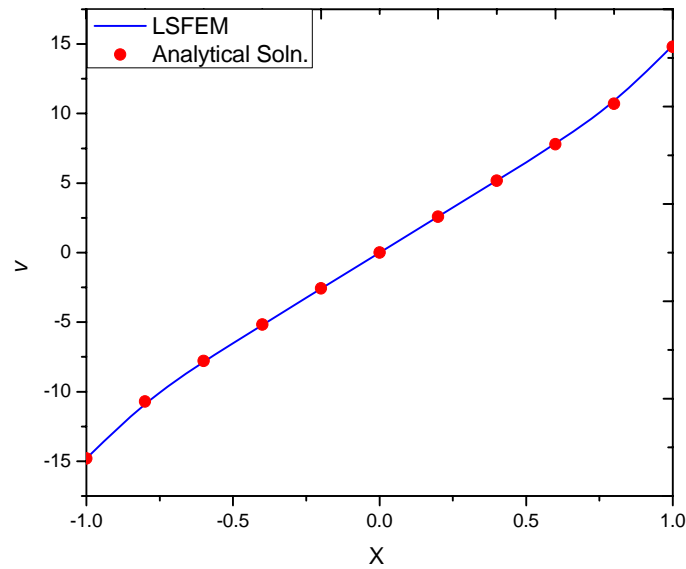


Figure 6. Comparison of primary variable v for $P=3$ and 5 with analytical solution at $Y=-0.8$

Conclusions

From the above results we can conclude that as the order of polynomial approximation functions is increased, the numerical solution becomes more and more close to the exact solution. As the dimension of the approximation spaces (i.e. P is varied from 2 to 7) is increased in the finite element method, it gets more and closer to the dimension of the solution space to the exact differential equation, hence the solution becomes accurate.

CHAPTER III

LEAST-SQUARES FORMULATION OF VORTICITY BASED FIRST-ORDER SYSTEM FOR NEWTONIAN FLUIDS

Introduction

As seen in the previous chapter the Least-Squares method has the property of minimizing the residuals in the differential equations. For the Stokes and Navier-Stokes equations, which have no underlying minimum principles, the Least-Squares method provides a variational framework. The main ideas of the Least-Squares method are described using the steady Stokes flow problem, which can be represented in vector form as:

$$\nabla \cdot V = 0 \text{ in } \Omega, \quad (3.1)$$

$$-\mu \nabla \cdot [(\nabla V) + (\nabla V)^T] + \nabla p = \rho_0 f \text{ in } \Omega, \quad (3.2)$$

$$V = V^s \text{ on } \Gamma_v, \quad (3.3)$$

$$\hat{n} \cdot \sigma = f^s \text{ on } \Gamma_f \quad (3.4)$$

where $\Gamma = \Gamma_v \cup \Gamma_f$ and $\phi = \Gamma_v \cap \Gamma_f$, f is the force term, \hat{n} is the outward unit normal on the boundary of Ω , μ is the viscosity of the fluid,

$\sigma = -(p)I - 2\mu [(\nabla V) + (\nabla V)^T]$, V^s is the prescribed value of velocity on the

boundary, and f^s is the prescribed value of tractions on the boundary Γ_f . Now choosing

the approximation functions for (p, V) as,

$$p(x, y) = \sum_{j=1}^n p_j \Psi_j(x, y), V(x, y) = \sum_{j=1}^n V_j \Psi_j(x, y),$$

and substituting in the governing equations results in residuals:

$$R_1 = \nabla \cdot V \quad (3.5)$$

$$R_2 = -\mu \nabla \cdot \left[(\nabla V) + (\nabla V)^T \right] + \nabla p - \rho_0 f \quad (3.6)$$

The Least-Squares functional associated with the above set over a typical element Ω^e is:

$$I(p, V) = \frac{1}{2} \int_{\Omega^e} \left[(R_1)^2 + (R_2)^2 \right] d\Omega \quad (3.7)$$

The variational problem associated with the above functional is obtained from the minimization condition $\delta I = 0$. It can be stated as: find (p, V) in a suitable vector space for all $(\delta p, \delta V)$ in the same vector space such that the following equation holds:

$$B((p, V), (\delta p, \delta V)) = l(\delta p, \delta V) \quad (3.8)$$

where $B(\bullet, \bullet)$ is a *bilinear form* [i.e., an expression that is linear in (p, V) as well as $(\delta p, \delta V)$] and $l(\bullet)$ is a *linear form* [in $(\delta p, \delta V)$], defined by:

$$B((p, V), (\delta p, \delta V)) = \int_{\Omega^e} \left(-\mu \nabla \cdot \left[(\nabla V) + (\nabla V)^T \right] + \nabla p \right) \cdot \left(-\mu \nabla \cdot \left[(\nabla \delta V) + (\nabla \delta V)^T \right] + \nabla \delta p \right) d\Omega + \int_{\Omega^e} (\nabla \cdot V)(\nabla \cdot \delta V) d\Omega \quad (3.9)$$

$$l(p, \delta V) = \int_{\Omega^e} \rho_0 f \cdot \left\{ -\mu \nabla \cdot \left[(\nabla \delta V) + (\nabla \delta V)^T \right] + \nabla \delta p \right\} d\Omega \quad (3.10)$$

This variational problem has some mathematical and computational advantages. For example, the coefficient matrix obtained from the above is symmetric and positive definite. But since, the variational problem is based on the original differential equation rather than on the weak form, it involves same order derivatives as that appearing in the differential equation. And also the variational form does not include the natural boundary terms; hence the approximation functions selected must be such that both the natural and essential boundary conditions can be imposed. This requires use of at Least C^1 -continuous functions for the velocity field. This higher order differentiability requirement is a practical disadvantage. To avoid the use of C^1 -continuous functions the differential equations are cast into equivalent first-order equations. The most common transformation to equivalent first-order system is to introduce the vorticity vector. The total number of variables is increased by one, but there is a benefit of directly solving the vorticity. Yet another approach is to introduce stresses as independent variables. In this case the total number of variables is increased by three. The third approach is to introduce all the partial derivatives of the velocities as independent variables. In two-dimensions the total number of variables is increased by four. But one can easily post-compute any physical quantity from these.

The Vorticity Based First-Order System

In this chapter the vorticity based first-order equations are presented. To write the second-order equations the vorticity vector $\omega = \nabla \times V$ is introduced. By making use of the vector identity $\nabla \times \nabla \times V = -\nabla^2 V + \nabla(\nabla \cdot V)$ and the incompressibility

condition $\nabla \cdot V = 0$, the original equations can be cast as following equivalent first-order equations:

$$\nabla \cdot V = 0 \text{ in } \Omega, \quad (3.11)$$

$$\rho_0 (V \cdot \nabla) V + \nabla p + \mu [\nabla \times \omega] = \rho_0 f \text{ in } \Omega, \quad (3.12)$$

$$\omega - \nabla \times V = 0 \text{ in } \Omega, \quad (3.13)$$

$$\nabla \cdot \omega = 0 \text{ in } \Omega, \quad (3.14)$$

$$V = V^s \text{ on } \Gamma_v, \quad (3.15)$$

$$\hat{n} \cdot \sigma = f^s \text{ on } \Gamma_\omega \quad (3.16)$$

Typically $\phi = \Gamma_v \cap \Gamma_\omega$, i.e., if velocity is specified at a boundary, vorticity need not be specified there.

Least-Squares Formulation

The Least-Squares functional associated with the above first-order system is given by:

$$I(p, V, \omega) = \frac{1}{2} \int_{\Omega^e} \left[(R_1)^2 + (R_2)^2 + (R_3)^2 \right] d\Omega \quad (3.17)$$

where R_1, R_2, R_3 are residuals obtained after substituting the element approximation spaces in the above first-order equations. The variational problem associated with the above functional is obtained from the minimization condition $\delta I = 0$. It can be stated as: find (p, V, ω) in a suitable vector space for all $(\delta p, \delta V, \delta \omega)$ in the same vector space such that the following equation holds:

$$B((p, V, \omega), (\delta p, \delta V, \delta \omega)) = l(\delta p, \delta V, \delta \omega) \quad (3.18)$$

where

$$B((p, V, \omega), (\delta p, \delta V, \delta \omega)) = \int_{\Omega^e} \left[(-\nabla \cdot V)(-\nabla \cdot \delta V) + (\rho_0 (V_0 \cdot \nabla) V + \nabla p + \mu [\nabla \times \omega]) \cdot \left(\rho_0 (V_0 \cdot \nabla) \delta V + \nabla \delta p + \mu [\nabla \times \delta \omega] \right) + (\omega - \nabla \times V) \cdot (\delta \omega - \nabla \times \delta V) \right] d\Omega$$

is the bilinear form and $l(\delta p, \delta V, \delta \omega) = \int_{\Omega^e} \left[(f_0) (\rho_0 (V_0 \cdot \nabla) \delta V + \nabla \delta p + \mu [\nabla \times \delta \omega]) \right] d\Omega$

is the linear form. Note here V_0 is assumed to be known from previous iteration, i.e., it is linearized before minimization.

Finite Element Model

In two dimensions the above equations in dimensionless form can be written as:

$$\frac{\partial u}{\partial x} + \frac{\partial v}{\partial y} = 0 \quad \text{in } \Omega \quad (3.19)$$

$$u \frac{\partial u}{\partial x} + v \frac{\partial u}{\partial y} + \frac{\partial p}{\partial x} + \frac{1}{\text{Re}} \frac{\partial \omega}{\partial y} = f_x \quad \text{in } \Omega \quad (3.20)$$

$$u \frac{\partial v}{\partial x} + v \frac{\partial v}{\partial y} + \frac{\partial p}{\partial y} - \frac{1}{\text{Re}} \frac{\partial \omega}{\partial y} = f_y \quad \text{in } \Omega \quad (3.21)$$

$$\omega + \frac{\partial u}{\partial y} - \frac{\partial v}{\partial x} = 0 \quad \text{in } \Omega \quad (3.22)$$

$$V = V^s \quad \text{on } \Gamma_v, \quad (3.23)$$

$$\hat{n} \cdot \sigma = f^s \quad \text{on } \Gamma_\omega \quad (3.24)$$

where $Re = \rho_0 VL / \mu$ is the Reynolds number. Note that in two-dimensions the vorticity vector is $\omega = (0, 0, \omega)$ i.e. it has component only in Z-direction. The following finite element approximation functions for (p, V, ω) can be chosen:

$$\begin{aligned} p(x, y) &= \sum_{j=1}^n p_j \Psi_j(x, y), u(x, y) = \sum_{j=1}^n u_j \Psi_j(x, y), \\ v(x, y) &= \sum_{j=1}^n v_j \Psi_j(x, y), \omega(x, y) = \sum_{j=1}^n \omega_j \Psi_j(x, y) \end{aligned} \quad (3.25)$$

where Ψ_j are the Lagrange family interpolation functions. The minimum requirement on approximation functions is that they all be Lagrange family of C^0 -continuity. Since the formulation is based on variational frame work there are no compatibility restrictions between velocity and pressure approximation spaces, so same Lagrange basis can be used for all primary variables (p, V, ω) . Substituting them in the governing equations results in residuals:

$$R_1 = \frac{\partial u}{\partial x} + \frac{\partial v}{\partial y} \quad (3.26)$$

$$R_2 = u \frac{\partial u}{\partial x} + v \frac{\partial u}{\partial y} + \frac{\partial p}{\partial x} + \frac{1}{Re} \frac{\partial \omega}{\partial y} - f_x \quad (3.27)$$

$$R_3 = u \frac{\partial v}{\partial x} + v \frac{\partial v}{\partial y} + \frac{\partial p}{\partial y} - \frac{1}{Re} \frac{\partial \omega}{\partial x} - f_y \quad (3.28)$$

$$R_4 = \omega + \frac{\partial u}{\partial y} - \frac{\partial v}{\partial x} \quad (3.29)$$

The Least-Squares functional associated with the above set over a typical element Ω^e with the residuals is:

$$I(p, V, \omega) = \frac{1}{2} \int_{\Omega^e} [(R_1)^2 + (R_2)^2 + (R_3)^2 + (R_4)^2] d\Omega \quad (3.30)$$

By minimization of the Least-Squares functional with nodal values of velocities, pressure, and vorticity, we obtain:

$$\delta I = \frac{\partial I}{\partial p} \delta p + \frac{\partial I}{\partial u} \delta u + \frac{\partial I}{\partial v} \delta v + \frac{\partial I}{\partial \omega} \delta \omega = 0 \quad (3.31)$$

which yields four sets of ‘n’ equations each over a typical element:

$$\frac{\partial I}{\partial p} \delta p = 0, \frac{\partial I}{\partial u} \delta u = 0, \frac{\partial I}{\partial v} \delta v = 0, \frac{\partial I}{\partial \omega} \delta \omega = 0 \quad (3.32)$$

The finite element model after substituting the approximation spaces is of the form shown below:

$$\begin{bmatrix} [K^{11}] [K^{12}] [K^{13}] [K^{14}] \\ [K^{21}] [K^{22}] [K^{23}] [K^{24}] \\ [K^{31}] [K^{32}] [K^{33}] [K^{34}] \\ [K^{41}] [K^{42}] [K^{43}] [K^{44}] \end{bmatrix} \begin{Bmatrix} \{p\} \\ \{u\} \\ \{v\} \\ \{\omega\} \end{Bmatrix} = \begin{Bmatrix} \{f^1\} \\ \{f^2\} \\ \{f^3\} \\ \{f^4\} \end{Bmatrix} \quad (3.33)$$

Note that the elemental equation $[K^e \{u^e\}] \{u^e\} = \{f^e\}$ cannot be solved until they are assembled and the boundary conditions are imposed.

In developing the finite element model, two cases have been considered. In the first case the convective terms in the residuals associated with the momentum equations are linearized before taking the minimum of the functional (this is not in consistent with the principles of mathematics). Here they are taken to be known from previous iteration. This amounts to linearization of Least-Squares functional before minimization. This kind

of linearization can be found in references ([15] and [73]). In this case the residuals become:

$$R_2 = u_0 \frac{\partial u}{\partial x} + v_0 \frac{\partial u}{\partial y} + \frac{\partial p}{\partial x} + \frac{1}{\text{Re}} \frac{\partial \omega}{\partial y} - f_x \quad (3.34)$$

$$R_3 = u_0 \frac{\partial v}{\partial x} + v_0 \frac{\partial v}{\partial y} + \frac{\partial p}{\partial y} - \frac{1}{\text{Re}} \frac{\partial \omega}{\partial x} - f_y \quad (3.35)$$

where (u_0, v_0) are known from previous iteration. Hence their variational is taken to be zero in minimization step. In the other case minimization precedes the linearization (this is believed to be consistent with the principles of mathematics). In this chapter only direct iteration procedure is used to solve the assembled algebraic system of equations. The results for both the cases are compared using the numerical example below.

Numerical Example

A two-dimensional steady flow in $\bar{\Omega} = [-0.5, 1.5] \times [-0.5, 1.5]$ as shown in the Figure 7 is considered. The figure shows the discretization of the domain using 2×4 mesh. The Kovasznay's exact solution [38] for stationary incompressible Navier-Stokes equation is given by:

$$u = 1 - e^{\lambda x} \cos(2\pi y), v = \frac{\lambda}{2\pi} e^{\lambda x} \sin(2\pi y), p = \frac{1}{2}(1 - e^{2\lambda x}) \quad (3.36)$$

where $\lambda = \text{Re}/2 - (\text{Re}^2/4 + 4\pi^2)^{1/2}$. A Reynolds number of 40 is used for this case. The exact solution is used to compute the velocity boundary conditions on Γ and pressure is specified at a point. No boundary conditions on vorticity are necessary.

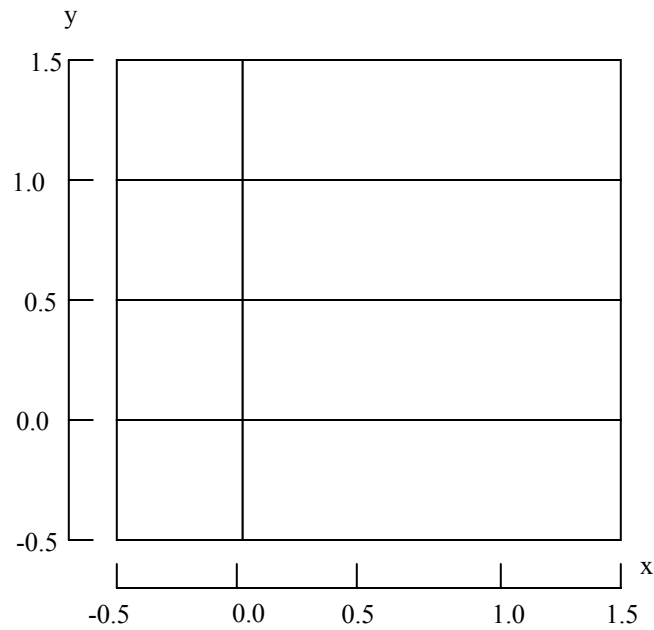


Figure 7. Computational domain using eight rectangular elements

The above problem is solved by direct-iteration method with order of polynomials ranging from $P=2$ to $P=7$. The coefficient matrix is evaluated using a Gaussian quadrature of $(P+1)$ in both the co-ordinate directions. The Reynolds number Re is fixed as 1000 for all the cases. Convergence is declared when the Euclidean norm is less than 10^{-3} , which typically took 5-7 iterations.

Results

For $P=2$, the program did not give correct results when compared to the exact solution. For $P=3$, the results were better compared to the previous case. For $P=5$, the results matched the exact solution for all the variables. And, for $P=7$, there was hardly

any improvement in the solution compared to the previous case. Figure 8 and Figure 9 show the isobar profile and velocity contour profile over the domain for polynomial order of $P=3$.

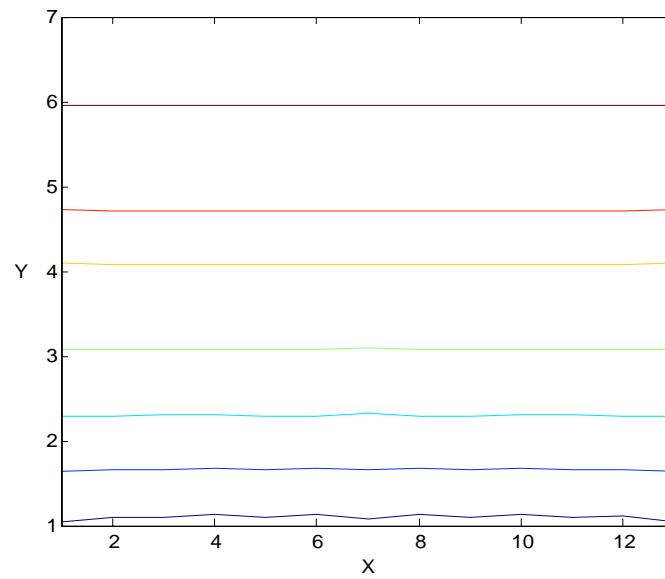


Figure 8. Isobars over the domain for $P=3$

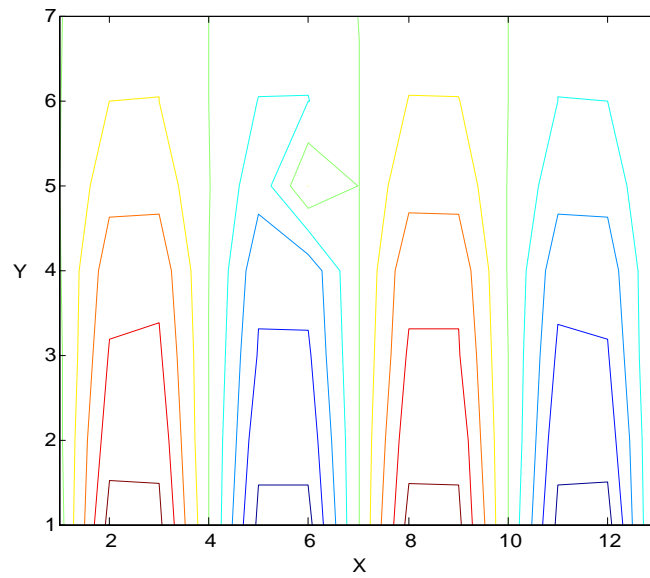


Figure 9. Velocity contour plot for polynomial order of $P=3$

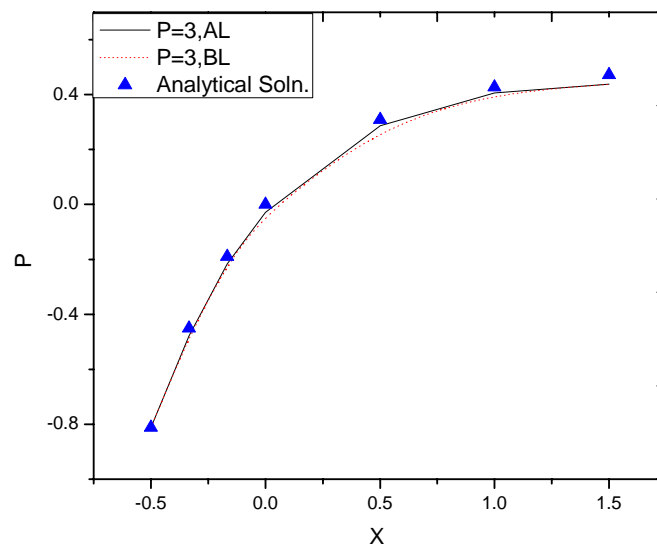


Figure 10. Comparison of pressure p for $P=3$ for linearization before (BL) and after (AL) minimization cases with analytical solution at $Y=-0.5$

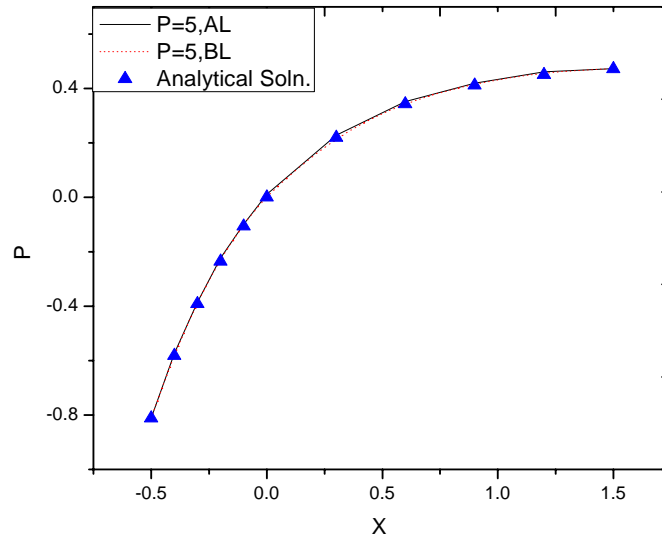


Figure 11. Comparison of pressure p for $P=5$ for linearization before (BL) and after (AL) minimization cases with analytical solution at $Y=-0.5$

Figure 10 and Figure 11 show the comparison of pressure p for $P=3$ and $P=5$ for linearization before (BL) and after (AL) minimization cases with analytical solution at $Y=-0.5$. Figure 12 and Figure 13 show the comparison of horizontal velocity u for $P=3$ and $P=5$ for linearization before (BL) and after (AL) minimization cases with analytical solution at $Y=-0.5$.

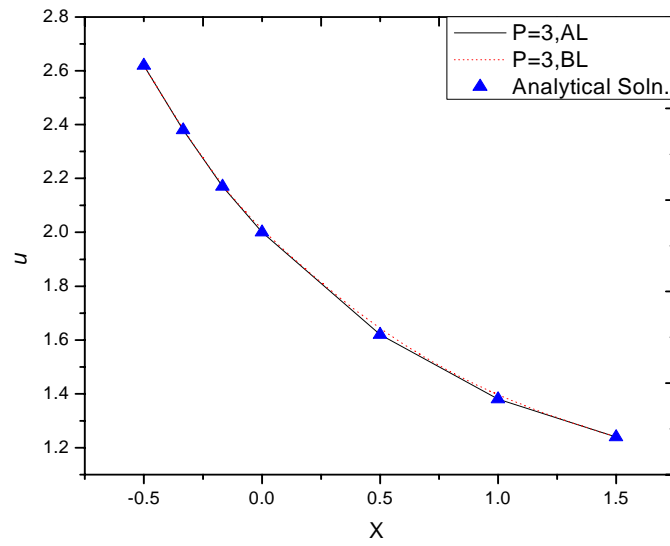


Figure 12. Comparison of horizontal velocity u for $P=3$ for linearization before (BL) and after (AL) minimization cases with analytical solution at $Y=-0.5$

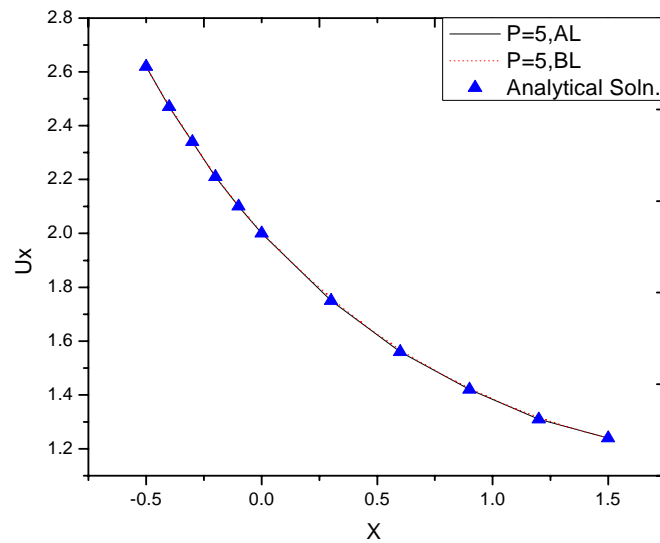


Figure 13. Comparison of horizontal velocity u for $P=5$ for linearization before (BL) and after (AL) minimization cases with analytical solution at $Y=-0.5$

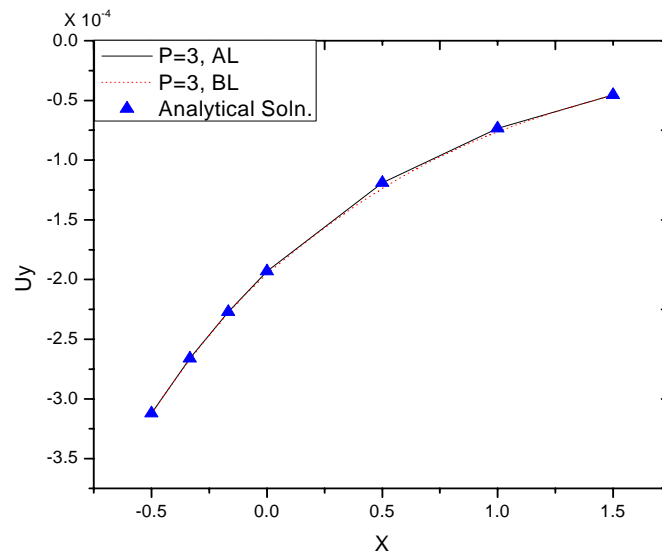


Figure 14. Comparison of vertical velocity v for $P=3$ for linearization before (BL) and after (AL) minimization cases with analytical solution at $Y=-0.5$

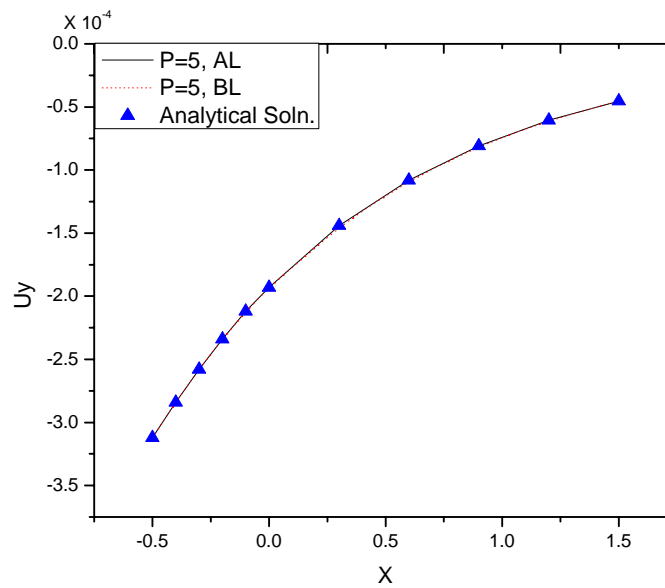


Figure 15. Comparison of vertical velocity v for $P=5$ for linearization before (BL) and after (AL) minimization cases with analytical solution at $Y=-0.5$

Figure 14 and Figure 15 show the comparison of vertical velocity v for $P=3$ and $P=5$ for linearization before (BL) and after (AL) minimization cases with analytical solution at $Y=-0.5$. The accuracy of the solution can be noted from the figures. In all the cases there is hardly any difference in the solution for linearization before and after minimization cases.

Conclusions

From the above results we can conclude that there is almost a negligible effect of linearization before and after minimization on the accuracy of the solution. And in both the cases it took almost the same number of iterations to converge, hence we can conclude that it has no impact on the rate of convergence of the iterative process. As explained in the previous chapter as the order of polynomial approximation functions is increased, the numerical solutions became more and more close to the exact solutions. Also there is no phenomenon of locking for both the cases considered.

CHAPTER IV

LEAST-SQUARES FORMULATION OF STRESS BASED FIRST-ORDER SYSTEM FOR NEWTONIAN FLUIDS

Introduction

Vorticity based Least-Squares formulation is the most popular first order formulation for the solution of Stokes and Navier-Stokes equations since only one additional independent variable is introduced in two-dimensions compared to three in stress based formulation and four in velocity-flux formulation. In this chapter the stress based first-order equations are presented. In the present chapter two kinds of stress based Least-Squares finite element methods are considered, one carries six independent variables and other carries five independent variables. In the latter case, continuity equation becomes an algebraic equation and is eliminated from the system of governing equations with suitable modifications. The effects of linearization before and after minimization are studied for both the formulations using suitable numerical examples.

To define the equivalent first-order velocity-pressure-stress system, stress tensor $\Gamma = \left[(\nabla V) + (\nabla V)^T \right]$ (symmetric part of velocity gradient tensor) is introduced as auxiliary variables. The Navier-Stokes flow can be represented in vector form as:

$$\nabla \cdot V = 0 \text{ in } \Omega, \quad (4.1)$$

$$(V \cdot \nabla)V + \nabla p - \frac{1}{\text{Re}} \nabla \cdot \Gamma = f \text{ in } \Omega, \quad (4.2)$$

$$\Gamma - \left[(\nabla V) + (\nabla V)^T \right] = 0 \text{ in } \Omega, \quad (4.3)$$

$$V = V^s \text{ on } \Gamma_v, \quad (4.4)$$

$$\hat{n} \cdot \Gamma = \Gamma^s \text{ on } \Gamma_\Gamma \quad (4.5)$$

where $\Gamma = \Gamma_v \cup \Gamma_\Gamma$ and $\phi = \Gamma_v \cap \Gamma_\Gamma$, f is the force term, \hat{n} is the outward unit normal on the boundary of Ω , Re is the Reynolds number of fluid, V^s is the prescribed value of velocity on the boundary Γ_v , and Γ^s is the prescribed value of tractions on the boundary Γ_Γ .

Least-Squares Formulation

The Least-Squares functional associated with the above first-order system is given by:

$$I(p, V, \Gamma) = \frac{1}{2} \int_{\Omega} \left[(R_1)^2 + (R_2)^2 + (R_3)^2 \right] d\Omega \quad (4.6)$$

where R_1, R_2, R_3 are residuals obtained after substituting the element approximation spaces in the above first-order equations. The variational problem associated with the above functional is obtained from the minimization condition $\delta I = 0$. It can be stated as: find (p, V, Γ) in a suitable vector space for all $(\delta p, \delta V, \delta \Gamma)$ in the same vector space such that the following equation holds:

$$B((p, V, \Gamma), (\delta p, \delta V, \delta \Gamma)) = l(\delta p, \delta V, \delta \Gamma) \quad (4.7)$$

where

$$B((p, V, \Gamma), (\delta p, \delta V, \delta \Gamma)) = \int_{\Omega} \left[\begin{aligned} & (-\nabla \cdot V)(-\nabla \cdot \delta V) + \left((V_0 \cdot \nabla) V + \nabla p - \frac{1}{\text{Re}} \nabla \cdot \Gamma \right) \cdot \left((V_0 \cdot \nabla) \delta V + \nabla \delta p - \frac{1}{\text{Re}} \nabla \cdot \delta \Gamma \right) \\ & + \left(\Gamma - [(\nabla V) + (\nabla V)^T] \right) \cdot \left(\delta \Gamma - [(\nabla \delta V) + (\nabla \delta V)^T] \right) \end{aligned} \right] d\Omega$$

is the bilinear form and $l(\delta p, \delta V, \delta \omega) = \int_{\Omega} \left[(f_0) \left((V_0 \cdot \nabla) \delta V + \nabla \delta p - \frac{1}{\text{Re}} \nabla \cdot \delta \Gamma \right) \right] d\Omega$ is

the linear form. Note here V_0 is assumed to be known from previous iteration, i.e., it is linearized before minimization. The governing equations for two-dimensional case are given by:

$$\frac{\partial u}{\partial x} + \frac{\partial v}{\partial y} = 0 \quad \text{in } \Omega \quad (4.8)$$

$$u \frac{\partial u}{\partial x} + v \frac{\partial u}{\partial y} + \frac{\partial p}{\partial x} - \left(\frac{\partial \Gamma_{xx}}{\partial x} + \frac{\partial \Gamma_{xy}}{\partial y} \right) = f_x \quad \text{in } \Omega \quad (4.9)$$

$$u \frac{\partial v}{\partial x} + v \frac{\partial v}{\partial y} + \frac{\partial p}{\partial y} - \left(\frac{\partial \Gamma_{xy}}{\partial x} + \frac{\partial \Gamma_{yy}}{\partial y} \right) = f_y \quad \text{in } \Omega \quad (4.10)$$

$$\Gamma_{xx} - 2\mu \frac{\partial u}{\partial x} = 0 \quad \text{in } \Omega \quad (4.11)$$

$$\Gamma_{xy} - \mu \left(\frac{\partial u}{\partial y} + \frac{\partial v}{\partial x} \right) = 0 \quad \text{in } \Omega \quad (4.12)$$

$$\Gamma_{yy} - 2\mu \frac{\partial v}{\partial y} = 0 \quad \text{in } \Omega \quad (4.13)$$

$$V = V^s \quad \text{on } \Gamma_V, \quad (4.14)$$

$$\hat{n} \cdot \Gamma = \Gamma^s \quad \text{on } \Gamma_\Gamma \quad (4.15)$$

Like before, we can describe the variational problem by minimizing the above functional with respect to chosen approximation spaces. The minimum requirement on approximation functions is that they all be Lagrange family of C^0 -continuity. Since the formulation is based on variational frame work there are no compatibility restrictions between velocity, pressure and stress approximation spaces, so same Lagrange basis can be used for all primary variables $(p, V, \Gamma_{xx}, \Gamma_{xy}, \Gamma_{yy})$.

Method I

In 2D the above equations in dimensionless form [33] can be written as:

$$\frac{\partial u}{\partial x} + \frac{\partial v}{\partial y} = 0 \text{ in } \Omega \quad (4.16)$$

$$u \frac{\partial u}{\partial x} + v \frac{\partial u}{\partial y} + \frac{\partial p}{\partial x} - \frac{1}{\text{Re}} \left(\frac{\partial \Gamma_{xx}}{\partial x} + \frac{\partial \Gamma_{xy}}{\partial y} \right) = f_x \text{ in } \Omega \quad (4.17)$$

$$u \frac{\partial v}{\partial x} + v \frac{\partial v}{\partial y} + \frac{\partial p}{\partial y} - \frac{1}{\text{Re}} \left(\frac{\partial \Gamma_{xy}}{\partial x} + \frac{\partial \Gamma_{yy}}{\partial y} \right) = f_y \text{ in } \Omega \quad (4.18)$$

$$\Gamma_{xx} - 2 \frac{\partial u}{\partial x} = 0 \text{ in } \Omega \quad (4.19)$$

$$\Gamma_{xy} - \left(\frac{\partial u}{\partial y} + \frac{\partial v}{\partial x} \right) = 0 \text{ in } \Omega \quad (4.20)$$

$$\Gamma_{yy} - 2 \frac{\partial v}{\partial y} = 0 \text{ in } \Omega \quad (4.21)$$

$$V = V^s \text{ on } \Gamma_v \quad (4.22)$$

$$\hat{n} \cdot \Gamma = \Gamma^s \text{ on } \Gamma_\Gamma \quad (4.23)$$

The Least-Squares functional associated with the above set over a typical element Ω^e with the residuals is:

$$I(p, V, \Gamma_{xx}, \Gamma_{xy}, \Gamma_{yy}) = \frac{1}{2} \int_{\Omega^e} \left[(R_1)^2 + (R_2)^2 + (R_3)^2 + (R_4)^2 + (R_5)^2 + (R_6)^2 \right] d\Omega \quad (4.24)$$

where

$$R_1 = \frac{\partial u}{\partial x} + \frac{\partial v}{\partial y} \quad (4.25)$$

$$R_2 = u \frac{\partial u}{\partial x} + v \frac{\partial u}{\partial y} + \frac{\partial p}{\partial x} - \frac{1}{\text{Re}} \left(\frac{\partial \Gamma_{xx}}{\partial x} + \frac{\partial \Gamma_{xy}}{\partial y} \right) - f_x \quad (4.26)$$

$$R_3 = u \frac{\partial v}{\partial x} + v \frac{\partial v}{\partial y} + \frac{\partial p}{\partial y} - \frac{1}{\text{Re}} \left(\frac{\partial \Gamma_{xy}}{\partial x} + \frac{\partial \Gamma_{yy}}{\partial y} \right) - f_y \quad (4.27)$$

$$R_4 = \Gamma_{xx} - 2 \frac{\partial u}{\partial x} \quad (4.28)$$

$$R_5 = \Gamma_{xy} - \left(\frac{\partial u}{\partial y} + \frac{\partial v}{\partial x} \right) \quad (4.29)$$

$$R_6 = \Gamma_{yy} - 2 \frac{\partial v}{\partial y} \quad (4.30)$$

and the primary variables $(p, V, \Gamma_{xx}, \Gamma_{xy}, \Gamma_{yy})$ are approximated by the expansions of the form:

$$\begin{aligned} p(x, y) &= \sum_{j=1}^n p_j \Psi_j(x, y), u(x, y) = \sum_{j=1}^n u_j \Psi_j(x, y), \\ v(x, y) &= \sum_{j=1}^n v_j \Psi_j(x, y), \Gamma_{xx}(x, y) = \sum_{j=1}^n \Gamma_{xx,j} \Psi_j(x, y) \\ \Gamma_{xy}(x, y) &= \sum_{j=1}^n \Gamma_{xy,j} \Psi_j(x, y), \Gamma_{yy}(x, y) = \sum_{j=1}^n \Gamma_{yy,j} \Psi_j(x, y) \end{aligned} \quad (4.31)$$

where ψ_j are the Lagrange family interpolation functions.

Finite Element Model

By minimization of the Least-Squares functional with nodal values of velocities, pressure, and stresses, we obtain:

$$\delta I = \frac{\partial I}{\partial p} \delta p + \frac{\partial I}{\partial u} \delta u + \frac{\partial I}{\partial v} \delta v + \frac{\partial I}{\partial \Gamma_{xx}} \delta \Gamma_{xx} + \frac{\partial I}{\partial \Gamma_{xy}} \delta \Gamma_{xy} + \frac{\partial I}{\partial \Gamma_{yy}} \delta \Gamma_{yy} = 0 \quad (4.32)$$

which yields six sets of 'n' equations each over a typical element:

$$\frac{\partial I}{\partial p} \delta p = 0, \frac{\partial I}{\partial u} \delta u = 0, \frac{\partial I}{\partial v} \delta v = 0, \frac{\partial I}{\partial \Gamma_{xx}} \delta \Gamma_{xx} = 0, \frac{\partial I}{\partial \Gamma_{xy}} \delta \Gamma_{xy} = 0, \frac{\partial I}{\partial \Gamma_{yy}} \delta \Gamma_{yy} = 0 \quad (4.33)$$

The finite element model after substituting the approximation spaces is of the form shown below:

$$\begin{bmatrix} [K^{11}] [K^{12}] [K^{13}] [K^{14}] [K^{15}] [K^{16}] \\ [K^{21}] [K^{22}] [K^{23}] [K^{24}] [K^{25}] [K^{26}] \\ [K^{31}] [K^{32}] [K^{33}] [K^{34}] [K^{35}] [K^{36}] \\ [K^{41}] [K^{42}] [K^{43}] [K^{44}] [K^{45}] [K^{46}] \\ [K^{51}] [K^{52}] [K^{53}] [K^{54}] [K^{55}] [K^{56}] \\ [K^{61}] [K^{62}] [K^{63}] [K^{64}] [K^{65}] [K^{66}] \end{bmatrix} \begin{Bmatrix} \{p\} \\ \{u\} \\ \{v\} \\ \{\Gamma_{xx}\} \\ \{\Gamma_{xy}\} \\ \{\Gamma_{yy}\} \end{Bmatrix} = \begin{Bmatrix} \{f^1\} \\ \{f^2\} \\ \{f^3\} \\ \{f^4\} \\ \{f^5\} \\ \{f^6\} \end{Bmatrix} \quad (4.34)$$

Note that the elemental equation $[K^e \{u^e\}] \{u^e\} = \{f^e\}$ cannot be solved until they are assembled and the boundary conditions are imposed.

In developing the finite element model, two cases have been considered. In the first case the convective terms in the residuals associated with the momentum equations are linearized before taking the minimum of the functional (this is not in consistent with

the principles of mathematics). Here they are taken to be known from previous iteration. This amounts to linearization of Least-Squares functional before minimization. This kind of linearization can be found in references ([15]-[73]). In this case the residuals become:

$$R_2 = u_0 \frac{\partial u}{\partial x} + v_0 \frac{\partial u}{\partial y} + \frac{\partial p}{\partial x} - \frac{1}{\text{Re}} \left(\frac{\partial \Gamma_{xx}}{\partial x} + \frac{\partial \Gamma_{xy}}{\partial y} \right) - f_x \quad (4.35)$$

$$R_3 = u_0 \frac{\partial v}{\partial x} + v_0 \frac{\partial v}{\partial y} + \frac{\partial p}{\partial y} - \frac{1}{\text{Re}} \left(\frac{\partial \Gamma_{xy}}{\partial x} + \frac{\partial \Gamma_{yy}}{\partial y} \right) - f_y \quad (4.36)$$

where (u_0, v_0) are known from previous iteration. Hence their variational is taken to be zero in minimization step. In the other case minimization precedes the linearization (this is believed to be consistent with the principles of mathematics). In this chapter only direct iteration procedure is used to solve the assembled algebraic system of equations.

Numerical Example

The ‘lid-driven’ cavity is a standard test problem in the computational fluid dynamics. The problem is characterized by a square cavity in which the driving force for the flow is the shear created by the lid. Figure 16 shows a schematic of the cavity with the boundary conditions and the finite element discretization.

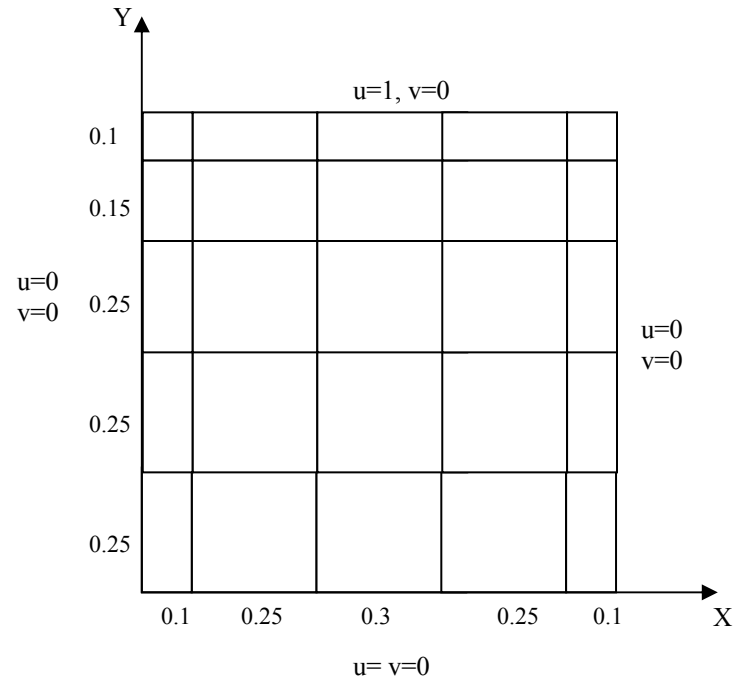


Figure 16. Computational domain using graded 25 rectangular elements

The above problem is solved by direct-iteration method with order of polynomials ranging from $P=2$ to $P=7$. The coefficient matrix is evaluated using a Gaussian quadrature of $(P+1)$ in both the co-ordinate directions. The Reynolds number Re is fixed as 1000 for all the cases. Convergence is declared when the Euclidean norm is less than 10^{-3} , which typically took 5-7 iterations.

Results

For $P=2$, the program did not give correct results when compared to the benchmark solution. For $P=3$, the results were better compared to the previous case. For $P=5$, the results matched the exact solution for all the variables. And, for $P=7$, there was hardly any improvement in the solution compared to the previous case.

Case-I (Linearization before Minimization)

Figure 17 shows the plots of horizontal velocity u at $X=0.5$ with $P=5$ using. Figure 18 shows the plots of vertical velocity v at $Y=0.5$ with $P=5$.

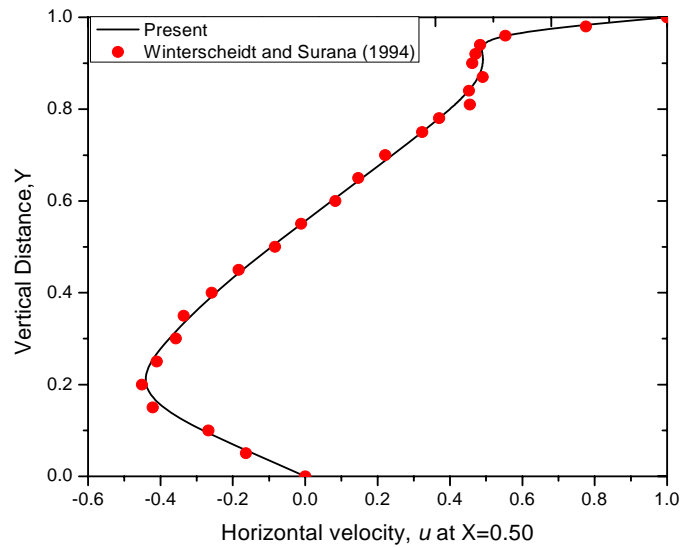


Figure 17. Plots of horizontal velocity u at $X=0.5$ with $P=5$ for linearization before minimization case

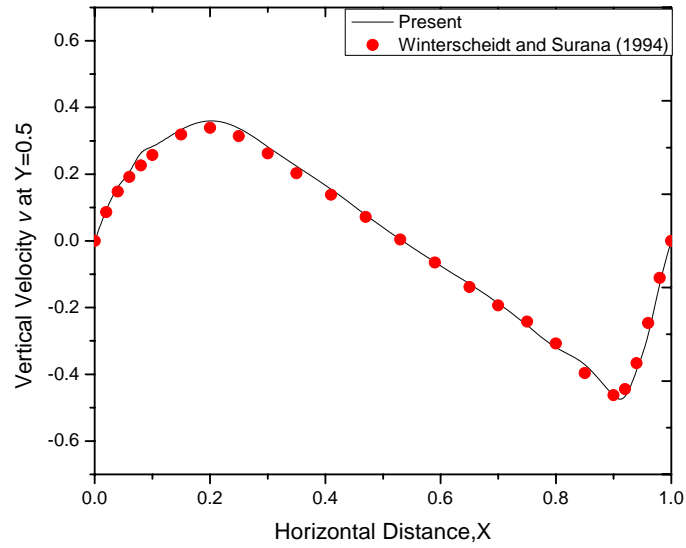


Figure 18. Plots of vertical velocity v at $Y=0.5$ with $P=5$ for linearization before minimization case

Case-II (Linearization after Minimization)

Figure 19 shows the plots of horizontal velocity u at $X=0.5$ with $P=5$ using.

Figure 20 shows the plots of vertical velocity v at $Y=0.5$ with $P=5$.

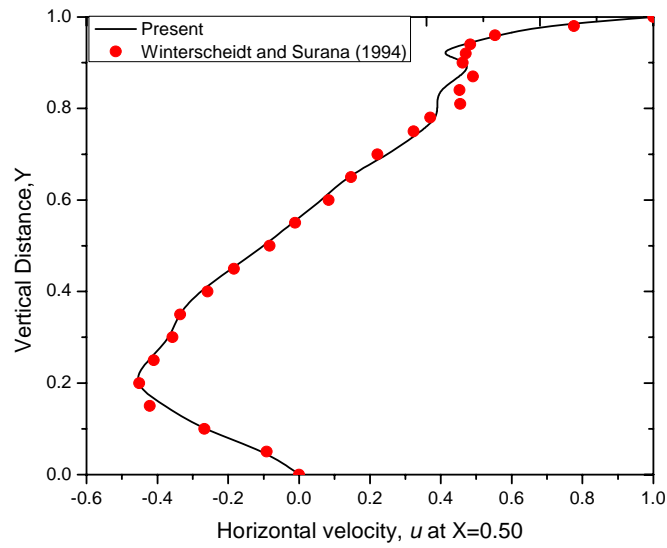


Figure 19. Plots of horizontal velocity u at $X=0.5$ with $P=5$ for linearization after minimization case

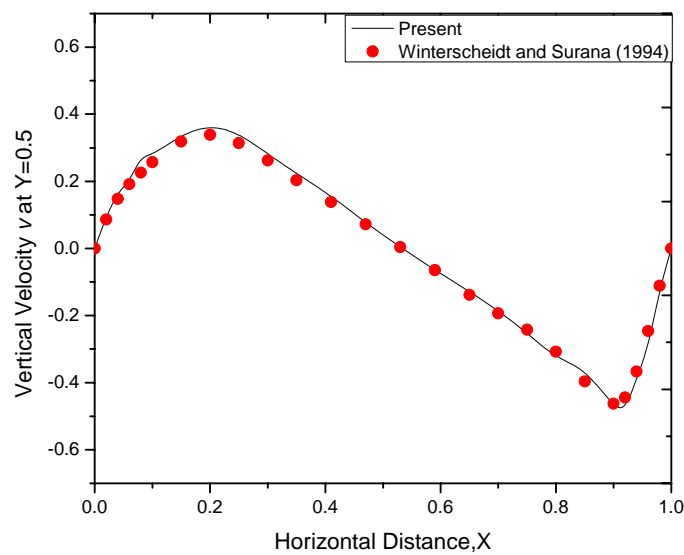


Figure 20. Plots of vertical velocity v at $Y=0.5$ with $P=5$ for linearization after minimization case

The accuracy of the solution can be noted from the figures. In all the above cases there is hardly any difference in the solution for linearization before and after minimization cases.

Method II

From the previous method the continuity equation can be written as:

$$\frac{\partial u}{\partial x} + \frac{\partial v}{\partial y} = 0 \text{ in } \Omega \quad (4.37)$$

$$\Rightarrow \Gamma_{xx} = -\Gamma_{yy} \quad (4.38)$$

Hence the continuity equation can be eliminated and Γ_{yy} is replaced by $-\Gamma_{xx}$ in the governing equations. The equivalent first-order system of equations can be represented in two-dimensions as:

$$u \frac{\partial u}{\partial x} + v \frac{\partial u}{\partial y} + \frac{\partial p}{\partial x} - \frac{1}{\text{Re}} \left(\frac{\partial \Gamma_{xx}}{\partial x} + \frac{\partial \Gamma_{xy}}{\partial y} \right) = f_x \text{ in } \Omega \quad (4.39)$$

$$u \frac{\partial v}{\partial x} + v \frac{\partial v}{\partial y} + \frac{\partial p}{\partial y} - \frac{1}{\text{Re}} \left(\frac{\partial \Gamma_{xy}}{\partial x} + \frac{\partial \Gamma_{yy}}{\partial y} \right) = f_y \text{ in } \Omega \quad (4.40)$$

$$\Gamma_{xx} - 2 \frac{\partial u}{\partial x} = 0 \text{ in } \Omega \quad (4.41)$$

$$\Gamma_{xy} - \left(\frac{\partial u}{\partial y} + \frac{\partial v}{\partial x} \right) = 0 \text{ in } \Omega \quad (4.42)$$

$$-\Gamma_{xx} - 2 \frac{\partial v}{\partial y} = 0 \text{ in } \Omega \quad (4.43)$$

$$V = V^s \text{ on } \Gamma_v, \quad (4.44)$$

$$\hat{n} \cdot \Gamma = \Gamma^s \text{ on } \Gamma_\Gamma \quad (4.45)$$

The Least-Squares functional associated with the above set over a typical element Ω^e with the residuals is:

$$I(p, V, \Gamma_{xx}, \Gamma_{xy}) = \frac{1}{2} \int_{\Omega^e} \left[(R_1)^2 + (R_2)^2 + (R_3)^2 + (R_4)^2 + (R_5)^2 \right] d\Omega \quad (4.46)$$

where

$$R_1 = u \frac{\partial u}{\partial x} + v \frac{\partial u}{\partial y} + \frac{\partial p}{\partial x} - \frac{1}{\text{Re}} \left(\frac{\partial \Gamma_{xx}}{\partial x} + \frac{\partial \Gamma_{xy}}{\partial y} \right) - f_x \quad (4.47)$$

$$R_2 = u \frac{\partial v}{\partial x} + v \frac{\partial v}{\partial y} + \frac{\partial p}{\partial y} - \frac{1}{\text{Re}} \left(\frac{\partial \Gamma_{xy}}{\partial x} + \frac{\partial \Gamma_{yy}}{\partial y} \right) - f_y \quad (4.48)$$

$$R_3 = \Gamma_{xx} - 2 \frac{\partial u}{\partial x} \quad (4.49)$$

$$R_4 = \Gamma_{xy} - \left(\frac{\partial u}{\partial y} + \frac{\partial v}{\partial x} \right) \quad (4.50)$$

$$R_5 = -\Gamma_{xx} - 2 \frac{\partial v}{\partial y} \quad (4.51)$$

and the primary variables $(p, V, \Gamma_{xx}, \Gamma_{xy})$ are approximated by the expansions of the form

$$\begin{aligned} p(x, y) &= \sum_{j=1}^n p_j \Psi_j(x, y), u(x, y) = \sum_{j=1}^n u_j \Psi_j(x, y), \\ v(x, y) &= \sum_{j=1}^n v_j \Psi_j(x, y), \Gamma_{xx}(x, y) = \sum_{j=1}^n \Gamma_{xxj} \Psi_j(x, y) \\ \Gamma_{xy}(x, y) &= \sum_{j=1}^n \Gamma_{xyj} \Psi_j(x, y) \end{aligned} \quad (4.52)$$

where Ψ_j are the Lagrange family interpolation functions.

Finite Element Model

By minimization of the Least-Squares functional with nodal values of velocities, pressure, and vorticity, we obtain

$$\delta I = \frac{\partial I}{\partial u} \delta u + \frac{\partial I}{\partial v} \delta v + \frac{\partial I}{\partial p} \delta p + \frac{\partial I}{\partial \Gamma_{xx}} \delta \Gamma_{xx} + \frac{\partial I}{\partial \Gamma_{xy}} \delta \Gamma_{xy} = 0 \quad (4.53)$$

which yields five sets of 'n' equations each over a typical element:

$$\frac{\partial I}{\partial p} \delta p = 0, \frac{\partial I}{\partial u} \delta u = 0, \frac{\partial I}{\partial v} \delta v = 0, \frac{\partial I}{\partial \Gamma_{xx}} \delta \Gamma_{xx} = 0, \frac{\partial I}{\partial \Gamma_{xy}} \delta \Gamma_{xy} = 0 \quad (4.54)$$

The finite element model after substituting the approximation spaces is of the form shown below:

$$\begin{bmatrix} [K^{11}] [K^{12}] [K^{13}] [K^{14}] [K^{15}] [K^{16}] \\ [K^{21}] [K^{22}] [K^{23}] [K^{24}] [K^{25}] [K^{26}] \\ [K^{31}] [K^{32}] [K^{33}] [K^{34}] [K^{35}] [K^{36}] \\ [K^{41}] [K^{42}] [K^{43}] [K^{44}] [K^{45}] [K^{46}] \\ [K^{51}] [K^{52}] [K^{53}] [K^{54}] [K^{55}] [K^{56}] \end{bmatrix} \begin{Bmatrix} \{p\} \\ \{u\} \\ \{v\} \\ \{\Gamma_{xx}\} \\ \{\Gamma_{xy}\} \end{Bmatrix} = \begin{Bmatrix} \{f^1\} \\ \{f^2\} \\ \{f^3\} \\ \{f^4\} \\ \{f^5\} \end{Bmatrix} \quad (4.55)$$

Note that the elemental equation $[K^e \{u^e\}] \{u^e\} = \{f^e\}$ cannot be solved until they are assembled and the boundary conditions are imposed.

In developing the finite element model, two cases have been considered. In the first case the convective terms in the residuals associated with the momentum equations are linearized before taking the minimum of the functional (this is not in consistent with the theories of mathematics). Here they are taken to be known from previous iteration. This amounts to linearization of Least-Squares functional before minimization. In this case the residuals become:

$$R_1 = u_0 \frac{\partial u}{\partial x} + v_0 \frac{\partial u}{\partial y} + \frac{\partial p}{\partial x} - \frac{1}{\text{Re}} \left(\frac{\partial \Gamma_{xx}}{\partial x} + \frac{\partial \Gamma_{xy}}{\partial y} \right) - f_x \quad (4.56)$$

$$R_2 = u_0 \frac{\partial v}{\partial x} + v_0 \frac{\partial v}{\partial y} + \frac{\partial p}{\partial y} - \frac{1}{\text{Re}} \left(\frac{\partial \Gamma_{xy}}{\partial x} + \frac{\partial \Gamma_{yy}}{\partial y} \right) - f_y \quad (4.57)$$

where (u_0, v_0) are known from previous iteration. Hence their variational is taken to be zero in minimization step. In the other case minimization precedes the linearization (this is believed to be consistent with the principles of mathematics). In this chapter only direct iteration procedure is used to solve the assembled algebraic system of equations.

Numerical Example

A two-dimensional steady flow in $\bar{\Omega} = [-0.5, 1.5] \times [-0.5, 1.5]$ as shown in the Figure 21 is considered. The figure shows the discretization of the domain using 2×4 mesh. The Kovasznay's exact solution [38] for stationary incompressible Navier-Stokes equation is given by:

$$u = 1 - e^{\lambda x} \cos(2\pi y), v = \frac{\lambda}{2\pi} e^{\lambda x} \sin(2\pi y), p = \frac{1}{2}(1 - e^{2\lambda x}) \quad (4.58)$$

where $\lambda = \text{Re}/2 - (\text{Re}^2/4 + 4\pi^2)^{1/2}$. A Reynolds number of 40 is used for this case. The exact solution is used to compute the velocity boundary conditions on Γ and pressure is specified at a point. No boundary conditions on vorticity are necessary.

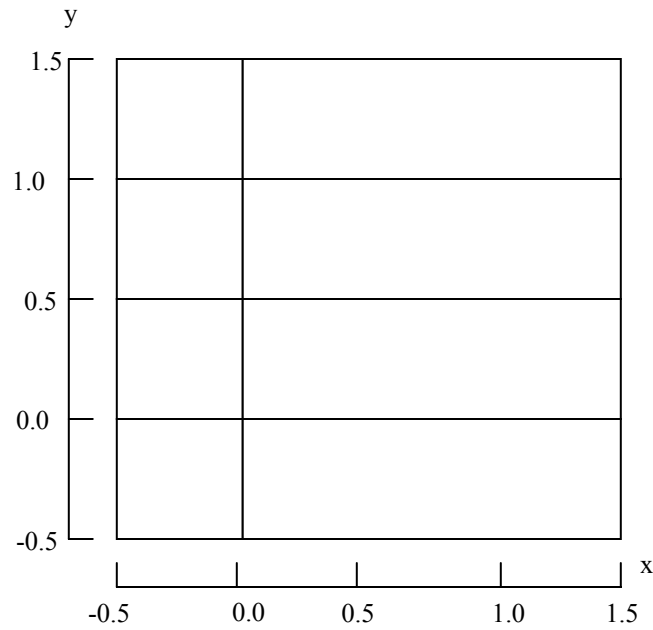


Figure 21. Computational domain using 2x4 rectangular elements

The above problem is solved by direct-iteration method with order of polynomials ranging from $P=2$ to $P=7$. The coefficient matrix is evaluated using a Gaussian quadrature of $(P+1)$ in both the co-ordinate directions. The Reynolds number Re is fixed as 1000 for all the cases. Convergence is declared when the Euclidean norm is less than 10^{-3} , which typically took 5-7 iterations.

Results

For $P=2$, the program did not give correct results when compared to the exact solution. For $P=3$, the results were better compared to the previous case. For $P=5$, the results matched the exact solution for all the variables. And, for $P=7$, there was hardly any improvement in the solution compared to the previous case. Figure 22 and Figure 23

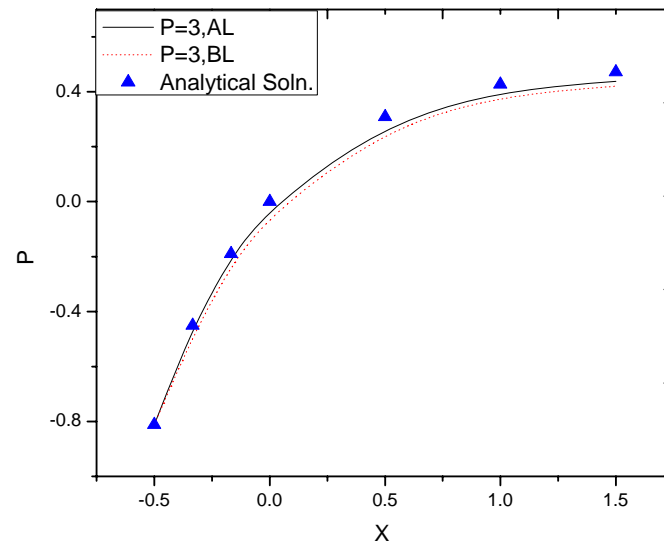


Figure 22. Comparison of pressure p for $P=3$ for linearization before (BL) and after (AL) minimization cases with analytical solution at $Y=-0.5$

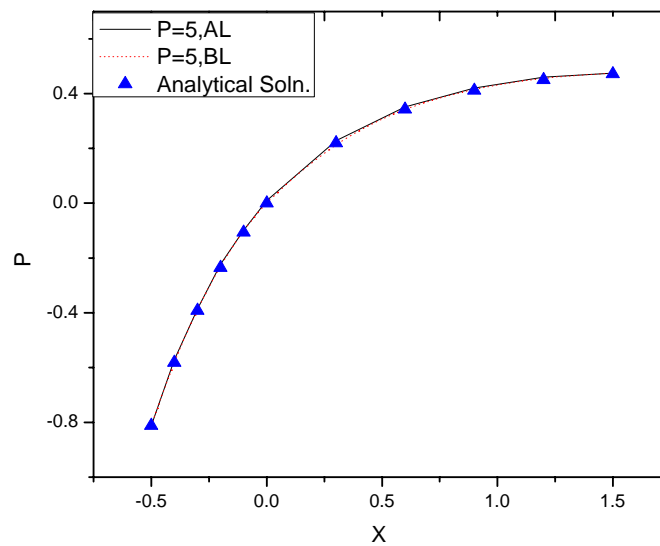


Figure 23. Comparison of pressure p for $P=5$ for linearization before (BL) and after (AL) minimization cases with analytical solution at $Y=-0.5$

show the comparison of pressure p for $P=3$ and $P=5$ for linearization before (BL) and after (AL) minimization cases with analytical solution at $Y=-0.5$. Figure 24 and Figure 25 show the comparison of horizontal velocity u for $P=3$ and $P=5$ for linearization before (BL) and after (AL) minimization cases with analytical solution at $Y=-0.5$.

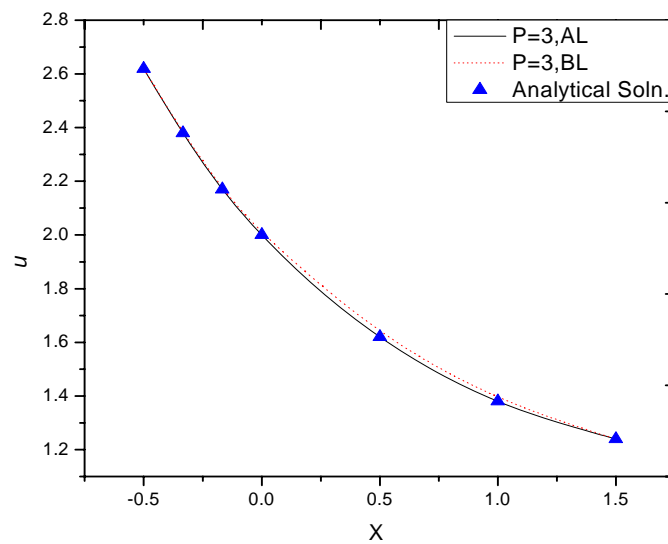


Figure 24. Comparison of horizontal velocity u for $P=3$ for linearization before (BL) and after (AL) minimization cases with analytical solution at $Y=-0.5$

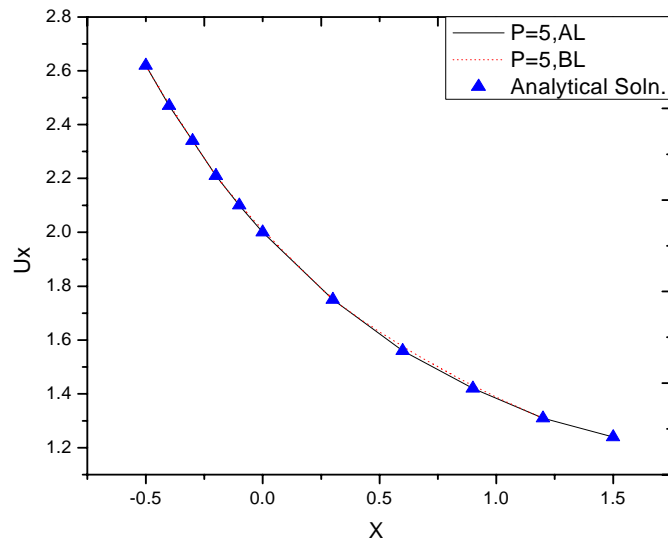


Figure 25. Comparison of horizontal velocity u for $P=5$ for linearization before (BL) and after (AL) minimization cases with analytical solution at $Y=-0.5$

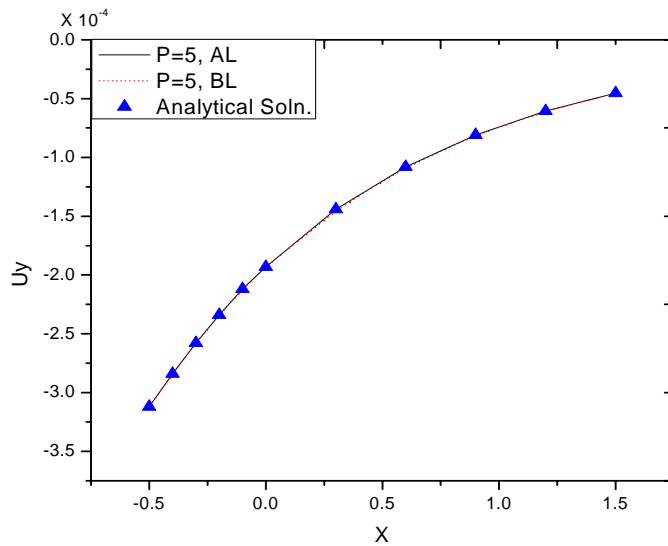


Figure 26. Comparison of vertical velocity v for $P=3$ for linearization before (BL) and after (AL) minimization cases with analytical solution at $Y=-0.5$

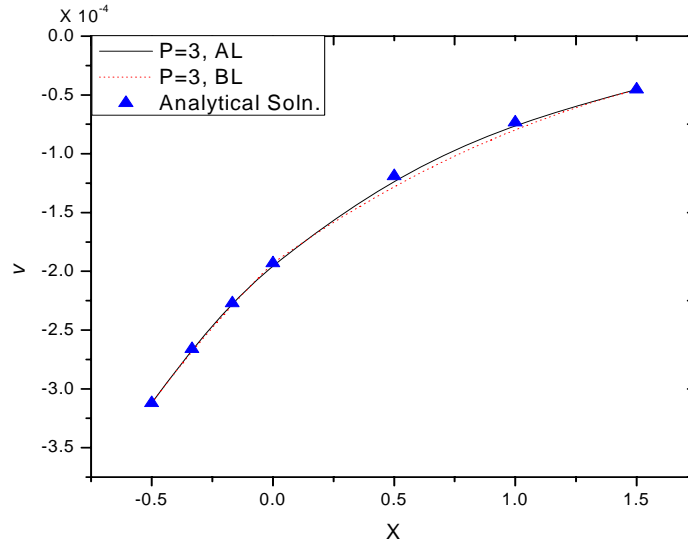


Figure 27. Comparison of vertical velocity v for $P=5$ for linearization before (BL) and after (AL) minimization cases with analytical solution at $Y=-0.5$

Figure 26 and Figure 27 show the comparison of vertical velocity v for $P=3$ and $P=5$ for linearization before (BL) and after (AL) minimization cases with analytical solution at $Y=-0.5$. The accuracy of the solution can be noted from the figures. In all the above cases there is hardly any difference in the solution for linearization before and after minimization cases.

Conclusions

From the above results we can conclude that there is almost a negligible effect of linearization before or after minimization on the accuracy of the solution. And in both the

cases it took almost the same number of iterations to converge, hence we can conclude that it has no impact on the rate of convergence of the iterative process. As explained in the previous chapter as the order of polynomial approximation functions is increased, the numerical solutions became more and more close to the exact solutions. Also there is no phenomenon of locking for both the cases considered.

CHAPTER V

LEAST-SQUARES FORMULATION OF STRESS BASED FIRST-ORDER SYSTEM FOR POWER-LAW FLUIDS

Introduction

Non-Newtonian fluid flows are the most challenging and widely investigated areas in computational fluid mechanics. A non-Newtonian fluid is defined to be the one whose constitutive behavior is nonlinear, i.e. stresses are nonlinear functions of strain rates. If such fluids have the memory of past deformation then they are called viscoelastic fluids. Practical examples of non-Newtonian fluids are multigrade oils, liquid detergents, paints, and printing inks. Polymer solutions and polymer melts also fall within this category. All such flows are extremely important in forming processes of various kinds of applied to metals, plastics, or glass.

Numerical approaches used for analyzing the non-Newtonian fluids differ very little from the ones used for Newtonian fluids. When shear viscosity is a function of rate of deformation tensor (i.e. as in case of Power-Law fluids), the equation of motion can still be explicitly written in terms of velocity components. For such fluids the same formulation as used for Newtonian fluids can be used. The constitutive equations for viscoelastic fluids are described in terms of *extra stress* components and it is not covered in my research.

Power-Law Fluids

Many fluids in industrial applications are characterized by so-called Power-Law constitutive behavior. Power-Law fluids exhibit nonlinear material behavior according to relation:

$$\boldsymbol{\sigma} = \tau - p\mathbf{I}, \quad \tau = 2\mu(I_2)\mathbf{D} \quad (5.1)$$

$$\mu = \mu_0(I_2)^{\frac{(n-1)}{2}} \quad (5.2)$$

$$I_2 = \frac{1}{2} D_{ij} D_{ij} \quad (\text{sum on } i \text{ and } j) \quad (5.3)$$

$$\Rightarrow I_2 = 2\left(\frac{\partial u}{\partial x}\right)^2 + 2\left(\frac{\partial v}{\partial x}\right)^2 + \left(\frac{\partial u}{\partial y} + \frac{\partial v}{\partial x}\right)^2 \text{ in two-dimensions.} \quad (5.4)$$

where τ is the viscous part of the stress tensor $\boldsymbol{\sigma}$, \mathbf{I} is the unit tensor, I_2 is the second invariant of \mathbf{D} , and the parameters μ_0 and n characterize the fluid (have to be determined experimentally). For many non-Newtonian fluids, the viscosity μ decreases with increase in shear rate. These are called shear thinning fluids and for these the Power-Law index $n < 1$. Fluids with Power-Law index $n > 1$ are called shear thickening fluids. For such fluids the viscosity μ increases with increase in shear rate. For $n = 1$ it can be seen that the viscosity $\mu = \mu_0$ (constant) and gives a Newtonian relation. For all other values of n , the Power-Law constitutive relation makes the problem nonlinear even when the convective terms are negligible. In fact the nonlinearity due to Power-Law is more dominant compared to that of the convective terms.

To illustrate how the Power-Law constitutive equation affects the finite element formulation, a steady state, isothermal, incompressible, non-Newtonian fluid is considered. To define the equivalent first-order velocity-pressure-stress system, stress tensor $\Gamma - \mu \left[(\nabla V) + (\nabla V)^T \right] = 0$ (symmetric part of velocity gradient tensor) is introduced as auxiliary variables. The Navier-Stokes flow can be represented in vector form as:

$$\nabla \cdot V = 0 \text{ in } \Omega, \quad (5.5)$$

$$(V \cdot \nabla) V + \nabla p - \nabla \cdot \Gamma = f \text{ in } \Omega, \quad (5.6)$$

$$\Gamma - \mu \left[(\nabla V) + (\nabla V)^T \right] = 0 \text{ in } \Omega, \quad (5.7)$$

$$V = V^s \text{ on } \Gamma_v, \quad (5.8)$$

$$\hat{n} \cdot \Gamma = \Gamma^s \text{ on } \Gamma_r \quad (5.9)$$

where $\Gamma = \Gamma_v \cup \Gamma_r$ and $\phi = \Gamma_v \cap \Gamma_r$, f is the force term, \hat{n} is the outward unit normal on the boundary of Ω , μ is the viscosity of fluid which varies as per Power-Law, V^s is the prescribed value of velocity on the boundary Γ_v , and Γ^s is the prescribed value of tractions on the boundary Γ_r .

Least-Squares Formulation

The Least-Squares functional associated with the above first-order system is given by:

$$I(p, V, \Gamma) = \frac{1}{2} \int_{\Omega^e} \left[(R_1)^2 + (R_2)^2 + (R_3)^2 \right] d\Omega \quad (5.10)$$

where R_1, R_2, R_3 are residuals obtained after substituting the element approximation spaces in the above first-order equations. The variational problem associated with the above functional is obtained from the minimization condition $\delta I = 0$. It can be stated as: find (p, V, Γ) in a suitable vector space for all $(\delta p, \delta V, \delta \Gamma)$ in the same vector space such that the following equation holds:

$$B((p, V, \Gamma), (\delta p, \delta V, \delta \Gamma)) = l(\delta p, \delta V, \delta \Gamma) \quad (5.11)$$

$$B((p, V, \Gamma), (\delta p, \delta V, \delta \Gamma)) = \int_{\Omega^e} (-\nabla \cdot V)(-\nabla \cdot \delta V) + ((V_0 \cdot \nabla)V + \nabla p - \nabla \cdot \Gamma) \cdot$$

where $((V_0 \cdot \nabla)\delta V + (\delta V \cdot \nabla)V_0 + \nabla \delta p - \nabla \cdot \delta \Gamma)$

$$\left(\Gamma - \mu \left[(\nabla V) + (\nabla V)^T \right] \right) \cdot \left(\delta \Gamma - \mu_0 \left[(\nabla \delta V) + (\nabla \delta V)^T \right] - \delta \mu \left[(\nabla V_0) + (\nabla V_0)^T \right] \right) d\Omega$$

is the bilinear form and

$$l(\delta p, \delta V, \delta \omega) = \int_{\Omega^e} \left[(f_0) ((V_0 \cdot \nabla)\delta V + (\delta V \cdot \nabla)V_0 + \nabla \delta p - \nabla \cdot \delta \Gamma) \right] d\Omega \text{ is the linear form.}$$

Note, here linearization of both convective and viscous terms is done after minimization and (V_0, μ_0) are known from previous iteration. And this μ_0 is the value of viscosity calculated based on the previous iteration solution and is different from the μ_0 defined in equation (5.2), which is used to characterize the fluid. And the variation of viscosity is obtained from:

$$\delta \mu = \mu_0 \frac{(n-1)}{2} (I_2)^{\frac{(n-3)}{2}} \delta I_2 \quad (5.12)$$

The governing equations in dimensionless form for two-dimensional case are given by:

$$\frac{\partial \hat{u}}{\partial \hat{x}} + \frac{\partial \hat{v}}{\partial \hat{y}} = 0 \quad \text{in } \Omega \quad (5.13)$$

$$\hat{u} \frac{\partial \hat{u}}{\partial \hat{x}} + \hat{v} \frac{\partial \hat{u}}{\partial \hat{y}} + \frac{\partial \hat{p}}{\partial \hat{x}} - \left(\frac{\partial \hat{\Gamma}_{xx}}{\partial \hat{x}} + \frac{\partial \hat{\Gamma}_{xy}}{\partial \hat{y}} \right) = \hat{f}_x \quad \text{in } \Omega \quad (5.14)$$

$$\hat{u} \frac{\partial \hat{v}}{\partial \hat{x}} + \hat{v} \frac{\partial \hat{v}}{\partial \hat{y}} + \frac{\partial \hat{p}}{\partial \hat{y}} - \left(\frac{\partial \hat{\Gamma}_{xy}}{\partial \hat{x}} + \frac{\partial \hat{\Gamma}_{yy}}{\partial \hat{y}} \right) = \hat{f}_y \quad \text{in } \Omega \quad (5.15)$$

$$\hat{\Gamma}_{xx} - 2\hat{\mu} \frac{\partial \hat{u}}{\partial \hat{x}} = 0 \quad \text{in } \Omega \quad (5.16)$$

$$\hat{\Gamma}_{xy} - \hat{\mu} \left(\frac{\partial \hat{u}}{\partial \hat{y}} + \frac{\partial \hat{v}}{\partial \hat{x}} \right) = 0 \quad \text{in } \Omega \quad (5.17)$$

$$\hat{\Gamma}_{yy} - 2\hat{\mu} \frac{\partial \hat{v}}{\partial \hat{y}} = 0 \quad \text{in } \Omega \quad (5.18)$$

$$\hat{V} = \hat{V}^s \quad \text{on } \hat{\Gamma}_v, \quad (5.19)$$

$$\hat{n} \cdot \hat{\Gamma} = \hat{\Gamma}^s \quad \text{on } \hat{\Gamma}_r \quad (5.20)$$

where $\hat{\mu} = \hat{\mu}_0 \left(\hat{I}_2 \right)^{\frac{(n-1)}{2}}$ is the viscosity and $\hat{I}_2 = 2 \left(\frac{\partial \hat{u}}{\partial x} \right)^2 + 2 \left(\frac{\partial \hat{v}}{\partial x} \right)^2 + \left(\frac{\partial \hat{u}}{\partial y} + \frac{\partial \hat{v}}{\partial x} \right)^2$ is the second invariant.

The above equations can be non dimensionalized in two different forms. The choice of these forms has a dramatic effect on the convergence of the iterative process. These two forms arise as a result of choice of the characteristic scale for stresses. If the characteristic viscous stress $(\mu_0 V_0 / L)$ is chosen to scale the stresses, the Reynolds number appears in the momentum equation. If the characteristic kinetic energy $(\rho_0 V_0^2)$ is used to scale the stresses, the Reynolds number appears in the stress equations. It is

demonstrated by Surana and others that the first choice has undesirable effects which lead to non-convergence of the iterative process or convergence to a spurious solution. The complete details on this can be found in [32]. The Navier-Stokes equation is transformed to:

$$\frac{\partial u}{\partial x} + \frac{\partial v}{\partial y} = 0 \text{ in } \Omega \quad (5.21)$$

$$u \frac{\partial u}{\partial x} + v \frac{\partial u}{\partial y} + \frac{\partial p}{\partial x} - \left(\frac{\partial \Gamma_{xx}}{\partial x} + \frac{\partial \Gamma_{xy}}{\partial y} \right) = f_x \text{ in } \Omega \quad (5.22)$$

$$u \frac{\partial v}{\partial x} + v \frac{\partial v}{\partial y} + \frac{\partial p}{\partial y} - \left(\frac{\partial \Gamma_{xy}}{\partial x} + \frac{\partial \Gamma_{yy}}{\partial y} \right) = f_y \text{ in } \Omega \quad (5.23)$$

$$\Gamma_{xx} - 2\mu \frac{\partial u}{\partial x} = 0 \text{ in } \Omega \quad (5.24)$$

$$\Gamma_{xy} - \mu \left(\frac{\partial u}{\partial y} + \frac{\partial v}{\partial x} \right) = 0 \text{ in } \Omega \quad (5.25)$$

$$\Gamma_{yy} - 2\mu \frac{\partial v}{\partial y} = 0 \text{ in } \Omega \quad (5.26)$$

$$V = V^s \text{ on } \Gamma_v, \quad (5.27)$$

$$\hat{n} \cdot \Gamma = \Gamma^s \text{ on } \hat{\Gamma}_\Gamma \quad (5.28)$$

where $\mu = \frac{1}{\text{Re}_n} (I_2)^{\frac{(n-1)}{2}}$ and $I_2 = 2 \left(\frac{\partial u}{\partial x} \right)^2 + 2 \left(\frac{\partial v}{\partial x} \right)^2 + \left(\frac{\partial u}{\partial y} + \frac{\partial v}{\partial x} \right)^2$.

Like with the case of Newtonian fluids, we can describe a variational problem by minimizing the above functional with respect to chosen approximation spaces. The minimum requirement on approximation functions is that they all be Lagrange family of

C^0 -continuity. . Since the formulation is based on variational frame work there are no compatibility restrictions between velocity, pressure and stress approximation spaces, so same Lagrange basis can be used for all primary variables $(p, V, \Gamma_{xx}, \Gamma_{xy}, \Gamma_{yy})$.

The Least-Squares functional associated with the above set over a typical element Ω^e with the residuals is:

$$I(p, V, \Gamma_{xx}, \Gamma_{xy}, \Gamma_{yy}) = \frac{1}{2} \int_{\Omega^e} \left[(R_1)^2 + (R_2)^2 + (R_3)^2 + (R_4)^2 + (R_5)^2 + (R_6)^2 \right] d\Omega \quad (5.29)$$

where

$$R_1 = \frac{\partial u}{\partial x} + \frac{\partial v}{\partial y} \quad (5.30)$$

$$R_2 = u \frac{\partial u}{\partial x} + v \frac{\partial u}{\partial y} + \frac{\partial p}{\partial x} - \left(\frac{\partial \Gamma_{xx}}{\partial x} + \frac{\partial \Gamma_{xy}}{\partial y} \right) - f_x \quad (5.31)$$

$$R_3 = u \frac{\partial v}{\partial x} + v \frac{\partial v}{\partial y} + \frac{\partial p}{\partial y} - \left(\frac{\partial \Gamma_{xy}}{\partial x} + \frac{\partial \Gamma_{yy}}{\partial y} \right) - f_y \quad (5.32)$$

$$R_4 = \Gamma_{xx} - 2\mu \frac{\partial u}{\partial x} \quad (5.33)$$

$$R_5 = \Gamma_{xy} - \mu \left(\frac{\partial u}{\partial y} + \frac{\partial v}{\partial x} \right) \quad (5.34)$$

$$R_6 = \Gamma_{yy} - 2\mu \frac{\partial v}{\partial y} \quad (5.35)$$

and the primary variables $(p, V, \Gamma_{xx}, \Gamma_{xy}, \Gamma_{yy})$ are approximated by the expansions of the form:

$$\begin{aligned}
p(x, y) &= \sum_{j=1}^n p_j \Psi_j(x, y), u(x, y) = \sum_{j=1}^n u_j \Psi_j(x, y), \\
v(x, y) &= \sum_{j=1}^n v_j \Psi_j(x, y), \Gamma_{xx}(x, y) = \sum_{j=1}^n \Gamma_{xx}^j \Psi_j(x, y) \quad (5.36) \\
\Gamma_{xy}(x, y) &= \sum_{j=1}^n \Gamma_{xy}^j \Psi_j(x, y), \Gamma_{yy}(x, y) = \sum_{j=1}^n \Gamma_{yy}^j \Psi_j(x, y)
\end{aligned}$$

where Ψ_j are the Lagrange family interpolation functions.

Finite Element Model

By minimization of the Least-Squares functional with nodal values of velocities, pressure, and vorticity, we obtain:

$$\delta I = \frac{\partial I}{\partial p} \delta p + \frac{\partial I}{\partial u} \delta u + \frac{\partial I}{\partial v} \delta v + \frac{\partial I}{\partial \Gamma_{xx}} \delta \Gamma_{xx} + \frac{\partial I}{\partial \Gamma_{xy}} \delta \Gamma_{xy} + \frac{\partial I}{\partial \Gamma_{yy}} \delta \Gamma_{yy} = 0 \quad (5.37)$$

which yields six sets of 'n' equations each over a typical element:

$$\frac{\partial I}{\partial p} \delta p = 0, \frac{\partial I}{\partial u} \delta u = 0, \frac{\partial I}{\partial v} \delta v = 0, \frac{\partial I}{\partial \Gamma_{xx}} \delta \Gamma_{xx} = 0, \frac{\partial I}{\partial \Gamma_{xy}} \delta \Gamma_{xy} = 0, \frac{\partial I}{\partial \Gamma_{yy}} \delta \Gamma_{yy} = 0 \quad (5.38)$$

The finite element model after substituting the approximation spaces is of the form shown below:

$$\begin{bmatrix} [K^{11}] [K^{12}] [K^{13}] [K^{14}] [K^{15}] [K^{16}] \\ [K^{21}] [K^{22}] [K^{23}] [K^{24}] [K^{25}] [K^{26}] \\ [K^{31}] [K^{32}] [K^{33}] [K^{34}] [K^{35}] [K^{36}] \\ [K^{41}] [K^{42}] [K^{43}] [K^{44}] [K^{45}] [K^{46}] \\ [K^{51}] [K^{52}] [K^{53}] [K^{54}] [K^{55}] [K^{56}] \\ [K^{61}] [K^{62}] [K^{63}] [K^{64}] [K^{65}] [K^{66}] \end{bmatrix} \begin{Bmatrix} \{p\} \\ \{u\} \\ \{v\} \\ \{\Gamma_{xx}\} \\ \{\Gamma_{xy}\} \\ \{\Gamma_{yy}\} \end{Bmatrix} = \begin{Bmatrix} \{F^1\} \\ \{F^2\} \\ \{F^3\} \\ \{F^4\} \\ \{F^5\} \\ \{F^6\} \end{Bmatrix} \quad (5.39)$$

Note that the elemental equation $\left[K^e \{u^e\} \right] \{u^e\} = \{f^e\}$ cannot be solved until they are assembled and the boundary conditions are imposed.

In developing the finite element model, two cases have been considered. In the first case the convective terms in the residuals associated with the momentum equations and the viscous terms in the stress equations are linearized before taking the minimum of the functional (this is not in consistent with the theories of mathematics). Here they are taken to be known from previous iteration. This amounts to linearization of Least-Squares functional before minimization. In this case the residuals become:

$$R_2 = u_0 \frac{\partial u}{\partial x} + v_0 \frac{\partial u}{\partial y} + \frac{\partial p}{\partial x} - \left(\frac{\partial \Gamma_{xx}}{\partial x} + \frac{\partial \Gamma_{xy}}{\partial y} \right) - f_x \quad (5.40)$$

$$R_3 = u_0 \frac{\partial v}{\partial x} + v_0 \frac{\partial v}{\partial y} + \frac{\partial p}{\partial y} - \left(\frac{\partial \Gamma_{xy}}{\partial x} + \frac{\partial \Gamma_{yy}}{\partial y} \right) - f_y \quad (5.41)$$

$$R_4 = \Gamma_{xx} - 2\mu_0 \frac{\partial u}{\partial x} \quad (5.42)$$

$$R_5 = \Gamma_{xy} - \mu_0 \left(\frac{\partial u}{\partial y} + \frac{\partial v}{\partial x} \right) \quad (5.43)$$

$$R_6 = \Gamma_{yy} - 2\mu_0 \frac{\partial v}{\partial y} \quad (5.44)$$

where (u_0, v_0, μ_0) are know from previous iteration. Hence their variational is taken to be zero in minimization step. In the other case minimization precedes the linearization (this is believed to be in consistent with the theories of mathematics). Here the viscosity also contributes to the stiffness coefficients in the finite element model, as it is not constant anymore.

Numerical Example

The ‘lid-driven’ cavity is a standard test problem in the computational fluid dynamics. The problem is characterized by a square cavity in which the driving force for the flow is the shear created by the lid. Figure 28 shows a schematic of the cavity with the boundary conditions and the finite element discretization.

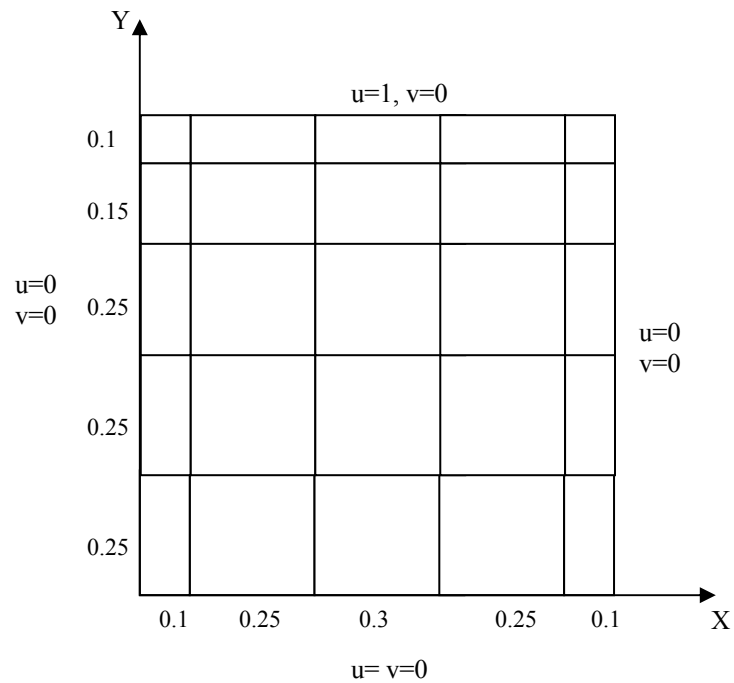


Figure 28. Computational domain using graded 5x5 rectangular elements

The above problem is solved by direct-iteration and tangent method with order of polynomials ranging from $P=3$ to $P=7$. The coefficient matrix is evaluated using a Gaussian quadrature of $(2P+1)$ in both the co-ordinate directions. The Reynolds number Re_n for Power-Law fluid is fixed as 100 for all the cases. Convergence is declared when

the Euclidean norm is less than 10^{-3} , which typically took 7-12 iterations. However the number of iterations for the linearization before minimization case was less compared to case of linearization after minimization.

Results

For $P=3$, the program did not converge for lower values of Power-Law index (0.25, 0.5 and 0.75) and did not give correct results for other values of Power-Law index (1.0, 1.25 and 1.5). The results from direct iteration method were not good when compared to that of the tangent method. For $P=5$, the program did not converge for lower values of Power-Law index (0.25 and 0.5) and did not give correct results for other values of Power-Law index (0.75, 1.0, 1.25 and 1.5). But the results were improved when compared to the previous case. For this case also the results from direct iteration method were not good when compared to that of the tangent method. For $P=7$, the program did not converge for lower values of Power-Law index (0.25 and 0.5) but the results for other values of Power-Law index (0.75, 1.0, 1.25 and 1.5) were good. As with the previous cases the results from direct iteration method were not good when compared to that of the tangent method. Also, for $P=7$, the results from linearization before minimization case were not good compared to case of linearization after minimization.

Case-I (Linearization before Minimization)

Figure 29 shows the plots of horizontal velocity u at $X=0.5$ with $P=7$ for various values of Power-Law index using Tangent method. Figure 30 shows the plots of vertical

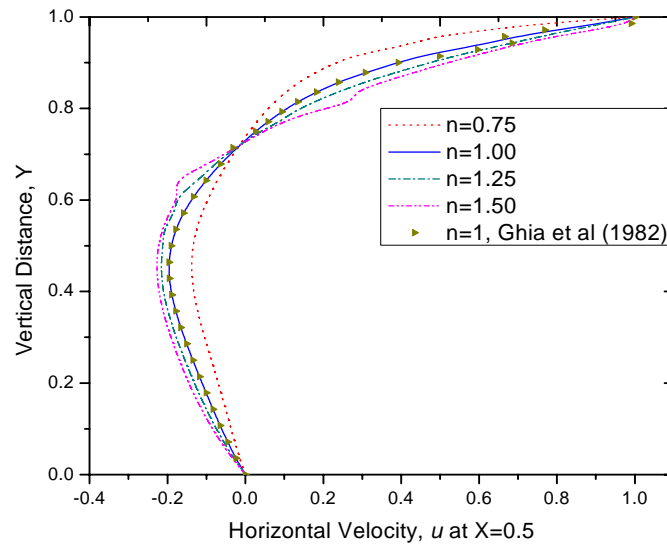


Figure 29. Plots of horizontal velocity u at $X=0.5$ with $P=7$ for various values of Power-Law index for linearization before minimization

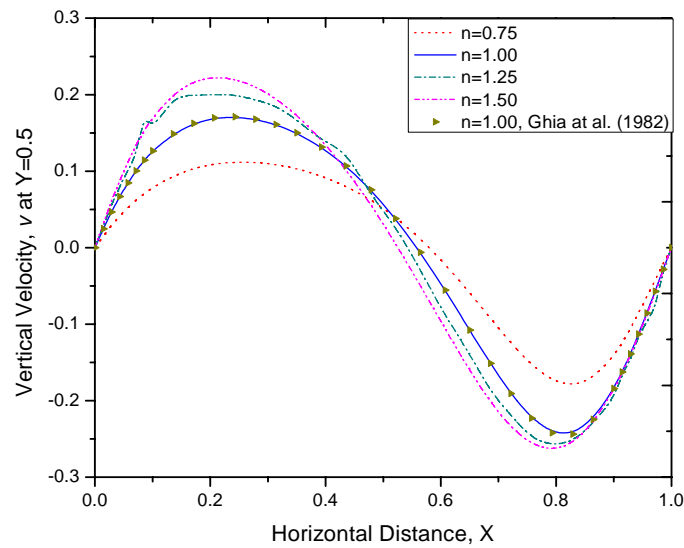


Figure 30. Plots of vertical velocity v at $Y=0.5$ with $P=7$ for various values of Power-Law index for linearization before minimization

velocity v at $Y=0.5$ with $P=7$ for various values of Power-Law index using Tangent method.

Case-II (Linearization after Minimization)

Figure 31 shows the plots of horizontal velocity u at $X=0.5$ with $P=7$ for various values of Power-Law index using Tangent method. Figure 32 shows the plots of vertical velocity v at $Y=0.5$ with $P=7$ for various values of Power-Law index using Tangent method.

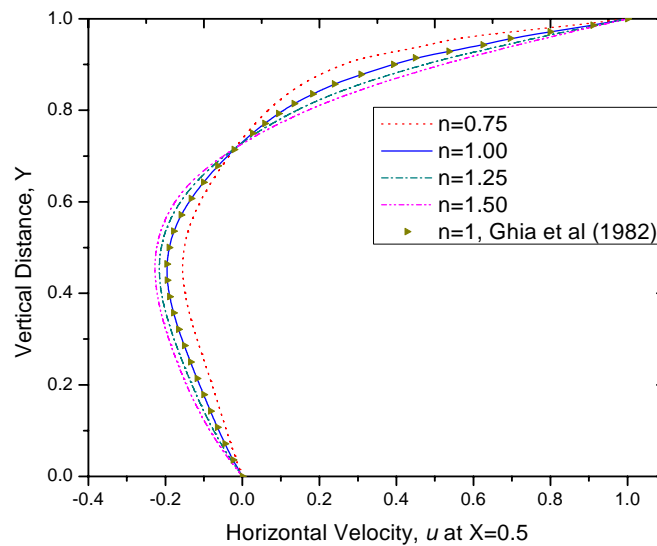


Figure 31. Plots of horizontal velocity u at $X=0.5$ with $P=7$ for various values of Power-Law index

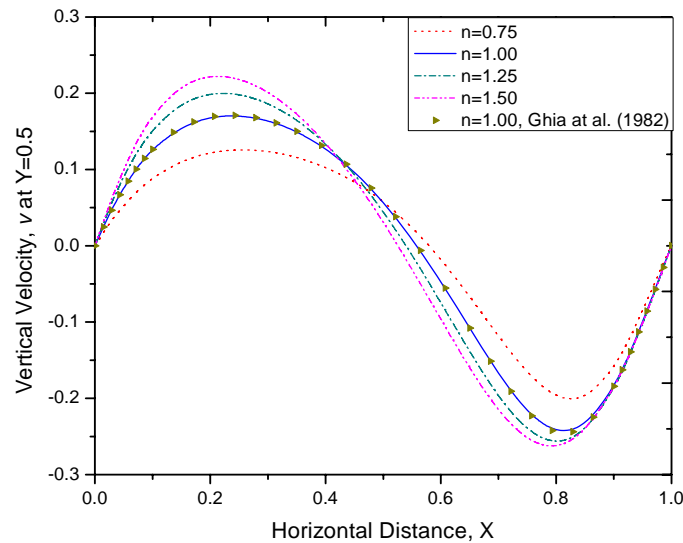


Figure 32. Plots of vertical velocity v at $Y=0.5$ with $P=7$ for various values of Power-Law index

Conclusions

From the above results we can conclude that the non-Newtonian fluids require higher order polynomial approximation functions and higher order Gaussian quadrature compared to Newtonian fluids. There is some tangible effect of linearization before and after minimization on the accuracy of the solution. The effect is more pronounced for lower Power-Law indices compared to higher Power-Law indices. The linearization before minimization case converges at a faster rate compared to the case of linearization after minimization. And there seems to be some kind of locking that is causing the matrices to be ill-conditioned esp. for lower values of Power-Law indices. As explained in the previous chapters as the order of polynomial approximation functions is increased, the numerical solutions became more and more close to the benchmark solutions.

CHAPTER VI

LEAST-SQUARES FORMULATION OF VORTICITY BASED SYSTEM FOR POWER-LAW FLUIDS

Introduction

In this chapter the vorticity based Power-Law fluids are considered. To illustrate how the Power-Law constitutive equation affects the finite element equations, a steady state, isothermal, incompressible, non-Newtonian fluid is considered. The equivalent system is defined by introducing vorticity $\hat{\omega} = \nabla \times \hat{V}$ as an auxiliary variable. By making use of the vector identity $\nabla \times \nabla \times \hat{V} = -\nabla^2 \hat{V} + \nabla(\nabla \cdot \hat{V})$ and the incompressibility condition $\nabla \cdot \hat{V} = 0$, the original equations in 2D can be cast as following equivalent equations:

$$\frac{\partial \hat{u}}{\partial x} + \frac{\partial \hat{v}}{\partial y} = 0 \quad \text{in } \Omega, \quad (5.1)$$

$$\hat{u} \frac{\partial \hat{u}}{\partial x} + \hat{v} \frac{\partial \hat{u}}{\partial y} + \frac{\partial \hat{p}}{\partial x} + \hat{\mu} \frac{\partial \hat{\omega}}{\partial y} - \frac{\partial \hat{\mu}}{\partial x} \left(2 \frac{\partial \hat{u}}{\partial x} \right) - \frac{\partial \hat{\mu}}{\partial y} \left(\frac{\partial \hat{u}}{\partial y} + \frac{\partial \hat{v}}{\partial x} \right) = \hat{f}_x \quad \text{in } \Omega, \quad (5.2)$$

$$\hat{u} \frac{\partial \hat{u}}{\partial x} + \hat{v} \frac{\partial \hat{u}}{\partial y} + \frac{\partial \hat{p}}{\partial y} - \hat{\mu} \frac{\partial \hat{\omega}}{\partial x} - \frac{\partial \hat{\mu}}{\partial y} \left(2 \frac{\partial \hat{v}}{\partial y} \right) - \frac{\partial \hat{\mu}}{\partial x} \left(\frac{\partial \hat{u}}{\partial y} + \frac{\partial \hat{v}}{\partial x} \right) = \hat{f}_y \quad \text{in } \Omega, \quad (5.3)$$

$$\hat{\omega} + \frac{\partial \hat{u}}{\partial y} - \frac{\partial \hat{v}}{\partial x} = 0 \quad \text{in } \Omega, \quad (5.4)$$

$$\hat{V} = \hat{V}^s \quad \text{on } \Gamma_v, \quad (5.5)$$

$$\hat{n} \cdot \hat{\sigma} = \hat{f}^s \quad \text{on } \Gamma_\omega \quad (5.6)$$

where $\hat{\mu} = \hat{\mu}_0 (\hat{I}_2)^{\frac{(n-1)}{2}}$ and $\hat{I}_2 = 2 \left(\frac{\partial \hat{u}}{\partial x} \right)^2 + 2 \left(\frac{\partial \hat{v}}{\partial x} \right)^2 + \left(\frac{\partial \hat{u}}{\partial y} + \frac{\partial \hat{v}}{\partial x} \right)^2$. Typically $\phi = \Gamma_v \cap \Gamma_\omega$ i.e.,

if velocity is specified at a boundary, vorticity need not be specified there. Also for 2D case the vorticity vector $\hat{\omega} = (0, 0, \hat{\omega})$ i.e. it has component only in Z-direction. The above equations can be non dimensionalized as explained in the previous chapter. The Navier-Stokes equation is transformed to:

$$\frac{\partial u}{\partial x} + \frac{\partial v}{\partial y} = 0 \text{ in } \Omega, \quad (5.7)$$

$$u \frac{\partial u}{\partial x} + v \frac{\partial u}{\partial y} + \frac{\partial p}{\partial x} + \mu \frac{\partial \omega}{\partial y} - \frac{\partial \mu}{\partial x} \left(2 \frac{\partial u}{\partial x} \right) - \frac{\partial \mu}{\partial y} \left(\frac{\partial u}{\partial y} + \frac{\partial v}{\partial x} \right) = f_x \text{ in } \Omega, \quad (5.8)$$

$$u \frac{\partial u}{\partial x} + v \frac{\partial u}{\partial y} + \frac{\partial p}{\partial y} - \mu \frac{\partial \omega}{\partial x} - \frac{\partial \mu}{\partial y} \left(2 \frac{\partial v}{\partial y} \right) - \frac{\partial \mu}{\partial x} \left(\frac{\partial u}{\partial y} + \frac{\partial v}{\partial x} \right) = f_y \text{ in } \Omega, \quad (5.9)$$

$$\omega + \frac{\partial u}{\partial y} - \frac{\partial v}{\partial x} = 0 \text{ in } \Omega, \quad (5.10)$$

$$V = V^s \text{ on } \Gamma_v, \quad (5.11)$$

$$\hat{n} \cdot \sigma = f^s \text{ on } \Gamma_\omega \quad (5.12)$$

where $\mu = \frac{1}{\text{Re}_n} (I_2)^{\frac{(n-1)}{2}}$ and $I_2 = 2 \left(\frac{\partial u}{\partial x} \right)^2 + 2 \left(\frac{\partial v}{\partial x} \right)^2 + \left(\frac{\partial u}{\partial y} + \frac{\partial v}{\partial x} \right)^2$

The terms $\left(\frac{\partial \mu}{\partial x}, \frac{\partial \mu}{\partial y} \right)$ make the above equations to be of the same order

derivatives as that of the original differential equation. This requires use of at Least C^1 -continuous functions for the velocity field. This higher order differentiability requirement is again a practical disadvantage. And it is also very difficult to derive the

approximation functions that belong to C^1 -continuous space. One new method that is tried out is to see if the higher order approximation functions that belong to Lagrange family of C^0 -continuity can be used to solve the problem. It should be noted that in all the previous chapters, only the first order derivatives of the approximation functions are required to be evaluated, but for this problem both the first order and the second order derivatives of the approximation functions have to be evaluated. Like before, we can describe the variational problem by minimizing the above functional with respect to chosen approximation spaces. The minimum requirement on approximation functions is again taken to be that of C^0 -continuity. Since the formulation is based on variational frame work there are no compatibility restrictions between velocity and pressure approximation spaces, so same Lagrange basis can be used for all primary variables (V, p, ω) .

Least-Squares Formulation

The Least-Squares functional associated with the above set over a typical element Ω^e with the residuals is:

$$I(V, p, \omega) = \frac{1}{2} \int_{\Omega^e} [(R_1)^2 + (R_2)^2 + (R_3)^2 + (R_4)^2] d\Omega \quad (5.13)$$

where

$$R_1 = \frac{\partial u}{\partial x} + \frac{\partial v}{\partial y} \quad (5.14)$$

$$R_2 = u \frac{\partial u}{\partial x} + v \frac{\partial u}{\partial y} + \frac{\partial p}{\partial x} + \mu \frac{\partial \omega}{\partial y} - \frac{\partial \mu}{\partial x} \left(2 \frac{\partial u}{\partial x} \right) - \frac{\partial \mu}{\partial y} \left(\frac{\partial u}{\partial y} + \frac{\partial v}{\partial x} \right) - f_x \quad (5.15)$$

$$R_3 = u \frac{\partial u}{\partial x} + v \frac{\partial u}{\partial y} + \frac{\partial p}{\partial y} - \mu \frac{\partial \omega}{\partial x} - \frac{\partial \mu}{\partial y} \left(2 \frac{\partial v}{\partial y} \right) - \frac{\partial \mu}{\partial x} \left(\frac{\partial u}{\partial y} + \frac{\partial v}{\partial x} \right) - f_y \quad (5.16)$$

$$R_4 = \omega + \frac{\partial u}{\partial y} - \frac{\partial v}{\partial x} \quad (5.17)$$

and the primary variables (u, v, p, ω) are approximated by the expansions of the form

$$\begin{aligned} u(x, y) &= \sum_{j=1}^n u_j \Psi_j(x, y), \quad v(x, y) = \sum_{j=1}^n v_j \Psi_j(x, y), \\ p(x, y) &= \sum_{j=1}^n p_j \Psi_j(x, y), \quad \omega(x, y) = \sum_{j=1}^n \omega_j \Psi_j(x, y) \end{aligned} \quad (5.18)$$

where Ψ_j are the Lagrange family interpolation functions.

Finite Element Model

By minimization of the Least-Squares functional with nodal values of velocities, pressure, and vorticity, we obtain

$$\delta I = \frac{\partial I}{\partial p} \delta p + \frac{\partial I}{\partial u} \delta u + \frac{\partial I}{\partial v} \delta v + \frac{\partial I}{\partial \omega} \delta \omega = 0 \quad (5.19)$$

which yields four sets of 'n' equations each over a typical element:

$$\frac{\partial I}{\partial p} \delta p = 0, \quad \frac{\partial I}{\partial u} \delta u = 0, \quad \frac{\partial I}{\partial v} \delta v = 0, \quad \frac{\partial I}{\partial \omega} \delta \omega = 0 \quad (5.20)$$

The finite element model after substituting the approximation spaces is of the form shown below:

$$\begin{bmatrix} [K^{11}][K^{12}][K^{13}][K^{14}] \\ [K^{21}][K^{22}][K^{23}][K^{24}] \\ [K^{31}][K^{32}][K^{33}][K^{34}] \\ [K^{41}][K^{42}][K^{43}][K^{44}] \end{bmatrix} \begin{Bmatrix} \{p\} \\ \{u\} \\ \{v\} \\ \{\omega\} \end{Bmatrix} = \begin{Bmatrix} \{f^1\} \\ \{f^2\} \\ \{f^3\} \\ \{f^4\} \end{Bmatrix} \quad (5.21)$$

In developing the finite element model, two cases have been considered. In the first case the convective terms in the residuals associated with the momentum equations are linearized before taking the minimum of the functional (this is not in consistent with the theories of mathematics). Here they are taken to be known from previous iteration. This amounts to linearization of Least-Squares functional before minimization. In this case the residuals become:

$$R_2 = u_0 \frac{\partial u}{\partial x} + v_0 \frac{\partial u}{\partial y} + \frac{\partial p}{\partial x} + \mu_0 \frac{\partial \omega}{\partial y} - \frac{\partial \mu_0}{\partial x} \left(2 \frac{\partial u}{\partial x} \right) - \frac{\partial \mu_0}{\partial y} \left(\frac{\partial u}{\partial y} + \frac{\partial v}{\partial x} \right) - f_x \quad (5.22)$$

$$R_3 = u_0 \frac{\partial u}{\partial x} + v_0 \frac{\partial u}{\partial y} + \frac{\partial p}{\partial y} - \mu_0 \frac{\partial \omega}{\partial x} - \frac{\partial \mu_0}{\partial y} \left(2 \frac{\partial v}{\partial y} \right) - \frac{\partial \mu_0}{\partial x} \left(\frac{\partial u}{\partial y} + \frac{\partial v}{\partial x} \right) - f_y \quad (5.23)$$

where $(u_0, v_0, \mu_0, \partial \mu_0 / \partial x, \partial \mu_0 / \partial y)$ are know from previous iteration. Hence their variational is taken to be zero in minimization step. In the other case minimization precedes the linearization (this is believed to be in consistent with the theories of mathematics). Here the viscosity also contributes to the stiffness coefficients in the finite element model, as it is not constant anymore.

Numerical Example

The ‘lid-driven’ cavity is a standard test problem in the computational fluid dynamics. The problem is characterized by a square cavity in which the driving force for

the flow is the shear created by the lid. Figure 33 shows a schematic of the cavity with the boundary conditions and the finite element discretization.

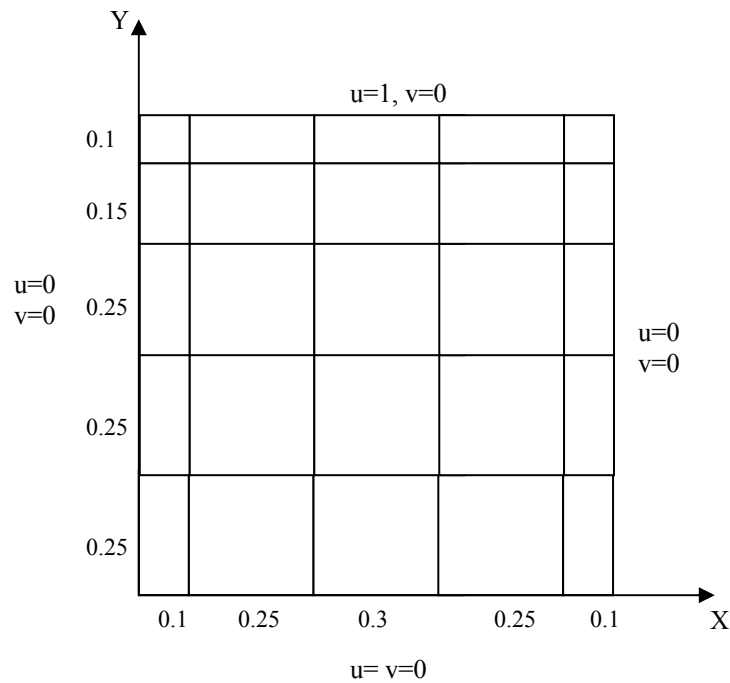


Figure 33. Computational domain using non-uniform 5x5 rectangular elements

The above problem is solved by direct-iteration and tangent method with order of polynomials ranging from $P=3$ to $P=5$. The coefficient matrix is evaluated using a Gaussian quadrature of $(2P+1)$ in both the co-ordinate directions. The Reynolds number Re_n for Power-Law fluid is fixed as 100 for all the cases. Convergence is declared when the Euclidean norm is less than 10^{-3} , which typically took 7-10 iterations. However the

number of iterations for the linearization before minimization case was less compared to case of linearization after minimization.

Results

For $P=3$, the program did not converge for lower values of Power-Law index (0.25) and did not give correct results for other values of Power-Law index (0.5, 0.75, 1.0, 1.25 and 1.5). The results from direct iteration method were not good when compared to that of the tangent method. For $P=5$, the program did not converge for lower values of Power-Law index (0.25) but the results for other values of Power-Law index (0.75, 1.0, 1.25 and 1.5) were good. As with the previous cases the results from direct iteration method were not good when compared to that of the tangent method. Also, for $P=5$, the results from linearization before minimization case were not good compared to case of linearization after minimization.

Case-I (Linearization before Minimization)

Figure 34 shows the plots of horizontal velocity u at $X=0.5$ with $P=5$ for various values of Power-Law index using Tangent method. Figure 35 shows the plots of vertical velocity v at $Y=0.5$ with $P=5$ for various values of Power-Law index using Tangent method.

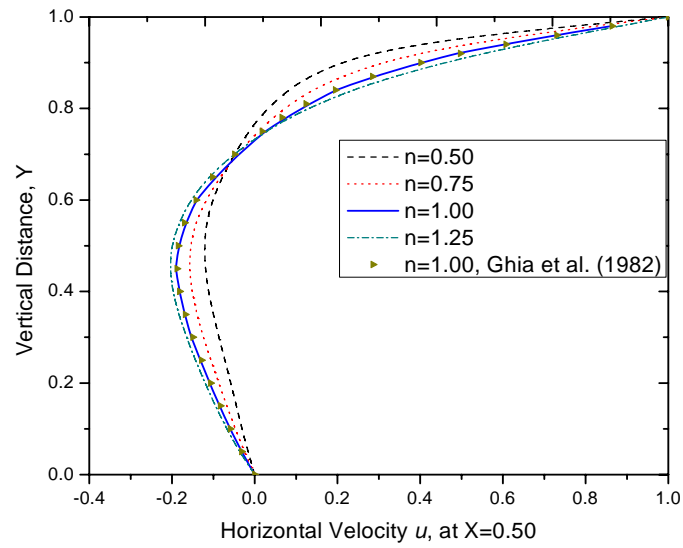


Figure 34. Plots of horizontal velocity u at $X=0.5$ with $P=5$ for various values of Power-Law index for linearization before minimization

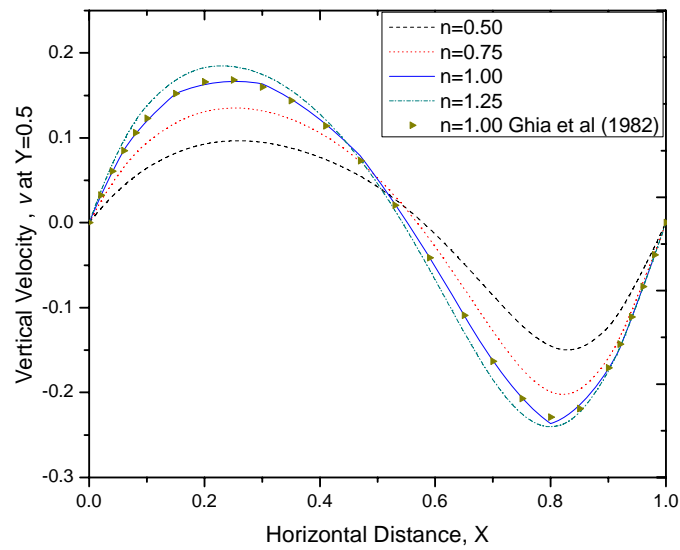


Figure 35. Plots of vertical velocity v at $Y=0.5$ with $P=5$ for various values of Power-Law index for linearization before minimization

Case-II (Linearization after Minimization)

Figure 36 shows the plots of horizontal velocity u at $X=0.5$ with $P=5$ for various values of Power-Law index using Tangent method. Figure 37 shows the plots of vertical velocity v at $Y=0.5$ with $P=5$ for various values of Power-Law index using Tangent method.

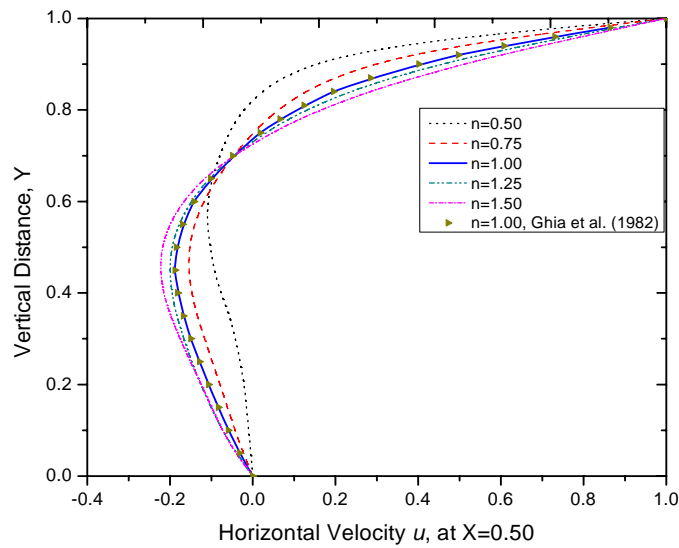


Figure 36. Plots of horizontal velocity u at $X=0.5$ with $P=5$ for various values of Power-Law index

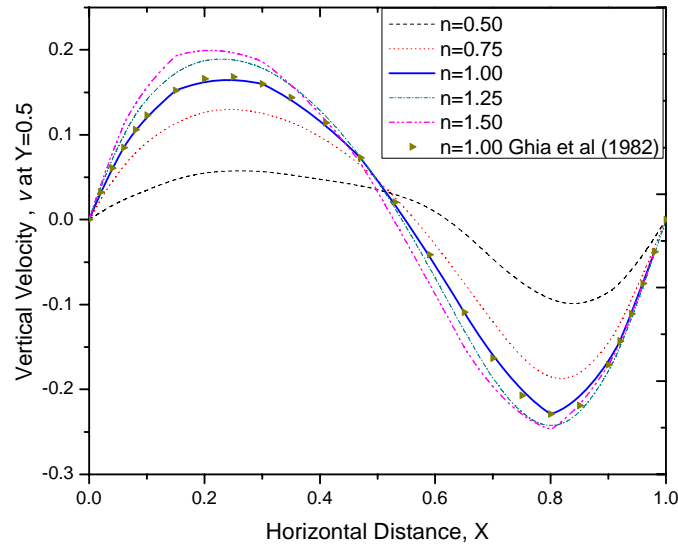


Figure 37. Plots of vertical velocity v at $Y=0.5$ with $P=5$ for various values of Power-Law index

Conclusions

From the above results we can conclude that the non-Newtonian fluids require higher order polynomial approximation functions and higher order Gaussian quadrature compared to Newtonian fluids. There is some tangible effect of linearization before and after minimization on the accuracy of the solution. The effect is more pronounced for lower Power-Law indices compared to higher Power-Law indices. The linearization before minimization case converges at a faster rate compared to the case of linearization after minimization. And there seems to be some kind of locking that is causing the matrices to be ill-conditioned esp. for lower values of Power-Law indices. As explained in the previous chapters as the order of polynomial approximation functions is increased, the numerical solutions became more and more close to the benchmark solutions. And

finally the new method of using the higher order approximation functions that belong to Lagrange family of C^0 -continuity to solve the present problem seems to give good results.

CHAPTER VII

REDUCED INTEGRATION PENALTY FINITE ELEMENT MODEL FOR POWER-LAW FLUIDS

Introduction

The governing equations for steady state, incompressible, viscous, Newtonian fluids under isothermal conditions are:

$$\nabla \cdot V = 0 \text{ in } \Omega, \quad (7.1)$$

$$\rho_0 (V \cdot \nabla) V + \nabla p - \mu \nabla \cdot \left[(\nabla V) + (\nabla V)^T \right] = \rho_0 f \text{ in } \Omega, \quad (7.2)$$

$$V = V^s \text{ on } \Gamma_v, \quad (7.3)$$

$$\hat{n} \cdot \sigma = f^s \text{ on } \Gamma_f \quad (7.4)$$

where $\Gamma = \Gamma_v \cup \Gamma_f$ and $\phi = \Gamma_v \cap \Gamma_f$, f is the force term, \hat{n} is the outward unit normal on the boundary of Ω , μ is the viscosity of the fluid, $\sigma = -(p)I - 2\mu \left[(\nabla V) + (\nabla V)^T \right]$, V^s is the prescribed value of velocity on the boundary Γ_v , and f^s is the prescribed value of tractions on the boundary Γ_f . The above equations in two-dimensional form can be represented as:

$$\frac{\partial u}{\partial x} + \frac{\partial v}{\partial y} = 0 \text{ in } \Omega, \quad (7.5)$$

$$\rho_0 \left(u \frac{\partial u}{\partial x} + v \frac{\partial u}{\partial y} \right) - \frac{\partial}{\partial x} \left(2\mu \frac{\partial u}{\partial x} \right) - \frac{\partial}{\partial y} \left[\mu \left(\frac{\partial u}{\partial y} + \frac{\partial v}{\partial x} \right) \right] + \frac{\partial p}{\partial x} = \rho_0 f_x \text{ in } \Omega, \quad (7.6)$$

$$\rho_0 \left(u \frac{\partial v}{\partial x} + v \frac{\partial v}{\partial y} \right) - \frac{\partial}{\partial y} \left(2\mu \frac{\partial v}{\partial y} \right) - \frac{\partial}{\partial x} \left[\mu \left(\frac{\partial u}{\partial y} + \frac{\partial v}{\partial x} \right) \right] + \frac{\partial p}{\partial y} = \rho_0 f_y \text{ in } \Omega, \quad (7.7)$$

$$V = V^s \text{ on } \Gamma_v, \quad (7.8)$$

$$\hat{n} \cdot \sigma = f^s \text{ on } \Gamma_f \quad (7.9)$$

where (u, v) are the horizontal and vertical components of velocity vector “ V ” and (f_x, f_y) are the horizontal and vertical components of body force vector f .

There several different finite element models for the above equations. The conventional one is a natural formulation in which the weak forms of the above equations are used are to construct the finite element model. The resulting finite element model is termed the *mixed model*. The phrase “mixed” is used because velocity variables are mixed with the force-like variable, pressure, and both types of variables are retained in a single formulation. More details on the mixed model can be found in the book on nonlinear finite element analysis by Dr. Reddy [72]. The second model is based on the interpretation that the continuity equation (7.1) is an additional relation among the velocity components (i.e., a constraint among the v_i), and the constraint is satisfied in a Least-Squares (i.e. approximate) sense.

This particular method of including the constraint in the formulation is known as the *penalty function method*, and the model is termed the *penalty-finite element model*. In this case, the pressure variable is effectively eliminated from the formulation. It is informative to note that the velocity-pressure (or mixed) formulation is the same as the

Lagrange multiplier formulation, wherein the constraint is included by means of the Lagrange multiplier method. The Lagrange multiplier turns out to be the negative of the pressure.

Penalty Finite Element Formulation

The penalty function method allows us to reformulate a problem with constraints as one without constraints. In order to use the penalty function method for the flow of a viscous incompressible fluid, first it is reformulated as a variational problem subjected to a constraint. For the purpose of describing the penalty function method, we consider the steady Stokes flow problem (i.e. without time-dependent and nonlinear terms) in two dimensions. Then the penalty method is applied to the variational problem with a constraint. The development will then be extended to unsteady Navier-Stokes equations. The weak forms of the above equations can be expressed in the form (neglecting time derivatives and nonlinear terms):

$$B\left((w_x, w_y, q), (u, v, p)\right) = l(w_x, w_y, q) \quad (7.10)$$

where (w_x, w_y, q) are the weight functions used for the momentum and continuity equations, respectively, $B(\bullet, \bullet)$ is a *bilinear form* [i.e., an expression that is linear in (w_x, w_y, q) as well as (u, v, p)] and $l(\bullet)$ is a *linear form*, defined by:

$$\begin{aligned}
B((w_x, w_y, q), (u, v, p)) = & \int_{\Omega^e} \mu \left[2 \left(\frac{\partial w_x}{\partial x} \frac{\partial u}{\partial x} + \frac{\partial w_y}{\partial y} \frac{\partial v}{\partial y} \right) + \left(\frac{\partial w_x}{\partial y} + \frac{\partial w_y}{\partial x} \right) \left(\frac{\partial u}{\partial y} + \frac{\partial v}{\partial x} \right) \right] dx dy \\
& - \int_{\Omega^e} \left[\left(\frac{\partial w_x}{\partial y} + \frac{\partial w_y}{\partial x} \right) p + \left(\frac{\partial u}{\partial y} + \frac{\partial v}{\partial x} \right) q \right] dx dy
\end{aligned} \tag{7.11}$$

$$l(w_x, w_y, q) = \int_{\Omega^e} \rho (w_x f_x + w_y f_y) dx dy + \oint_{\Gamma^e} (w_x t_x + w_y t_y) ds \tag{7.12}$$

and (t_x, t_y) are the boundary stress components defined as below:

$$t_x = \left(2\mu \frac{\partial u}{\partial x} - p \right) n_x + \mu \left(\frac{\partial u}{\partial y} + \frac{\partial v}{\partial x} \right) n_y \tag{7.13}$$

$$t_y = \mu \left(\frac{\partial u}{\partial y} + \frac{\partial v}{\partial x} \right) n_x + \left(2\mu \frac{\partial v}{\partial y} - p \right) n_y \tag{7.14}$$

The statement in Eq. (7.10) is known as the variational problem associated with steady-state Stokes problem.

Suppose that the velocity field (u, v) is such that the continuity equation is satisfied identically. Then the weight functions (w_x, w_y) , being virtual variations of the velocity components, also satisfy the continuity equation:

$$\nabla \cdot \mathbf{w} = \frac{\partial w_x}{\partial x} + \frac{\partial w_y}{\partial y} = 0 \tag{7.15}$$

As a result, the second integral expression in the bilinear form (7.10) drops out, and the pressure, and hence the weight function q , does not appear explicitly in the variational problem (7.10). The resulting variational problem now can be stated as follows: among

all vectors $V = u\hat{e}_x + v\hat{e}_y$ that satisfies the continuity equation (7.1), find the one that satisfies the variational problem:

$$B_0((w_x, w_y), (u, v)) = l_0(w_x, w_y) \quad (7.16)$$

for all admissible weight functions $w = w_x\hat{e}_x + w_y\hat{e}_y$ [i.e. that which satisfies the condition

$\nabla \cdot w = 0$]. The bilinear and linear forms in Eq. (7.16) are defined by:

$$B_0((w_x, w_y), (u, v)) = \int_{\Omega^e} \mu \left[2 \left(\frac{\partial w_x}{\partial x} \frac{\partial u}{\partial x} + \frac{\partial w_y}{\partial y} \frac{\partial v}{\partial y} \right) + \left(\frac{\partial w_x}{\partial y} + \frac{\partial w_y}{\partial x} \right) \left(\frac{\partial u}{\partial y} + \frac{\partial v}{\partial x} \right) \right] dx dy \quad (7.17)$$

$$l_0(w_x, w_y) = \int_{\Omega^e} \rho (w_x f_x + w_y f_y) dx dy + \oint_{\Gamma^e} (w_x t_x + w_y t_y) ds \quad (7.18)$$

The variational problem in Eq. (7.16) is a constrained variational problem, because the solution vector “ V ” is constrained to satisfy the continuity equation. The bilinear form $B_0(w, V)$ is symmetric i.e. $B_0(w, V) = B_0(V, w)$ and also linear in both its arguments. Whenever the bilinear form of a variational problem is symmetric in its arguments, it is possible to construct a quadratic functional such that the minimum of the quadratic functional is equivalent to the variational problem. The quadratic functional is given by the expression:

$$I_0(V) = \frac{1}{2} B_0(V, V) - l_0(V) \quad (7.19)$$

Now we can state that equations governing the steady flow of viscous incompressible fluids are equivalent to minimizing the quadratic functional $I_0(V)$ subjected to the constraint:

$$G(V) \equiv \nabla \cdot V = \frac{\partial w_x}{\partial x} + \frac{\partial w_y}{\partial y} = 0 \quad (7.20)$$

Reduced Integration Penalty Finite Element Formulation

The advantage of the constrained problem is that the pressure variable “ p ” does not appear in the formulation. In the penalty function method, the constrained problem is reformulated as an unconstrained problem as follows: minimize the modified functional:

$$I_p(V) = I_0(V) + \frac{\gamma_e}{2} \int_{\Omega^e} [G(V)]^2 dx \quad (7.21)$$

where γ_e is called the *penalty parameter*. Note that the constraint is included in a Least-Squares sense into the functional. Seeking the minimum of the modified functional $I_p(V)$ is equivalent to seeking the minimum of both $I_0(V)$ and $G(V)$, the latter with respect to the weight γ_e . The larger the value of γ_e , the more exactly the constraint is satisfied. The necessary condition for the minimum of $I_p(V)$ is:

$$\delta I_p(V) = 0 \quad (7.22)$$

from the above we have:

$$\begin{aligned} 0 = \int_{\Omega^e} \mu \left[2 \left(\frac{\partial \delta u}{\partial x} \frac{\partial u}{\partial x} \right) + \frac{\partial \delta u}{\partial y} \left(\frac{\partial u}{\partial y} + \frac{\partial v}{\partial x} \right) \right] dx dy - \int_{\Omega^e} \rho \delta u f_x dx dy \\ - \oint_{\Gamma^e} \delta u t_x ds + \int_{\Omega^e} \gamma_e \frac{\partial \delta u}{\partial x} \left(\frac{\partial u}{\partial x} + \frac{\partial v}{\partial y} \right) dx dy \end{aligned} \quad (7.23)$$

$$\begin{aligned}
0 = \int_{\Omega^e} \mu \left[2 \left(\frac{\partial \delta v}{\partial y} \frac{\partial v}{\partial y} \right) + \frac{\partial \delta v}{\partial x} \left(\frac{\partial u}{\partial y} + \frac{\partial v}{\partial x} \right) \right] dx dy - \int_{\Omega^e} \rho \delta v f_y dx dy \\
- \oint_{\Gamma^e} \delta v t_y ds + \int_{\Omega^e} \gamma_e \frac{\partial \delta v}{\partial y} \left(\frac{\partial u}{\partial x} + \frac{\partial v}{\partial y} \right) dx dy
\end{aligned} \tag{7.24}$$

These two statements provide the weak forms for the penalty finite element model with $\delta u = w_x$ and $\delta v = w_y$. The pressure does not explicitly appear in the above weak form equations although it is a part of the boundary stresses. The pressure can be post computed, from the relation:

$$p_\gamma = -\gamma_e \left(\frac{\partial u}{\partial x} + \frac{\partial v}{\partial y} \right) \tag{7.25}$$

Now the nonlinear terms can be added without affecting the above discussion. Also the time derivative terms can be added, but in this study only steady state flow is considered, hence they are not included. The complete equations are given as:

$$\begin{aligned}
0 = \int_{\Omega^e} \left[\delta u \rho \left(u \frac{\partial u}{\partial x} + v \frac{\partial v}{\partial y} \right) + 2\mu \left(\frac{\partial \delta u}{\partial x} \frac{\partial u}{\partial x} \right) + \mu \frac{\partial \delta u}{\partial y} \left(\frac{\partial u}{\partial y} + \frac{\partial v}{\partial x} \right) \right] dx dy - \int_{\Omega^e} \rho \delta u f_x dx dy \\
- \oint_{\Gamma^e} \delta u t_x ds + \int_{\Omega^e} \gamma_e \frac{\partial \delta u}{\partial x} \left(\frac{\partial u}{\partial x} + \frac{\partial v}{\partial y} \right) dx dy
\end{aligned} \tag{7.26}$$

$$\begin{aligned}
0 = \int_{\Omega^e} \left[\delta v \rho \left(u \frac{\partial u}{\partial x} + v \frac{\partial v}{\partial y} \right) + 2\mu \left(\frac{\partial \delta v}{\partial y} \frac{\partial v}{\partial y} \right) + \mu \frac{\partial \delta v}{\partial x} \left(\frac{\partial u}{\partial y} + \frac{\partial v}{\partial x} \right) \right] dx dy \\
- \int_{\Omega^e} \rho \delta v f_y dx dy - \oint_{\Gamma^e} \delta v t_y ds + \int_{\Omega^e} \gamma_e \frac{\partial \delta v}{\partial y} \left(\frac{\partial u}{\partial x} + \frac{\partial v}{\partial y} \right) dx dy
\end{aligned} \tag{7.27}$$

The penalty finite element model derived above falls into the category known as *reduced integration penalty* (RIP) method. The penalty terms in the above are evaluated

using reduced integration rule. The choice of the penalty parameter is largely dictated by the ratio of the magnitude of the penalty terms to the viscous and convective terms (or compared to the Reynolds number, Re), the mesh, and the precision of the computer. Generally the value of penalty parameter ranges from $\gamma = 10^4 Re$ to $\gamma = 10^{12} Re$. The penalty finite element model is obtained from the above equations by substituting the finite element approximation for velocity field, and $\delta u = \psi_i^e$ and $\delta v = \psi_i^e$:

$$\left[C(\rho, V) + K(\mu) + \bar{K}(\gamma) \right] V = F \quad (7.28)$$

where $C(\rho, V)$ is the contribution due to convective terms, $K(\mu)$ is contribution from viscous terms, and $\bar{K}(\gamma)$ is contribution from penalty terms, which come from the incompressibility constraint. In theory as we increase the value of γ , the conservation of mass is satisfied more exactly. However, in practice, for some large value of γ , the contribution viscous terms would be negligibly small compared to the penalty terms in the computer. Thus, if $\bar{K}(\gamma)$ is non-singular (i.e. invertible) matrix, the solution satisfies the continuity equation, it does not satisfy the momentum equations. In this case the discrete problem is said to be over constrained or “locked”. If $\bar{K}(\gamma)$ is singular, then the sum $\left[C(\rho, V) + K(\mu) + \bar{K}(\gamma) \right]$ is non-singular (because $\left[C(\rho, V) + K(\mu) \right]$ is non-singular), and a non-trivial solution to the problem is obtained.

The numerical problem described above is eliminated by proper evaluation of the integrals in $C(\rho, V)$, $K(\mu)$, and $\bar{K}(\gamma)$. It is found that if the coefficients of $\bar{K}(\gamma)$ (i.e. penalty matrix coefficients) are evaluated using a numerical integration rule of an order

less than that required integrating them exactly; the finite element equations give acceptable solutions for the velocity field. This technique of under-integrating the penalty terms is known in the literature as *reduced integration*. Of course, as the degree of interpolation goes up, or very refined meshes are used, the resulting equations become less sensitive to locking. In this chapter as higher order interpolation terms are used there is no need for reduced integration. The pressure should be computed by evaluating the equation (7.25) at integration points corresponding to the reduced Gauss rule. This corresponds to using an interpolation for pressure that is one order less than the one used for velocity field. The pressure computed using the above equation at reduced integration points is not always reliable and accurate. Various techniques have been proposed in the literature to obtain the accurate pressure fields.

Power-Law Fluids

Although the above equations are derived for Newtonian fluids they are the same in case of non-Newtonian fluids too as in the above formulation viscosity μ has never been treated as constant. The viscosity varies as per the Power-Law model as:

$$\mu = \mu_0 (I_2)^{\frac{(n-1)}{2}} \text{ where } I_2 = 2\left(\frac{\partial u}{\partial x}\right)^2 + 2\left(\frac{\partial v}{\partial x}\right)^2 + \left(\frac{\partial u}{\partial y} + \frac{\partial v}{\partial x}\right)^2 \text{ is the second invariant. The}$$

results for both the cases are compared using the 2D Lid Driven Cavity flow problem.

Numerical Example

The ‘lid-driven’ cavity is a standard test problem in the computational fluid dynamics. The problem is characterized by a square cavity in which the driving force for the flow is the shear created by the lid. Figure 38 shows a schematic of the cavity with the boundary conditions and the finite element discretization.

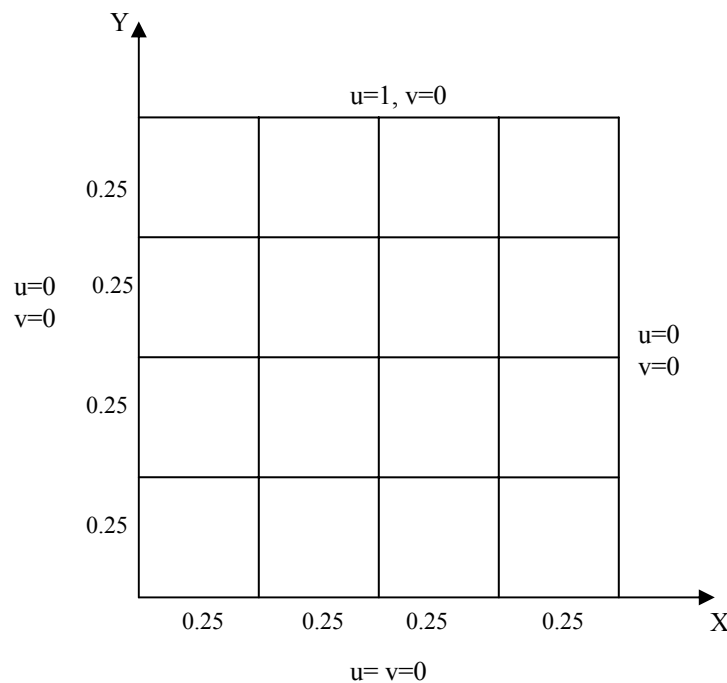


Figure 38. Computational domain using uniform 16 rectangular elements

The above problem is solved by direct-iteration with order of polynomials ranging from $P=2$ to $P=5$. The coefficient matrix is evaluated using a Gaussian quadrature of $(2P+1)$ in both the co-ordinate directions. For lower order P , reduced integration is used to evaluate the penalty terms, but for higher order P full integration is

used to evaluate the penalty terms. The Reynolds number Re_n for Power-Law fluid is fixed as 100 and the penalty parameter is taken as 10^8 for all the cases. Convergence is declared when the Euclidean norm is less than 10^{-3} , which typically took 7-10 iterations.

Results

For $P=2$, reduced integration is used to evaluate the penalty terms, the program converged for all values of Power-Law index, but the results were not good. For $P=3$, reduced integration is used to evaluate the penalty terms, the program converged for all values of Power-Law index and the results were better compared to the previous case. For $P=5$, full integration is used to evaluate the penalty terms, the program converged for all values of Power-Law index and the results are also good. Figure 39 shows the plots of horizontal velocity u at $X=0.5$ with $P=5$ for various values of Power-Law index $X=0.5$. Figure 40 shows the plots of vertical velocity v at $Y=0.5$ with $P=5$ for various values of Power-Law index $Y=0.5$.

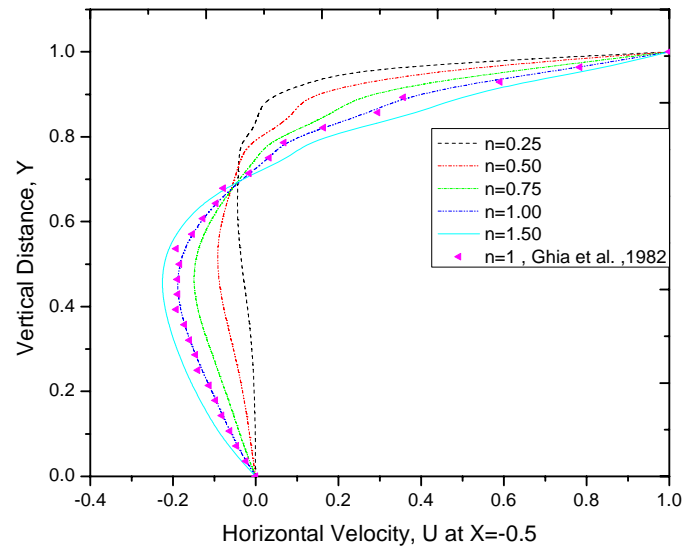


Figure 39. Plots of horizontal velocity u at $X=0.5$ with $P=5$ for various values of Power-Law index using RIP

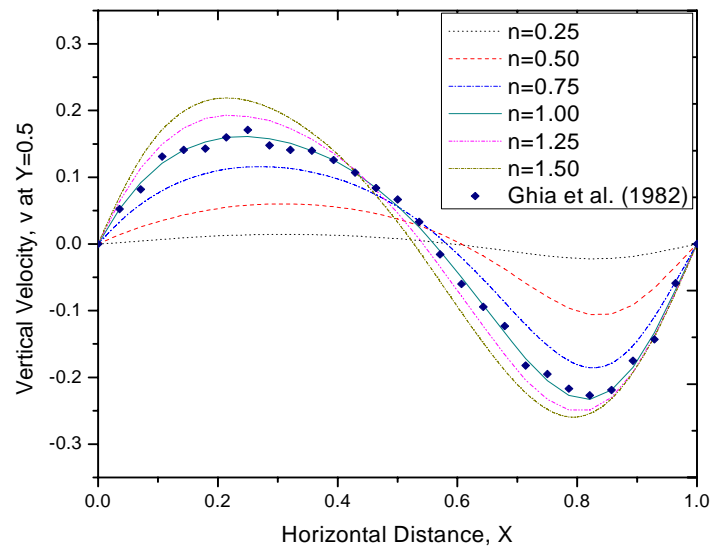


Figure 40. Plots of vertical velocity v at $Y=0.5$ with $P=5$ for various values of Power-Law index using RIP

Conclusions

From the above results we can conclude that there is some kind of locking occurring with lower order polynomial approximation functions. The effect is more pronounced for lower Power-Law indices compared to higher Power-Law indices. As explained in the previous chapters as the order of polynomial approximation functions is increased, the numerical solutions became more and more close to the benchmark solutions.

CHAPTER VIII

SUMMARY AND CONCLUSIONS

In this work alternative Least-Squares based finite element formulations of Navier-Stokes equation for Newtonian and non-Newtonian fluids are presented. Although the Least-Squares formulation can be considered as a special case of the weighted-residual method, it has its own standing as the true variational method since it is based on the minimization of a functional, whereas the other weighted-residual methods may not have corresponding functional whose first variation is equivalent to the governing equations. Variational methods (i.e., methods based on the existence of a functional whose extremum is equivalent to the governing equations) are considered to produce the ‘best’ approximation to the exact solution of the equations being modeled. The Least-Squares method satisfies the criteria desirable in a variational method. This has drawn a considerable attention for the solution of Stokes and Navier-Stokes equations ([11]-[17]). The Least-Squares method gives a more general, flexible and robust formulation procedure than weak form Galerkin-based finite element models and has several theoretical and computational advantages. Notably, it circumvents the ‘in-sup’ condition of LBB. As a result, equal order interpolation can be used for all the variables. It also results in symmetric, positive-definite coefficient matrix; hence robust iterative solvers can be employed to solve the system of algebraic equations.

In Chapter II, the steps involved in developing a Least-Squares based finite element model were presented for Poisson's equation. The *Direct-iteration* and *Newton-Raphson* iterative techniques were explained. The procedure was presented in a general setting by considering an abstract initial boundary value problem. The accuracy of the results was verified by increasing the order of the approximation spaces.

In Chapter III, the Least-Squares formulation of vorticity based Navier-Stokes equations for a steady state, isothermal, incompressible Newtonian fluids was presented. To transform the second-order equations to first-order the vorticity vector $\omega = \nabla \times V$ was introduced. The minimum requirement on approximation functions was that they all be Lagrange family of C^0 -continuity. Since the formulation was based on variational framework there were no compatibility issues between velocity and pressure approximation spaces, and so same Lagrange basis was used for all primary variables (p, V, ω) . The method of linearization of Least-Squares functional before and after minimization was explained. The effect of linearization was studied using Kovasznay flow problem with *Direct-iteration* iterative technique. The accuracy of the results was verified by increasing the order of the approximation spaces. From the results it was concluded that there is no significant impact of the linearization on the accuracy of the solution.

In Chapter IV, the Least-Squares formulation of stress based Navier-Stokes equations for a steady state, isothermal, incompressible Newtonian fluids was presented. To define the equivalent first-order velocity-pressure-stress system, stress tensor $\Gamma = \left[(\nabla V) + (\nabla V)^T \right]$ (symmetric part of velocity gradient tensor) was introduced as auxiliary variable. The minimum requirement on approximation functions used for all

variables was that they all require Lagrange family of approximation functions (i.e., C^0 -continuity). Since the formulation was based on variational framework there were no compatibility issues between velocity and pressure approximation spaces, and so the same Lagrange basis was used for all primary variables $(p, V, \Gamma_{xx}, \Gamma_{xy}, \Gamma_{yy})$. The method of linearization of Least-Squares functional before and after minimization was explained. The effect of linearization was studied by using ‘lid-driven’ cavity flow problem with *Direct-iteration* iterative technique. The accuracy of the results was verified by increasing the order of the approximation spaces. In the second formulation, continuity equation became an algebraic equation and was eliminated from the system with suitable modifications. This formulation carried one less degree of freedom compared to existing stress based first order formulations. The effect of linearization was studied using Kovasznay flow problem with *Direct-iteration* iterative technique. The accuracy of the results was verified by increasing the order of the approximation spaces. From the results it was concluded that there is no significant impact of the linearization before or after minimization on the accuracy of the solution.

In Chapter V, the Least-Squares formulation of stress based Navier-Stokes equations for a steady state, isothermal, incompressible non-Newtonian (Power-Law) fluids was presented. To define the equivalent first-order velocity-pressure-stress system, stress tensor $\Gamma - \mu \left[(\nabla V) + (\nabla V)^T \right] = 0$ (symmetric part of velocity gradient tensor) was introduced as auxiliary variables. The viscosity μ of the fluid was varied as per Power-Law. The Power-Law index was varied from 0.25 to 1.5 to study the shear thinning and

shear thickening fluids. The minimum requirement on approximation functions was that they all be Lagrange family of C^0 -continuity. Since the formulation was based on variational framework there were no compatibility issues between velocity and pressure approximation spaces, and so same Lagrange basis was used for all primary variables $(p, V, \Gamma_{xx}, \Gamma_{xy}, \Gamma_{yy})$. The method of linearization of Least-Squares functional before and after minimization was explained for Power-Law fluids. The effect of linearization was studied by using ‘lid-driven’ cavity flow problem with *Direct-iteration* and *Newton-Raphson* iterative techniques. The accuracy of the results was verified by increasing the order of the approximation spaces. From the results it was concluded that the non-Newtonian fluids require higher order polynomial approximation functions and higher order Gaussian quadrature compared to Newtonian fluids. The results were more accurate by tangent matrix than Direct-iteration technique for all Power-Law indices. The linearization before minimization case converged at a faster rate compared with linearization after minimization. There was some tangible effect of linearization before and after minimization on the accuracy of the solution. The effect was more pronounced for lower Power-Law indices compared to higher Power-Law indices. And there seemed to have some kind of locking that caused the matrices to be ill-conditioned especially for lower values of Power-Law indices. As with the case of Newtonian fluids, the numerical solutions became more and more close to the benchmark solutions with increase in the order of polynomial approximation functions.

In Chapter VI, the Least-Squares formulation of vorticity based Navier-Stokes equations for a steady state, isothermal, incompressible non-Newtonian (Power-Law)

fluids was presented. To define the equivalent velocity-pressure-vorticity system, vorticity vector $\omega = \nabla \times V$ was introduced as auxiliary variable. It was shown that, for Power-Law fluids, the vorticity vector did not reduce the original differential equations to first-order system. Hence it required use of at Least C^1 -continuous functions for the velocity field. The higher-order differentiability was a practical disadvantage and was also complex to derive the approximation functions that belong to C^1 -continuous space. A new method was tried to see if the higher-order approximation functions that belong to the Lagrange family of C^0 -continuity could be used instead of C^1 -continuity. The viscosity μ of the fluid was varied as per Power-Law. The Power-Law index was varied from 0.25 to 1.5 to study the shear thinning and shear thickening fluids. Since the formulation was based on variational framework there were no compatibility issues between velocity and pressure approximation spaces, and so the same Lagrange basis was used for all primary variables (p, V, ω) . The method of linearization of Least-Squares functional before and after minimization was explained for Power-Law fluids. The effect of linearization was studied by using ‘lid-driven’ cavity flow problem with *Direct-iteration* and *Newton-Raphson* iterative technique. The accuracy of the results was verified by increasing the order of the approximation spaces. From the results it was concluded that the non-Newtonian fluids require higher-order polynomial approximation functions and higher-order Gaussian quadrature compared to Newtonian fluids. The results were more accurate by tangent matrix than Direct-iteration technique for all Power-Law indices. The linearization before minimization case converged at a faster rate compared with linearization after minimization. There was some tangible effect of

linearization before and after minimization on the accuracy of the solution. The effect was more pronounced for lower Power-Law indices compared to higher Power-Law indices. There seemed to have some kind of locking that caused the matrices to be ill-conditioned especially for lower values of Power-Law indices. The new method which used higher-order approximation functions that belong to Lagrange family of C^0 -continuity instead of C^1 -continuity, seemed to give good results. As with the case of Newtonian fluids, the numerical solutions became more and more close to the benchmark solutions as the order of polynomial approximation functions was increased.

Finally, in Chapter VII, the reduced integration penalty finite element formulation of Navier-Stokes equations for a steady state, isothermal, incompressible non-Newtonian (Power-Law) fluids was presented. The continuity equation was an additional relation among the velocity components (i.e., a constraint among the v_i), and the constraint was satisfied in a Least-Squares (i.e. approximate) sense. The advantage of the constrained problem was that the pressure variable “ p ” does not appear in the formulation and it was post computed. The technique of under-integrating the penalty terms to reduce locking was explained. The viscosity μ of the fluid was varied as per Power-Law. The Power-Law index was varied from 0.25 to 1.5 to study the shear thinning and shear thickening fluids. The reduced integration penalty formulation was studied by using ‘lid-driven’ cavity flow problem with *Direct-iteration* iterative technique. The accuracy of the results was verified by increasing the order of the approximation spaces. From the results it was concluded that the non-Newtonian fluids require higher-order polynomial approximation functions and higher-order Gaussian quadrature compared to Newtonian fluids. Again, it

was found that there is some kind of locking with lower-order polynomial approximation functions. The effect was more pronounced for smaller values of Power-Law index compared to larger values of Power-Law index. As with the case of Newtonian fluids, the numerical solutions became more and more close to the benchmark solutions as the order of polynomial approximation functions was increased.

REFERENCES

- [1] I. Babuska, Errors bounds for finite element method, Numer. Math. 16 (1971) 322.
- [2] F. Brezzi and K.J. Bathe, A discourse on the stability conditions for mixed finite element formulations, Comput. Methods Appl. Mech. Engrg. 82 (1990) 27-57.
- [3] T. J. R. Hughes W. K. Liu and A. Brooks, Finite element analysis of incompressible viscous flows by the penalty function formulation. J. Comput. Phys. 30 I-60 (1979).
- [4] A. N. Brooks and T. J. R. Hughes, Streamline upwind/ Petrov galerkin formulations for convection dominated flows with particular emphasis on the incompressible Navier-Stokes equations, Comput. Methods Appl. Mech. Engrg. 32 (1982) 199-259.
- [5] G.F. Carey and R. Krishnan, Continuation techniques for a penalty approximation of Navier-Stokes equations, Comput. Methods Appl. Mech. Engrg. 48 (1985) 265-282.
- [6] T. J. R. Hughes, L. P. Franca and M. Balestra, A new finite element formulation for computational fluid dynamics: V. Circumventing the Babuska-Brezzi condition: A stable Petrov Galerkin formulation of the Stokes problem accommodating equal-order interpolations, Comput. Methods Appl. Mech. Engrg. 59 (1986) 85-99.
- [7] T. J. R. Hughes and L. P. Franca, A new finite element formulation for computational fluid dynamics: VII. The Stokes problem with various well-posed boundary conditions: Symmetric formulations that converge for all velocity/pressure spaces, Comput. Methods Appl. Mech. Engrg. 65 (1987) 85-96.
- [8] B. C. Bell and K. S. Surana, A space-time coupled p-version least-squares finite element formulation for unsteady fluid dynamics problems, Int. J. Numer. Methods Engrg. 37 (1994) 3545–3569.
- [9] B. C. Bell and K. S. Surana, A space-time coupled p-version least-squares finite element formulation for unsteady two-dimensional Navier-Stokes equations, Int. J. Numer. Methods Engrg. 39 (1996) 2593–2618.
- [10] D. Jespersen, A least-squares decomposition method for solving elliptic equations, Math. Comp., 31 (1977) 873–880.

- [11] B. N. Jiang, The Least-squares Finite Element Method, 1st ed., Berlin, Springer, 1998.
- [12] B. N. Jiang, On the least-squares method, *Comp. Methods in Appl. Mech. and Engrg.* (1997) 239-257.
- [13] P. V. Bochev and M. D. Gunzburger, Finite element methods of least-squares type, *SIAM Review*, 40 (1998) 789-837.
- [14] M. M. J. Proot and M. I. Gerritsma, Least-squares spectral elements applied to the Stokes problem, *J. of Comput. Phys.* 181 (2002) 454-477.
- [15] J. P. Pontaza and J. N. Reddy, Spectral/hp least-squares finite element formulation for the Navier-Stokes equations, *J. of Comput. Phys.* 190 (2003) 523-549.
- [16] V. Prabhakar and J. N. Reddy, Spectral/hp penalty least-squares finite element formulation for the steady incompressible Navier-Stokes equations, *J. of Comput. Phys.* 215 (2006) 274-297.
- [17] V. Prabhakar and J. N. Reddy, A stress based least-squares finite element formulation for the Incompressible Navier-Stokes equations, *Int. J. Numer. Methods Fluids* 54 (2007) 1369-1385.
- [18] A. P. Lynn and S. K. Arya, Use of the least squares criterion in the finite element formulation, *Int. J. Numer. Methods Enanz.* 6 (1973) 75-88.
- [19] G. F. Carey and B. N. Jiang, Least-squares finite elements for first order hyperbolic systems, *Int. J. Numer. Methods Engrg.* 26 (1988) 81-93.
- [20] G. J. Fix and M. D. Gunzburger, On least-squares approximations to indefinite problems of mixed type, *Int. J. Numer. Methods Engrg.* 12 (1978) 453-469.
- [21] P. P. Lynn, Least squares finite element analysis of laminar boundary layer flows, *Int. J. Numer. Methods Engrg.* 8 (1974) 865-876.
- [22] J. F. Polk and P. P. Lynn, A least squares finite element approach to unsteady gas dynamics, *Int. J. Numer. Methods Engrg.* 12 (1978) 3-10.
- [23] B. N. Jiang and C. L. Chang, Least-squares finite elements for the Stokes problem, *Comput. Methods Appl. Mech. Engrg.* 78 (1990) 297-311.
- [24] C. A. J. Fletcher, A primitive variable finite element formulation for inviscid, compressible flow, *J. Comput. Phys.* 33 (1979) 301-312.

- [25] H. Nguyen and J. Reynen, A space-time least-squares finite element scheme for advection-diffusion equations, *Comput. Methods Appl. Mech. Engrg.* 42 (1984) 331-342.
- [26] I. Kececioglu and B. Rubinsky, A mixed-variable continuously deforming finite element method for parabolic evolution problems. Part II: The coupled problem of phase change in porous media, *Internat. J. Numer. Methods Engrg.* 28 (1989) 2609-2634.
- [27] B.N. Jiang, A least-squares finite element method for incompressible Navier-Stokes problems, *Int. J. Numer. Methods Fluids* 14 (1992) 843-859.
- [28] B.N. Jiang, *The Least-squares Finite Element Method*, Springer-Verlag, New York, 1998.
- [29] B.N. Jiang, C.L. Chang, Least-squares finite elements for the Stokes problem, *Comput. Methods Appl. Mech. Engrg.* 78 (1990) 297-311.
- [30] B.N. Jiang, L.A. Povinelli, Least-squares finite element method for fluid dynamics, *Comput. Methods Appl. Mech. Engrg.* 81 (1990) 13-37.
- [31] B.N. Jiang, V. Sonnad, Least-squares solution of incompressible Navier-Stokes equations with the p-Version of finite elements, *Comput. Mech.* 15 (1994) 129.
- [32] B.C. Bell, K.S. Surana, A space-time coupled p-version least-squares finite element formulation for unsteady two-dimensional Navier-Stokes equations, *Int. J. Numer. Methods Engrg.* 39 (1996) 2593-2618.
- [33] D. Winterscheidt, K.S. Surana, p-Version least-squares finite element formulation for two-dimensional incompressible fluid flow, *Int. J. Numer. Methods Fluids* 18 (1994) 43-69.
- [34] Z. Cai, T.A. Manteuffel, S.F. McCormick, First-order system least-squares for the Stokes equations, with application to linear elasticity, *SIAM J. Numer. Anal.* 33 (1997) 1727-1741.
- [35] P.B. Bochev, Z. Cai, T.A. Manteuffel, S.F. McCormick, Analysis of velocity-flux first-order system least-squares principles for the Navier-Stokes equations: Part I, *SIAM J. Numer. Anal.* 35 (1998) 990-1099.
- [36] P.B. Bochev, T.A. Manteuffel, S.F. McCormick, Analysis of velocity-flux least-squares principles for the Navier-Stokes equations: Part II, *SIAM J. Numer. Anal.* 36 (1999) 1125-1144.

- [37] J. P. Pontaza and J. N. Reddy, Least-squares finite element formulations for viscous incompressible and compressible fluid flows, *Comput. Methods Appl. Mech. Engrg.* 195 (2006) 2454-2494.
- [38] L.I.G. Kovasznay, Laminar flow behind a two-dimensional grid, *Proc. Cambridge Philos. Soc.* 44 (1948) 58–62.
- [39] A.K. Aziz, R.B. Kellogg, A.B. Stephens, Least-squares methods for elliptic systems, *Math. Comput.* 44 (1985) 53–70.
- [40] Y. Cao, M.D. Gunzburger, Least-squares finite element approximations to solutions of interface problems, *SIAM J. Numer. Anal.* 35 (1998) 393–405.
- [41] M.I. Gerritsma, M.M.J. Proot, Analysis of a discontinuous least-squares spectral element method, *J. Sci. Comput.* 17 (2002) 297– 306.
- [42] W. Heinrichs, Least-squares spectral collocation for discontinuous and singular perturbation problems, *J. Comput. Appl. Math.* 157 (2003) 329–345.
- [43] J.P. Pontaza, J.N. Reddy, Space-time coupled spectral/hp least-squares finite element formulation for the incompressible Navier–Stokes equations, *J. Comput. Phys.* (accepted for publication).
- [44] O.C. Zienkiewicz, Constrained variational principles and penalty function methods in finite element analysis, in: G.A. Watson (Eds.), *Lecture Notes in Mathematics: Conference on the Numerical Solution of Differential Equations*, Springer-Verlag, Berlin, 1974.
- [45] D.S. Malkus, T.J.R. Hughes, Mixed finite element methods – reduced and selective integration techniques: A unification of concepts, *Comput. Methods Appl. Mech. Engrg.* 15 (1978) 63.
- [46] P. Bochoy, M.D. Gunzburger, Least-squares finite-element methods for optimization and control problems for the Stokes equations, *Comput. Math. Appl.* 48 (2004) 1035.
- [47] J.S. Hesthaven, Spectral penalty methods, *Appl. Numer. Math.* 33 (2000) 23.
- [48] P.J. Diamessis, J.A. Domaradzki, J.S. Hesthaven, A spectral multidomain penalty method model for the simulation of high Reynolds number localized incompressible stratified turbulence, *J. Comput. Phys.* 202 (2005) 298.
- [49] M.D. Gunzburger, Iterated penalty methods for the Stokes and Navier–Stokes equations, in: T.J. Chung, G.R. Karr (Eds.), *Finite Element Analysis in Fluids*,

Proceedings of the 7th International Conference on Finite Element Methods in Flow Problems, University of Alabama Press, Tuscaloosa, Alabama, 1989, 1040.

- [50] B.N. Jiang, T.L. Lin, L.A. Povinelli, Large-scale computation of incompressible viscous flow by least-squares finite element method, *Comput. Methods Appl. Mech. Engrg.* 114 (1994) 213.
- [51] D.K. Gartling, A test problem for outflow boundary conditions – flow over a backward-facing step, *Int. J. Numer. Methods Fluids* 11 (1990) 953.
- [52] A.S. Grove, F.H. Shair, E.E. Petersen, A. Acrivos, An experimental investigation of the steady separated flow past a circular cylinder, *J. Fluid Mech.* 19 (1964) 60.
- [53] G.D.V. Davis, Natural convection of air in a square cavity: A bench mark numerical solution, *Int. J. Numer. Methods Fluids* 3 (1983) 249.
- [54] J. N. Reddy and V. A. Padhye, A penalty finite element model for axisymmetric flows of non-Newtonian fluids. *Numer. Methods Partial Diff. Equ.* 4 (1988) 33-56.
- [55] M. Iga and J. N. Reddy, Penalty finite element analysis of free surface flows of Power-Law fluids, in: J.R. Whiteman (Eds.), *The Mathematics of Finite Elements and Applications VI (MAFELAP 1987)*, Academic Press, London (1988).
- [56] R. I. Tanner, Die-Swell reconsidered: Some numerical solutions using a finite element program, *Appl. Polymer Symp.* 20 (1973) 201-20s.
- [57] R. I. Tanner, R. E. Nickell and R. W. Bilger, Finite element methods for the solution of some incompressible non-Newtonian fluid mechanics problems with free surfaces, *Comput. Methods Appl. Mech. Engrg.* 6 (1975) 155-179.
- [58] R. E. Nickell, R. I. Tanner and B. Caswell, The solution of viscous incompressible jet and free surface flows using finite element methods, *J. Fluid Mech.* 65 (1974) 189-206.
- [59] R. I. Tanner, Some experiences using finite element methods in polymer processing and rheology, in: *Proceedings of the Seventh Int. Congress on Rheology* (Edited by C. Klason and J. Kubat) Gothenburg, Sweden, (1976) pp. 140-145.

- [60] K. R. Reddy and R. I. Tanner, Finite element approach to die-swell problems of non-Newtonian fluids .Proceedings of the Sixth Australian Hydraulics and Fluid Mechanics Conference, Adelaide, Australia, (1977) pp. 431-434.
- [61] B. Caswell and R. I. Tanner, Wirecoating die design using finite element methods, *Polymer. Engrg. Sci.* 18 (1978) 416-421.
- [62] D. V. Boger, R. Gupta and R. I. Tanner, The end-correction for Power-Law fluids in the capillary rheometer, *J. non-Newtonion Fluid Mech.* 4 (1978) 239-248.
- [63] O. C. Zienkiewicz, P. C. Jain and E. Onate, Flow of solids during forming and extrusion: Some aspects of numerical solutions, *Int. J. Solids Struct.* 14 (1978) 15-38.
- [64] O. C. Zienkiewicz and P. N. Godbole, Viscous incompressible flow with special reference to non-Newtonian (plastic) fluids, in: R. A. Gallagher, J. T. Oden, C. T. Taylor and O. C. Zienkiewicz (Eds.), *Finite Element Method in Flow Problems*, Chap. 2. Wiley, New York , 1975.
- [65] M. Kawahara and N. Takeuchi. Mixed finite element method for analysis of viscoelastic fluid flow, *Computers Fluids* 5 (1977) 33-45.
- [66] B. C. Bell, and K. S. Surana, p-Version least squares finite element formulation for two-dimensional, incompressible, non-Newtonian isothermal and non-isothermal fluid flow, *Int. J. Numer. Methods Fluids* 18 (1994) 127–162.
- [67] N. B. Edgar, and K. S. Surana, p-Version least squares finite element formulation for axisymmetric incompressible non-Newtonian fluid flow, *Comput. Methods Appl. Mech. Engrg.* 113 (1994) 271–300.
- [68] N. B. Edgar and K. S. Surana, p-Version least squares Newtonian and non-Newtonian fluids in rectangular ducts. Finite element formulation for axisymmetric incompressible non-Newtonian fluid flow, *Comput. Methods Appl. Mech. Engrg.* 113 (1994) 271-300.
- [69] H. S. Dalimunthe and K. S. Surana p-Version least squares finite element formulation for three-dimensional, incompressible, non-isothermal, non-Newtonian fluid flow, *Computers and Structures* 58 No. I EHOS, 1996.
- [70] Z. Feng and K. S. Surana, p-Version least squares finite element formulation for three-dimensional, isothermal, incompressible, non-Newtonian fluid flow, *Computers and Structures* 57 5 (1995) 799-816.

- [71] N. B. Edgar, K. S. Surana, p-Version least squares finite element formulation for axisymmetric incompressible non-Newtonian fluid flow, *Comput. Methods Appl. Mech. Engrg.* 113 (1994) 271-300.
- [72] J.N. Reddy *An Introduction to Nonlinear Finite Element Analysis* Oxford University Press, New York, 2004.

VITA

Venkat Pradeep Vallala received his baccalaureate (B.E.) degree in mechanical Engineering from Osmania University College of Engineering, OU, Hyderabad, AP, India in July 2004. After that, he worked as Associate Systems Engineer with companies like Syntel and IBM in India till Dec 2006. In January 2007, he joined the Mechanical Engineering Department at Texas A&M University for his graduate studies. Venkat's research at TAMU was concerned with alternative Least-Squares finite element formulations for Newtonian and non-Newtonian fluids. At TAMU, he worked as Graduate Assistant Research (GAR) with the Department of Veterinary Pathobiology, College of Medicine. He graduated with his Master's degree in May 2009.

He can be reached through Prof. J.N. Reddy, Department of Mechanical Engineering at Texas A&M University, College Station, TX-77843 (or) through his personal email pradeepvv82@gmail.com.